National Library of Canada
Bibliothèque nationale du Canada

Canadian Theses Service
Service des thèses canadiennes

Ottawa, Canada
K1A 0N4

NOTICE

The quality of this microform is heavily dependent upon the quality of the original thesis submitted for microfilming. Every effort has been made to ensure the highest quality of reproduction possible.

If pages are missing, contact the university which granted the degree.

Some pages may have indistinct print especially if the original pages were typed with a poor typewriter ribbon or if the university sent us an inferior photocopy.

Previously copyrighted materials (journal articles, published tests, etc.) are not filmed.

Reproduction in full or in part of this microform is governed by the Canadian Copyright Act, R.S.C. 1970, c. C-30.

AVIS

La qualité de cette microforme dépend grandement de la qualité de la thèse soumise au microfilmage. Nous avons tout fait pour assurer une qualité supérieure de reproduction.

S'il manque des pages, veuillez communiquer avec l'université qui a conféré le grade.

La qualité d'impression de certaines pages peut laisser à désirer, surtout si les pages originales ont été dactylographiées à l'aide d'un ruban usé ou si l'université nous a fait parvenir une photocopie de qualité inférieure.

Les documents qui font déjà l'objet d'un droit d'auteur (articles de revue, tests publiés, etc.) ne sont pas microfilmés.

La reproduction, même partielle, de cette microforme est soumise à la Loi canadienne sur le droit d'auteur, SRC 1970, c. C-30.

NL-339 (r. 88/04)

Canada

THE UNIVERSITY OF ALBERTA

STABILITY OF CONCRETE PLATES UNDER COMBINED IN-PLANE AND LATERAL LOADS

by

© ABIEYUWA O. AGHAYERE

A THESIS

SUBMITTED TO THE FACULTY OF GRADUATE STUDIES AND RESEARCH
IN PARTIAL FULFILMENT OF THE REQUIREMENTS FOR THE DEGREE
OF DOCTOR OF PHILOSOPHY

DEPARTMENT OF CIVIL ENGINEERING

EDMONTON, ALBERTA
SPRING 1988

Permission has been granted to the National Library of Canada to microfilm this thesis and to lend or sell copies of the film.

The author (copyright owner) has reserved other publication rights, and neither the thesis nor extensive extracts from it may be printed or otherwise reproduced without his/her written permission.

L'autorisation a été accordée à la Bibliothèque nationale du Canada de microfilmer cette thèse et de prêter ou de vendre des exemplaires du film.

L'auteur (titulaire du droit d'auteur) se réserve les autres droits de publication; ni la thèse ni de longs extraits de celle-ci ne doivent être imprimés ou autrement reproduits sans son autorisation écrite.

ISBN 0-315-42873-2

THE UNIVERSITY OF ALBERTA

RELEASE FORM

NAME OF AUTHOR ABIEYUWA O. AGHAYERE

TITLE OF THESIS STABILITY OF CONCRETE PLATES UNDER COMBINED IN-PLANE AND LATERAL LOADS

DEGREE FOR WHICH THESIS WAS PRESENTED DOCTOR OF PHILOSOPHY

YEAR THIS DEGREE GRANTED SPRING 1988

Permission is hereby granted to THE UNIVERSITY OF ALBERTA LIBRARY to reproduce single copies of this thesis and to lend or sell such copies for private, scholarly or scientific research purposes only.

The author reserves other publication rights, and neither the thesis nor extensive extracts from it may be printed or otherwise reproduced without the author's written permission.

(SIGNED) ....

PERMANENT ADDRESS:
No 41 Aruosa street
Benin-City
NIGERIA

DATED Feb. 1 1988

THE UNIVERSITY OF ALBERTA

FACULTY OF GRADUATE STUDIES AND RESEARCH

The undersigned certify that they have read, and recommend to the Faculty of Graduate Studies and Research, for acceptance, a thesis entitled STABILITY OF CONCRETE PLATES UNDER COMBINED IN-PLANE AND LATERAL LOADS submitted by ABIEYUWA O. AGHAYERE in partial fulfilment of the requirements for the degree of DOCTOR OF PHILOSOPHY.

....

Supervisor

....

....

....

Gary Faulkner

N. D. Na

External Examiner

Date January 19, 1988

DEDICATION

To my dearly beloved wife, Josephine, my rose of Sharon and lily of the valleys and to my darling daughters, Osarhieme and Itohan, the apples of my eye.

To my dearly beloved mother and to my cherished late great-grand mother for their selfless love and care when I needed it the most.

"Therefore, since we have been justified by faith, we have peace with God through our Lord Jesus Christ..." Romans 5:1

TO THE GLORY OF GOD

Abstract

Concrete plates supported along all edges are commonly used as structural elements in the hulls of concrete floating structures such as concrete ships, barges, pontoons, floating ports and bridges where they are subjected to combined compressive in-plane and lateral loads. Several analytical methods exist and test results are available for concrete plates under pure in-plane or pure lateral loads but to the author's knowledge, no test results are available for the combined load situation for plates supported on four edges and few analytical models exist.

The problem is to determine the maximum lateral load the plate can sustain under a given compressive in-plane load taking into account geometric and material nonlinearities. One analytical model exists for the analysis of concrete plates under combined loads but is limited to square plates under sinusoidally varying lateral loads.

Analytical models available for beam-columns under combined in-plane and lateral loads include the column-curvature-method and the assumed deflection method. In the first, iterative numerical integration of moment curvature diagrams is used to establish the deflected shape of the column at each stage of loading. In the assumed deflection method, a deflection function is assumed for the beam-column throughout the entire load range. This simplifies the beam-column problem reducing it to a one-degree of freedom problem requiring equilibrium between external loads and internal resistance only at the critical section, which occurs at the center of the span for symmetrically loaded uniform beam-columns.

A method of analysis is developed here based on the assumed deflection method. In this way calculation of the strength of a plate is reduced to a one-degree of freedom problem. A design method similar to the moment magnifier approach for slender columns is also developed based on a Fourier series expression of the deflection and lateral load.

Nine reinforced concrete plate specimens were tested; eight under combined in-plane and lateral loads, and one under lateral loads only. Parameters varied included aspect ratio, plate thickness, reinforcement ratio and loading history. The ultimate lateral loads computed using the proposed method of analysis show good agreement with test results.

AKNOWLEDGEMENTS

The author wishes to express his deep appreciation and gratitude to his thesis supervisor, Professor James G. MacGregor for his invaluable support, encouragement and guidance throughout this study. Financial assistance recieved from the National Science and Engineering Research Council through Operating Grant A1673 is gratefully acknowledged.

The assistance of L. Burden, R. Helfrich and Vijay Parmar of the I.F. Morrison Laboratory, University of Alberta in fabricating and testing the specimens and the help and encouragement of Dr. Brendan O'Flynn during the design stage of the test frame is gratefuly acknowledged.

I owe a debt of gratitude to my dearly beloved wife and children whose support, encouragement and perseverance was indispensable through out the course of this study. Many thanks to Alex Omoruyi and Ben Okorosobo for their support and encouragement.

My deep gratitude go to my parents for their prayers, moral and financial support during my student days.

My thanks go to Mr. and Mrs. Martin Bell for their love and support throughout the course of this study. I am indebted to my beloved grand-father, Pa A. Uwadiae and to Engr. G.O. Omonitan for encouraging me to take on this pursuit.

Finally, to my God and risen Savior Jesus Christ, the Alpha and the Omega, the First and the Last, the Beginning and the End, the Rock of all Ages, the Lord of lords, the King of kings, and the Fountain of all knowledge and wisdom, I owe all that I am and ever hope to be. The voices of a million angels could not express my gratitude for all the things You have done for me. Things so undeserved, yet You gave to prove Your love for me. To You, the only true God, be all praise, glory, honor and majesty forever and ever. Amen. Hallelujah, Hosanna in the highest.

Table of Contents

Chapter Page

1. INTRODUCTION 1
    - 1.1 Problem Statement 1
    - 1.2 Research Objectives 3
    - 1.3 Outline of Problem Solution 4

2. LITERATURE REVIEW 8
    - 2.1 General 8
    - 2.2 Related Previous Tests 8
        - 2.2.1 Tests of Metal Plates 8
        - 2.2.2 Tests of Reinforced Concrete Plates 14
    - 2.3 Related Previous Analyses 18
        - 2.3.1 Analyses of Elastic Plates 18
        - 2.3.2 Analyses of Steel Plates 20
        - 2.3.3 Analyses of Reinforced Concrete Plates 27
    - 2.4 Summary and Conclusions 31

3. EXPERIMENTAL PROGRAM 34
    - 3.1 Introduction 34
    - 3.2 Test Specimens 34
    - 3.3 Material Properties 37
        - 3.3.1 Reinforcing Steel 38
        - 3.3.2 Concrete 38
    - 3.4 Test Set-Up 39
    - 3.5 Instrumentation 43
        - 3.5.1 Displacement Measurement 43
        - 3.5.2 Steel Strains 44
    - 3.6 Test Procedure 45

4. TEST RESULTS 68

4.1 Introduction 68

4.2 General Test Observations 68

4.2.1 Maximum Loads and Modes of Failure 68

4.2.2 Load Deflection Response 72

4.2.3 Deflected Shapes 72

4.2.4 Strain Distribution 73

5. ANALYSES, DESIGN AND DISCUSSION OF RESULTS 101

5.1 Introduction 101

5.2 Moment-Load-Curvature Relationships 104

5.2.1 Tension Stiffening 107

5.3 Analytical Model 109

5.3.1 Modified Limit Analysis Method 111

5.4 Design Method 119

5.4.1 Formulation 120

5.5 DISCUSSION AND ANALYSIS OF RESULTS 125

5.5.1 Assumptions in Analytical Model 125

5.5.1.1 Small Deflection Theory 125

5.5.1.2 Deflected Shape 126

5.5.1.3 Poisson's Ratio 126

5.5.1.4 Independence of Moment Curvature Diagrams For Two Axes 127

5.5.1.5 Initial Imperfections 128

5.5.2 Comparison of Analytical Predictions With Test Results 129

5.5.3 Lateral load capacity of specimens for zero in-plane load 130

5.5.4 Effects of Various Parameters 130

6. SUMMARY, CONCLUSIONS AND RECOMMENDATIONS 167

6.1 Summary 167

6.2 Conclusions 169
6.3 Recommendations for Future Research 170
BIBLIOGRAPHY 171

List of Tables

Table Page

3.1 Average Measured Thickness of Specimens 46

3.2 Average Locations of Top and Bottom Reinforcement From Compressive Face 47

3.3 Area of Reinforcement in x and y Directions 48

3.4 Age at Testing for Each Specimen 49

3.5 Modulus of Elasticity, Compressive and Tensile Strength of Specimens 50

4.1 Maximum Lateral Load and Applied In-plane Load 75

5.1 Comparison of Dy/Dx Ratios 135

5.2 Ratio of Maximum Plate Deflection at Peak Lateral Load to Plate Thickness 136

5.3 Maximum Calculated Initial Deflections 137

5.4 Maximum Lateral Loads: Test versus Analytical Predictions 138

5.5 Maximum Lateral Loads: Test versus Design Predictions 139

5.6 Reduction in Lateral Load Capacity Due To In-plane Load 140

5.7 Ratio of Applied In-plane Load to Balanced Load 141

List of Figures

Figure Page

1.1 Typical Concrete Floating Structure 6

1.2 Loads Acting on The Bottom Plate of The Hull 7

3.1 Placement of Reinforcement 51

3.2 Stress Strain Curve for Reinforcement 52

3.3 Least Squares Estimate of Cylinder Strength/Time Curve for First Concrete Cast 53

3.4 Least Squares Estimate of Cylinder Strength/Time Curve for Second Concrete Cast 54

3.5 Schematic of Test Frame 55

3.6 Schematic of Rocker-Roller Assembly 56

3.7 Schematic of Corner Support Frame 57

3.8 Edge Rotation Measuring Device 58

3.9 LVDT Locations for Square Specimens 59

3.10 LVDT Locations for Rectangular Specimens 60

3.11 Strain Gage Layout for A Series 61

3.12 Strain Gage Layout for C and D Series 62

3.13 Strain Gage Layout for B Series 63

4.1 Lateral Load versus Out-of-Plane Center Deflection for Specimen A3 76

4.2 Lateral Load versus Out-of-Plane Center Deflection for Specimen A2 77

4.3 Lateral Load versus Out-of-Plane Center Deflection for Specimen B1 78

4.4 Lateral Load versus In-plane Deflection in the x Direction for Specimen A2 79

4.5 Lateral Load versus In-plane Deflection in the y Direction for Specimen A2 80

4.6 Lateral Load versus In-plane Deflection in the x Direction for Specimen B1 81

Figure Page

4.7 Lateral Load versus In-plane Deflection in the y Direction for Specimen B1 82

4.8 Lateral Load versus Edge Rotation in the x Direction for Specimen A2 83

4.9 Lateral Load versus Edge Rotation in the y Direction for Specimen A2 84

4.10 Lateral Load versus Edge Rotation in the x Direction for Specimen B1 85

4.11 Lateral Load versus Edge Rotation in the y Direction for Specimen B1 86

4.12 Deflection Profiles in the x Direction for Specimen A2 87

4.13 Deflection Profiles in the y Direction for Specimen A2 88

4.14 Deflection Profiles in the x Direction for Specimen B1 89

4.15 Deflection Profiles in the y Direction for Specimen B1 90

4.16 In-plane Strain Distribution for Specimen A1 91

4.17 In-plane Strain Distribution for Specimen D1 92

4.18 Lateral Load vs Transverse Steel Strains 93

5.1 Uniaxial Stress-Strain Curve for Concrete 142

5.2 Derivation of M-N-ϕ Relationship 143

5.3 Reinforced Concrete Element. Distribution of :(a) Bond Stress. (b)Concrete Tensile Stress. (c) Steel Tensile Stress. (d) Flexural Rigidity. 144

5.4 Moment-Curvature for a Typical Cross Section 145

5.5 Plate Dimensions, Coordinate axes and Loading. 146

5.6 Comparison of Deflected Shapes: Specimen A2 - x Direction 147

Figure Page

5.7 Comparison of Deflected Shapes: Specimen A2 - y Direction 148

5.8 Comparison of Deflected Shapes: Specimen B1- x Direction 149

5.9 Comparison of Deflected Shapes: Specimen B1- y Direction 150

5.10 Initial Deflected Shape in x Direction For Specimen A2 151

5.11 Initial Deflected Shape in y Direction For Specimen A2 152

5.12 Initial Deflected Shape in x Direction For Specimen B2 153

5.13 Initial Deflected Shape in y Direction For Specimen B2 154

5.14 Lateral Load Deflection Curves for Specimen A3: Test versus Analytical Predictions. 155

5.15 Lateral Load Deflection Curves for Specimen A2: Test versus Analytical Predictions. 156

5.16 Lateral Load Deflection Curves for Specimen A1: Test versus Analytical Predictions. 157

5.17 Lateral Load Deflection Curves for Specimen C1: Test versus Analytical Predictions. 158

5.18 Lateral Load Deflection Curves for Specimen C2: Test versus Analytical Predictions. 159

5.19 Lateral Load Deflection Curves for Specimen D1: Test versus Analytical Predictions. 160

5.20 Lateral Load Deflection Curves for Specimen D2: Test versus Analytical Predictions. 161

5.21 Lateral Load Deflection Curves for Specimen B1: Test versus Analytical Predictions. 162

Figure Page

5.22 Lateral Load Deflection Curves for Specimen B2: Test versus Analytical Predictions. 163

5.23 Lateral Load In-plane Load Interaction Diagram: Specimen B2 164

5.24 Lateral Load In-plane Load Interaction Diagram: Specimen D1 165

5.25 Lateral Load In-plane Load Interaction Diagram: Specimen A1 166

List of Plates

Plate Page

3.1 Reinforcement Cage for Square Specimen 64

3.2 In-plane Loading Frame Showing Clamps 65

3.3 Load Spreading Plate for Lateral Loading 66

3.4 An Over View of Test Frame 67

4.1 Tension Face of Specimen A1 After Failure, y Direction vertical 94

4.2 Compression Face of Specimen A1 After Failure, y Direction vertical 95

4.3 Tension Face of Specimen C1 After Failure, y Direction vertical 96

4.4 Compression Face of Specimen C1 After Failure, y Direction vertical 97

4.5 Tension Face of Specimen B2 After Failure, y Direction horizontal 98

4.6 Compression Face of Specimen B2 After Failure, y Direction horizontal 99

4.7 Buckling of Compression Reinforcement after Failure, y Direction horizontal 100

LIST OF SYMBOLS

b = length of plate in x direction

a = length of plate in y direction

D_x, D_y = bending stiffness per unit width in x and y directions, respectively

$2D_t$ = plate torsional rigidity per unit width

e_x = eccentricity of in-plane load in x direction

e_y = eccentricity of in-plane load in y direction

E = modulus of elasticity of reinforcement

EU = ultimate strain of reinforcement

E_c = concrete modulus of elasticity

f'_c = compressive strength of concrete at age of testing

f'_t = concrete tensile strength

f_c = compressive stress in concrete

f_t = tensile stress in concrete

f_s = tensile stress in steel

FU = ultimate stress of reinforcement

H = effective torsional rigidity

M_{cr} = cracking moment per unit length

M = moment per unit length

M_x, M_y = bending moment per unit length in x and y directions, respectively

M_{xy} = twisting moment per unit length

M_{xi}, M_{yi} = internal resisting moment per unit length in x and y directions, respectively

M_{xyi} = internal resisting twisting moment per unit length

N_x, N_y = in-plane load per unit length in x and y directions, respectively

q = uniform lateral load

q_x, q_y = lateral load carried by bending in x and y directions, respectively

q_{xy} = lateral load carried by twisting of plate

t = thickness of plate

u = bond stress

w = lateral plate deflection at point (x,y)

w_o = lateral deflection at center of the plate

ϵ = strain in concrete

ϵ_o = concrete strain at maximum stress

ϵ_{ult} = ultimate tensile strain

ϕ_x = curvature in x direction

ϕ_y = curvature in y direction

ϕ_{xy} = twist of the midplane of the plate with respect to x and y axes

ϕ_{xo} = maximum curvature in x direction

ϕ_{yo} = maximum curvature in y direction

ϕ_{xyo} = maximum twist of the midplane of the plate with respect to x and y axes

ϕ_m = average curvature

ϕ_1 = curvature in state 1

ϕ_2 = curvature in state 2

ν_x = Poisson's ratio in y direction

ν_y = Poisson's ratio in x direction

ρ_x = reinforcement ratio in one layer in x direction

ρ_y = reinforcement ratio in one layer in y direction.

1. INTRODUCTION

1.1 Problem Statement

The hulls of floating concrete structures such as concrete ships, barges, pontoons, floating ports and bridges, for simplicity and economy of construction are usually made up of a cellular system of rectangular plate elements supported along the four edges (Macleay, 1949; Magura and Mast, 1979; LaNier *et al.*, 1986). The loads acting on these plate elements include hydrostatic water pressures on the surface of the plate as well as compressive in-plane loads due to longitudinal hull bending and tranverse forces in the plane of the hull bottom arising directly from water pressure on the sides of the hull (Emi *et al.*, 1981). A schematic diagram of a typical floating concrete structure is shown in Fig. 1.1. The types of loads acting on the bottom plate of the hull are shown in Fig. 1.2. A hogging wave is one that lifts the middle of the ship more than the ends.

Conceivably, the application of combined in-plane and lateral loading can be achieved in three different sequences. The in-plane load may be applied first to its full value and then held constant while lateral load is applied from zero to failure. Secondly, lateral load may be applied to its full value and then held constant while in-plane load is applied until failure. Finally, both in-plane and lateral loading may be applied simultaneously while maintaining a constant ratio between them. This is the so-called proportional loading. The first sequence and the third (to a limited extent) are investigated in this thesis.

When in-plane compression and lateral loads act together, each of these loads can alter the effect which the other would have if it were acting alone. If the lateral load is sufficiently large it can influence both the deflected shape and the boundary conditions of a plate and thus influence the buckling stress. At the same time, the in-plane compression can alter the effects of the lateral loads. The significance of this influence and the way it is dealt with depends on whether the in-plane compression is moderate or large. If it is moderate such that there is no possibility of collapse under the in-plane load alone, then it merely magnifies the effects of the lateral loads and in this case the deflected shape and the boundary conditions which are used for the calculation of the elastic critical stress are those corresponding to the lateral load.

On the other hand, if the in-plane compression is large, such that there is a possibility of collapse under the in-plane load alone, then the analysis is concerned with the question of the actual buckling and/or collapse of the plate. For this case of buckling under pure in-plane load, test results and analytical models for reinforced concrete plates (Swartz *et al.*,1974) are available. However, to the author's knowledge there are no test results for reinforced concrete plates supported on four edges under combined in-plane and lateral loads. The only analytical model available for this load case is one by Aas Jakobsen (1983) and it is only applicable to simply supported plates with sinusoidal lateral loads.

The problem is to determine the maximum lateral load the plate can carry for a given in-plane load taking into consideration material and geometric nonlinearities.

1.2 Research Objectives

The general objective of this research is to develop a method of analysis for concrete plates under combined loads suitable for use in design calculations and to carry out an experimental program to obtain results against which the model could be calibrated. The nonlinear behavior of a concrete plate due to actual stress-strain relationships, effects of cracking, creep and deformations must be duly accounted for in order to carry out realistic strength predictions. The use of numerical based methods such as finite difference or nonlinear finite element methods is generally too costly for practical purposes.

Therefore, a method of analysis and a design approach are developed which are suitable for use in actual design situations and which allow for geometric and material nonlinear effects in a sufficiently accurate manner.

1.3 Outline of Problem Solution

As with all research, the search for a solution started with a review of existing literature. An overview of existing papers on both steel and concrete plates is presented in Chapter 2. The aim was to identify pertinent experimental data, establish the important variables and range of interest for each variable and critically examine any existing analytical models with a view to identifying defects or "gaps" in the formulations to determine the need for experiments.

From the literature review of Chapter 2, it was found that no experimental results are available for reinforced concrete plates supported on four edges under combined in-plane and lateral loads. This led to the development of the experimental program described in Chapter 3. The test program consisted of nine plates, simply supported on all four sides without in-plane restraints. Seven of the plates had an aspect ratio of 1.0 (square), while the remaining two specimens had an aspect ratio of 1.50. The tests provided quantitative information about the load-deflection behavior as well as qualitative behavioral observations. Chapter 4 consists of a description of the observed behavior.

From the literature review, it was found that only one simple calculation model by Aas Jakobsen(1983) exists. This model was restricted to square plates under sinusoidal lateral loads, or lateral pressures which could be approximated by a sinusoidal load, and had not been verified with any tests. This led to the development of an analytical model described in Chapter 5. Material nonlinearities are included in the formulations using analytically derived moment-load-curvature relationships. Second-order effect due to the in-plane load and the effects of initial deflections were considered. A design method similar to the moment magnifier approach for slender columns is developed in Chapter 5 followed by discussions of observed behavior and comparisons with predictions from the analytical model and design method.

In Chapter 6 a summary of the research, conclusions and recommendations for future research are presented.

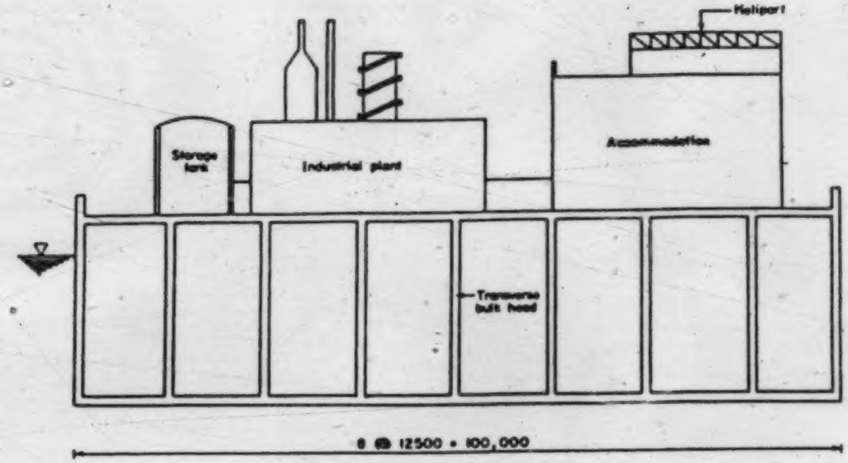
Heliport
Storage tank
Industrial plant
Accommodation
Transverse bulk head
8 @ 12500 = 100,000

LONGITUDINAL SECTION OF FLOATING PLANT

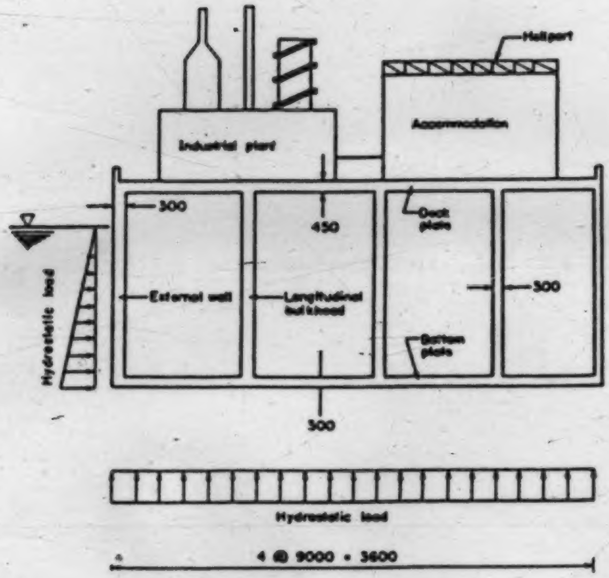
Heliport
Industrial plant
Accommodation
300
450
Deck plate
Hydrostatic load
External wall
Longitudinal bulkhead
300
Bottom plate
300
Hydrostatic load
4 @ 9000 = 3600

CROSS-SECTION OF FLOATING PLANT

Figure 1.1 Typical Concrete Floating Structure

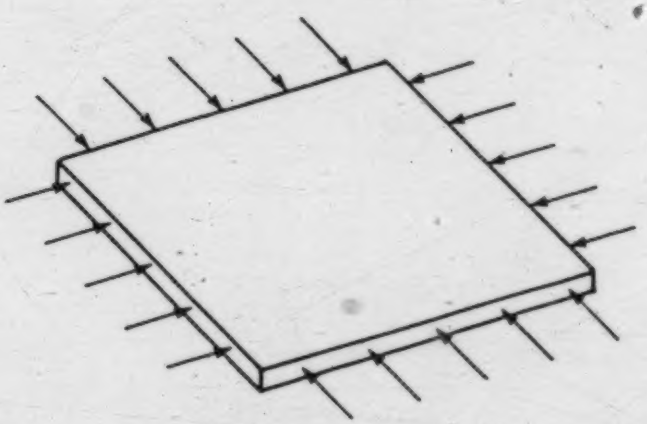

(a) UNIFORM IN-PLANE COMPRESSION DUE TO HYDROSTATIC LOADS AND LONGITUDINAL HULL BENDING UNDER HOGGING WAVE CONDITIONS.

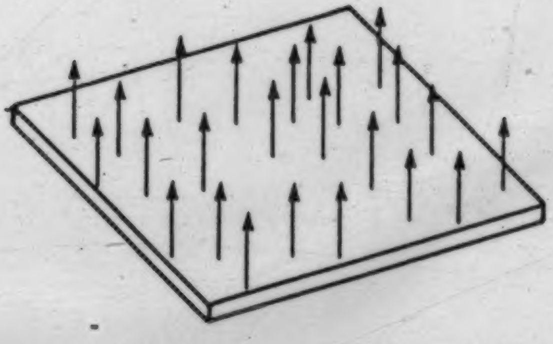

(b) UNIFORM LATERAL PRESSURE DUE TO HYDROSTATIC LOADS.

Figure 1.2 Loads Acting on The Bottom Plate of The Hull

2. LITERATURE REVIEW

2.1 General

This chapter reviews the existing literature on the behavior of concrete and steel plates under combined compressive in-plane and lateral loads. The first section contains a summary of previous experimental programs followed by a review of analytical studies.

2.2 Related Previous Tests

There is a scarcity of experimental information in this field. To the author's knowledge, most tests on plates under combined in-plane and lateral loads have been conducted by the ship building industry where the emphasis has been on steel plates and some by the aerospace industry where the emphasis has been on aluminium alloy plates. No tests are available in the literature for concrete plates under similar loads.

2.2.1 Tests of Metal Plates

McPherson *et al.*(1946) carried out tests under combined in-plane and lateral loads of 29 aluminium alloy sheet-stringer panels which had lengths of 305 and 483 mm, widths of 425 and 629 mm, and sheet thicknesses of 0.640 and 1.3 mm. These were reinforced by extruded Z stringers spaced 102 mm between centers. The in-plane load was applied through end blocks at the loaded edges and the lateral load was applied by means of an air cell made of rubberized balloon cloth. The loads for a particular panel were increased proportionally in small steps until the lateral load reached a predetermined value. It was then held constant while the panel was tested to failure with further increases in the axial load. For the 305 by 629 mm plates the test results showed that the presence of lateral load caused an increase in the elastic buckling load because it was not possible for the plate to buckle alternately above and below the plane of the plate. The lateral load also caused a reduction in the ultimate axial load of the sheet between stringers. Emperical equations were derived for the critical buckling strain and the ultimate load. To study the effect of loading history, for one of the panels, the load was increased from a low load to the test load by two sequences. For the first sequence, the axial load was applied first and then held constant while the lateral load was applied to a test value such that the panels were within the elastic range. In the second sequence, the order was reversed. The loading history had a negligible effect on the elastic buckling load.

Young (1957) carried out a series of tests of full scale, flat, clamped steel plates subjected to various combinations of lateral and compressive in-plane loads. Lateral loads were applied through a pressurized rubber bag on top of the plate. The bag was held down to the plate specimen by means of a steel pressure box attached by a system of rolled steel joists and tie rods to the very stiff support box on which the plate rested. The plate specimens were provided with a line support achieved by placing a set of roller-bearings between the support box and the plate. The compressive in-plane loads were applied by a series of hydraulic jacks attached to the specimen through fork-ended adaptors. The reactions of the jacks were taken by a rectangular frame made up of heavy rolled steel joists bolted together. To achieve uniform compressive in-plane load on the specimens, the plate overlapped the roller-bearing supports by about 305 mm all around. Furthermore the overhanging edges of the plate provided a means of applying fixed end moments to the boundary of the specimen in order to achieve rotational fixity at the roller-bearings. The fixed end moments were applied by screwing studs acting through sockets welded to the edges of the plate. Using the plate overhang as a lever with the roller-bearing supports as fulcra, a condition of zero slope could be attained at the boundary of the test specimen. Maximum compressive loads of 630 KN/m length and lateral loads of 172 KPa could be applied to the plates.

A total of four specimens, two square and two rectangular(aspect ratio 1:3) were tested. The width of the specimens were 610 mm while the width-to-thickness ratios varied from 62 to 99. Strains were measured using electrical resistance strain gages on both sides of each plate along the centerlines of the panel since the maximum stress occurs along these lines. Deflections were also measured on the plate in the transverse directions by means of dial gages. The test procedure consisted of the application of the particular in-plane loading required which was kept constant while the lateral load was applied. During the application of the load, the studs and bolts at the plate edges were also adjusted to maintain zero slope at the test panel boundary thus ensuring fixed end support. All four specimens were tested only within the elastic range and in-plane loads were applied first along a pair of opposite edges and along the four edges in a second test. The lateral loads were applied in increments of 34.5 KPa for the first three specimens with maximum pressures of 172, 103 and 138 KPa respectively. The fourth specimen (rectangular) had a maximum lateral pressure of 48.3 KPa and was loaded in increments of 6.9 or 13.8 KPa. The maximum in-plane load applied in the tests was 0.465 of the elastic buckling load of the plate.

A linear relationship between stress and lateral load and between deflection and lateral load were obtained for each plate. The results also showed that the application of in-plane load to the plate already subjected to lateral load magnifies the stresses and deflections of the plate, while retaining the general form of the distribution of the stresses and the deflections over the plate.

Two series of tests were conducted on rectangular steel plates (aspect ratio 3) in Japan (Yoshiki *et al.*, 1965 &

Yamamoto *et al.*,1970) with the lateral load applied first and then kept constant while the in-plane load was applied to the specimen until failure. The test was conducted in an apparatus with a water tank for applying the lateral load. The width-to-thickness ratios for the total of 48 specimens tested varied from 40.5 to 85. The test results indicate that the lateral pressure effects are maximum when the natural buckling mode of the in-plane loaded panel has predominant components in the one-half wave mode. Within the elastic range, it was found that the critical value of the in-plane load increased with lateral pressure when the mode shape involved more than one-half wave mode.

Sharman and Humpherson (1967) tested simply supported thin aluminium plates subjected to a trapezoidal lateral load and uniform uniaxial compression. The lateral loading was applied by a system of rods bearing on the plate surface connected to a pulley system designed to give a trapezoidal load distribution. Eight rows of rods were distributed along the length of the plate and four across the width. The simply supported edge condition was represented by rollers in the form of short pieces of slotted aluminium rod bonded around the plate edges at intervals, free to rotate and slide in grooves machined in the edge support member. The edge compression was applied through a rigid member (with appropriate edge conditions) sliding in the edge longitudinal members. The load was measured by an inductive load cell acting through a lever system.

Brown and Harvey (1969) tested rectangular aluminium alloy plates with an aspect ratio of 2 to determine the large deflection behavior under combined in-plane and lateral loads. The lateral load was applied by an airbag situated below the plate specimens and the inplane load applied through two calibrated tie bars loaded by means of internally threaded wormwheels. The edges of the specimens were all simply supported. Their test results indicate an increase in bending stresses with increase in the applied in-plane loads. Furthermore the tests showed that at large deflections, when membrane effects are predominant, the position of maximum bending stress shifts away from the plate center to somewhere between the plate edge and the plate center.

More recently, tests were conducted on isotropic mild steel plates (Aalami *et al.*,1972) using a box type model, the walls of which represented prototype plate panels under combined loading. Two rectangular steel sheets were bent and welded together to form the four sides of the box model. The ends of the box were covered by two stiff end pieces. Each wall of the box then represented a plate panel which can be tested under combined loading. The in-plane load was applied through a hydraulic ram to the end pieces of the box model. Lateral pressure was applied by oil under pressure inside the box and the lateral pressure and inplane load were increased simultaneously keeping the ratio constant through the test.

A total of 84 plate panels with width-to-thickness ratio of 50 were tested. All panels were square with side lengths of 100mm. The plates had a clearly defined yield point of 250 MPa and an ultimate tensile strength of 323 MPa. The panels were tested under six predetermined ratios of lateral-to-inplane loading (R=Q/N). For R less than 25, the plates collapsed suddenly due to plastic instability while for other load combinations, the plates exhibited excessive plastic deformation with increasing load.

2.2.2 Tests of Reinforced Concrete Plates

Reinforced concrete plates have been tested under concentric and eccentric in-plane loads with the plates either simply supported along all four edges or only along the two loaded edges.

Ernst (1952) carried out uni-directional edge compression tests on ten reinforced concrete panels having all four edges simply supported. Five of the panels were square while the others were rectangular with an aspect ratio of 2. Width-to-thickness ratios varied from 27 to 80. The specimens were centrally reinforced with 25.4 mm by 25.4 mm 15-gage welded wire mesh. Eccentricity-to-thickness ratios varied from 0.01 to 0.23 with the plate loaded to produce single curvature in the vertical and horizontal directions. The specimens were all loaded to failure and deflections, strains and angular rotations of edge tangents were taken at each load level. Failures ranged from crushing to stability failures followed by crushing.

Oberlander and Everard (1977) tested 54 reinforced concrete walls, 76.2 mm thick and 610 mm wide under in-plane loads supported along the loaded edges only. Because the walls were unsupported on two edges they behaved as essentially wide columns. The walls were tested to destruction and width-to-thickness ratios varied from 8 to 28. Vertical splitting was the failure pattern observed for width-to-thickness ratios less than 20 while for other ratios buckling failures were observed.

Swartz *et al.*(1974a) tested twenty-four walls with an aspect ratio of 2.0 and simply supported along all edges. The plates had dimensions of 2438 mm by 1219 mm and had no in-plane restraints along the edges. The reinforcement in the walls was in one or two layers in both directions and width-to-thickness ratios varied from 38 to 64. Total reinforcement ratios varied from 0.2 to 1 % in each direction and the in-plane load was applied concentrically. Some of the plates buckled in a single curvature mode while others buckled in a double curvature mode, depending on the width-to-thickness ratio, the aspect ratio and the extent of cracking in the plate. The buckling loads in the tests were determined using the measured deflection profiles, the application of Southwell's method, and the use of strains in the buckled portion of the plate. The ultimate loads were 1 to 24 percent higher than the buckling loads. It was also observed that the panels generally failed in a collapse mechanism approaching that for simply supported plates subjected to uniform lateral loads. That is, a panel failure mechanism was formed in one-half of the plate.

Recently 16 tests were carried out in Germany (Kordina *et al.* 1973,1979,1982) on square reinforced concrete walls under uni-axially eccentrically applied in-plane loads. Six walls were tested in the first test series, five each in the last two series. The wall width-to-thickness ratios varied from 20 to 35 while the eccentricity-to-thickness ratio of the in-plane load varied from 0.1 to 1.0. The walls were simply supported along the four edges without in-plane restraints. The walls were tested in a vertical position similar to the tests by Ernst (1952) and by Swartz *et al.* (1974a).

Six eccentrically applied concentrated loads simulated uniform vertical compression along the upper and lower horizontal edges of the wall. Specimens were loaded to failure in about fifteen load increments and strains were measured on both surfaces of the wall in the vertical, horizontal and diagonal directions. Displacements were measured at several points on the wall and crack distribution was noted at each load level. In the second series of tests (Kordina *et al.*,1979), columns of 0.5 meter width and 3 meter height were also tested to determine experimentally the influence on in-plane load carrying capacity of the horizontal or transverse bending of a plate. The columns were all loaded to failure and the following conclusions were drawn from the second series of tests:

1. Failure loads of the walls were approximately twice the column capacity expressed in terms of the uniaxial load bearing capacity of the plain cross-section.
2. A considerable increase in load carrying capacity is possible even after the first cracks have appeared.
3. The influence of wall slenderness on the load carrying capacity of the wall in the transverse direction was negligible.
4. A small amount of symmetrically placed reinforcement will cause a distinct finer crack distribution compared to unreinforced walls.
5. Failure occurred suddenly along a failure line similar to that of a simply supported plate under lateral loads.

Amrhein *et al.* (1985) carried out tests on twelve slender concrete walls under combined in-plane and lateral loads. The walls were 1.22 metres wide and 7.52 metres high. Height-to-thickness ratios varied between 30 and 60. The walls were supported along the horizontal edges only and therefore behaved as wide colums. There was no evidence of buckling in any of the walls tested because the maximum applied in-plane load was less than ten percent of the short column axial capacity.

2.3 Related Previous Analyses

Several analytical solutions are available for elastic plates or steel plates under combined compressive in-plane and lateral loads. Most of these are limited to isotropic plates. There is paucity of analytical solutions for reinforced concrete plates under similar loads.

2.3.1 Analyses of Elastic Plates

Levy (1944) investigated long rectangular elastic isotropic plates with an aspect ratio of 4 under combined axial ~~and~~ lateral loads using the von Karman large deflection equations and a Fourier series expression for the deflection function. The lateral loads were assumed to be applied first. The resulting nonlinear simultaneous equations were solved for the deflection in terms of the axial load and lateral pressure. The plate buckling load was found to be increased considerably by normal pressure. This is to be expected for an homogeneous elastic plate with the aspect ratio investigated because for low axial stresses the deflected shape of the plate is a single long bulge while the buckling mode consists of a series of square buckles alternately deflecting up and down. As the compressive stress was increased the deflected shape gradually approached the regular buckle pattern at increasing values of compressive stress. The initial general downward deflection of the plate due to lateral pressure tends to disappear at high axial loads.

Wang (1948) used the method of finite differences to solve the large deflection problem of isotropic plates with various boundary conditions under either lateral pressure or combined in-plane and lateral loading. Full elastic behavior was assumed in the analysis and the resulting nonlinear difference equations were solved using a modified form of the successive relaxation method.

Johns (1967) presented an analytical method by which the static instability of orthotropic panels subjected to uniform in-plane loads and lateral aerodynamic pressures may be obtained. The method, which assumes small deflection theory and linear elasticity, is based on the Galerkin method. A deflection function in the form of a double sine series was used.

Sharman and Humpherson (1967) presented a theoretical investigation of simply supported thin aluminium plates subjected to a trapezoidal lateral load and uniform uniaxial compression. The Galerkin integral technique is used in conjunction with an assumed two-mode deflection function which allows for the asymmetry of lateral load. The plate was assumed to be elastic and isotropic and the von Karman large deflection equations were used. The two resulting nonlinear simultaneous equations were solved graphically giving the ultimate axial load for a constant lateral load. It was noted that including more terms in the deflection function would increase theoretical deflections, since limiting the modal shape applies force constraints to the system.

Brown and Harvey(1969) analysed isotropic steel plates under combined loads using the finite difference method and considering large deflections. The analysis was carried out by writing the von Karman plate equations in finite difference form. This gave two sets of non-linear equations which were solved using an iterative approach. Because the convergence rate of this iterative process was very poor, a special form of interpolated iterative process was used. The analytical results were found to agree well with their test results. The analysis also indicates a shift of the position of maximum bending stress away from the plate center at large deflections, typically for deflections larger than the plate thickness. All the analysis was within the elastic range.

2.3.2 Analyses of Steel Plates

Lee (1961) carried out a theoretical study of the ultimate strength of simply supported rectangular isotropic steel plates under in-plane and lateral loading . A simple double cosine wave deflection function in the out-of-plane direction was first assumed and substituted into the first differential equation of von Karman's large deflection theory to determine the displacement functions in the two orthogonal in-plane directions. Assuming that these three displacement functions are approximately correct and thus applicable in the elastic-plastic range, the out-of-plane deflection at the center of the plate becomes the only parameter defining the displacement of a point in both the elastic and elastic-plastic ranges. By application of the principle of minimum potential energy and using a numerical integration procedure over five points through the plate thickness in the elastic-plastic range, the relationship between the deflection at the center of the plate and the loading was established. The loads considered include in-plane compression and lateral pressure. An ultimate strength analysis of a square plate with a slenderness ratio of 60 was carried out and the presence of lateral pressure was found to cause a reduction in the in-plane load capacity of the plate.

Aalami and Chapman (1969) carried out an elastic large deflection analysis of rectangular orthotropic plates under lateral and in-plane loads using a finite difference approach similar to the method used by Brown and Harvey(1969). Several flexural, extensional and tangential boundary conditions were investigated and the following conclusions were reached:

1. For simply supported plates the addition of in-plane loading shifts the position of maximum moment from the center to points between the center and edge of the plate at large deflections.
2. At large deflections the magnitude of the central moment in the direction transverse to the applied in-plane load is consistently higher than the corresponding central

moment in the direction of applied loading, but the maximum moment in the plate occurs in the latter direction near the loaded edges.

3. For simply supported plates under uniform uniaxial in-plane compression and uniform lateral load, the linearized solution proposed by Bleich(1952) gives a good estimate of initial stiffness. In the large deflection range linearized solutions are not adequate.

Mansour and Nagler(1970) carried out elastic, small deflection analysis on stiffened plates under combined loads using the equivalent orthotropic plate theory advanced by Huber. A single Fourier series solution was assumed for the deflection and lateral load. Several design curves were developed giving non-dimensional deflections and moments for a combination of non-dimensional in-plane and lateral loads and various edge conditions.

Mansour(1971) also carried out an elastic large deflection analysis of orthotropic plates under combined loads by extending the series solution developed by Levy (1942) for isotropic plates. The in-plane load was allowed to be several times the plate elastic buckling load and the governing large deflection equations were solved by an iterative process.

Supple (1979) presented an analysis of rectangular plates subjected to uni-axial in-plane compression together with a uniform lateral pressure over the surface of the plate. The analysis, which assumes the lateral load to be applied first, concentrates on the elastic post-buckling behavior and shows that lateral pressures produce similar effects as initial geometric imperfections with long wavelength. The Ritz (Galerkin) method was used to solve the von Karman large deflection equations using a two mode approximation. It was shown that sufficiently high lateral pressures induce stable post-buckling behavior in the long wavelength mode, though reversion to the short wavelength mode was possible.

Little (1987) presents an efficient method for the elastic large deflection analysis of rectangular orthotropic plates. The analysis initially proceeds along similar lines to that of Levy *et al.* (1944), with both the lateral deflection and the force function being represented as Fourier series. Each equilibrium shape, however, was determined by direct minimization of the total potential energy using a quasi-Newton minimization algorithm. The method was shown to reproduce previous results for isotropic and orthotropic plates and was more efficient than previous methods, ten plates being analyzed in less than one second of CPU time.

Limit analysis have also been applied to the analysis of isotropic steel plates under combined uniaxial compressive in-plane and lateral loads (Neale and Lind,1970; Fujita *et al.*,1979). The steel plates were assumed to be elastic-plastic. The analysis proceeds by postulating a collapse mechanism for the plate and determining the unloading load deflection curve for the rigid-plastic structure as a function of the in-plane and lateral loads and deflection. An elastic loading curve is derived for these combined loads. The failure in-plane load or failure lateral load is obtained from the intersection of these two curves. The analysis neglects any membrane effects but the effects of changes in geometry are taken into account in the derivation of the plastic unloading curve. Fujita *et al.*(1979) used this method to determine the in-plane load capacity of square and rectangular plates for a given lateral load considering large deflections. The following conclusions were reached:

1. Lateral load reduces the compressive strength of plates.
2. For rectangular plates with aspect ratios of 2.0 or 3.0 and a small lateral load, the collapse mode of the plate corresponds to the buckling pattern. On the other hand, in case of large lateral loads, the collapse mode approaches the pattern characteristic of lateral loads.
3. When a plate failure corresponds to a buckling mode pattern, the reduction of compressive strength due to lateral load is rather small. However in the case of collapse in the pattern which is induced by lateral load, the reduction in load capacity is larger because of the effect of the bending stress generated by the lateral load.

Herzog (1987) has presented design interaction equations for unstiffened and stiffened steel plates under combined in-plane and lateral loads. These equations were derived based on test results by Aalami *et al.* (1972) and using a yield line analytical approach.

Harding *et al.*(1977) used a finite difference formulation for the large deflection elasto-plastic analysis of initially imperfect thin rectangular steel plates under in-plane loads only. The elasto-plastic rigidities are calculated using a rigorous multilayer approach and the governing equations are solved in an incremental form using dynamic relaxation.

Dier and Dowling(1980) used a similar method for the analysis of steel plates under combined lateral pressure and bi-axial compression. In the analysis, the lateral pressure was assumed to be applied first followed by in-plane load to failure. They concluded from their study that flexural or membrane boundary conditions can increase this capacity considerably. Webb and Dowling (1980) used a similar approach to carry out a large deflection elasto-plastic analysis of stiffened plates under lateral and in-plane loads. They observed that the initial application of lateral load results in a significant reduction in compressive capacity and that the mode of deformation resulting from uniaxial load alone can be considerably modified by the addition of lateral forces.

Parsanajad (1986) presented a method for the nonlinear analysis of orthogonally stiffened plates under combined uniform lateral and uniform compressive axial loads. The lateral load was assumed constant as the axial load was applied until failure. The mathematical model treats the plate as a longitudinally stiffened panel continuous over a series of transverse stiffeners. Each transverse stiffener together with an assumed effective portion of the plate is assumed to provide only knife edge support for the longitudinal panel. Thus the orthogonally stiffened plate is divided into two separate systems subjected to the same redundant forces. The longitudinal system is treated as a series of beam columns. For a given value of axial load, values of the reactions provided by the transverse members are assumed. The large deflection inelastic beam column problem is solved using moment-load-curvature relationships and numerical integration along the length to determine the deflections, end slopes and the resultant forces at the ends of the beam column in terms of the redundant reactions provided by the transverse members. The transverse beams are subjected to forces equal and opposite to these redundant reactions and are analyzed using first order elasto-plastic beam theory. The analysis is repeated at the same load level with various assumed values of the redundant reactions until compatibility requirements at the junctions of the longitudinal and transverse beams are satisfied. The procedure is then repeated with an increased value of axial load. Comparison of results using this method with results of tests on seven grillages under combined loads was found to be satisfactory.

2.3.3 Analyses of Reinforced Concrete Plates

Several analytical approaches are available for concrete plates under uniaxial compression only and for concrete tilt-up walls under combined in-plane and lateral loads.

Wiegand(1970) presented an analysis for the buckling loads of concrete plates under concentric or eccentric in-plane loads using an energy method and taking into account material nonlinearities. Several design curves were presented for various slenderness ratios, eccentricity-to-thickness ratios and reinforcement ratios.

Swartz *et al.*(1974b) presented a method for calculating the buckling load of simply supported reinforced concrete plates using the isotropic tangent modulus approach based on the following assumptions:

1. Small deflection theory prevails and initial imperfections are neglected.
2. The concrete is assumed to be uncracked at the onset of buckling and only initial, short term buckling is considered.
3. The reinforcing steel is assumed not to have yielded at the onset of buckling and there is no interaction between longitudinal and transverse steel.

Design equations were proposed. The analytically predicted buckling loads showed good agreement with results from buckling tests on rectangular plates by Swartz *et al.*(1974a).

Lertbannaphong (1979) presented combined finite element/finite difference analyses for tilt-up concrete wall panels subjected to in-plane loads, edge couples caused by eccentricity of axial loads and uniformly distributed wind loads. The analysis which is based on an elastic plate model and small deflection theory, assumes that in-plane deformation due to lateral displacement is negligible. This assumption allows the analysis to be separated into two parts: the plane stress part which resists uniform in-plane loads is analysed using a finite element method to obtain the in-plane stress resultants; and the bending part, which includes the influence of the in-plane stress resultants from the first analysis and resists uniform lateral loads as well as uniformly distributed couples is analysed using a finite difference method to obtain moments, flexural stresses and flexural strains in the plate. In both the finite element and finite difference analyses, the same mesh was used. Several tilt-up walls supported along the loaded edges only were analysed and the ultimate load was assumed as the least of the following two capacities: the in-plane load causing a vertical compressive strain of 0.003 at any point in the plate, and the axial load that a section of the wall can carry as evaluated by the ultimate design method for columns. Design aids in form of tables and charts were presented.

DNV (1977) and Furnes(1981) presented simplified calculation methods for computing the buckling loads of reinforced and prestressed concrete members using the tangent modulus and the adjusted equilibrium methods. The tangent modulus method accounts approximately for material nonlinearities in combination with classical linear elastic buckling analysis. The method is useful for the approximate assessment of the buckling load of structures where the axial forces are predominant and also for obtaining non-linear magnification factors in order to evaluate the second order bending effects. This method was used to analyse three of the plates tested by Swartz *et al.* (1974). The critical buckling stress obtained from the analysis compared well with the test results. In general, the tangent modulus method tends to overestimate the critical buckling stress.

In the adjusted equilibrium method the direct superposition of the first and second order effects is carried out to obtain the total maximum loading effect. If, for certain strains and curvatures, a configuration can be found such that the design resistance is greater than or equal to the maximum loading effect, then the design is deemed adequate. To enable the use of moment-curvature tables, the maximum loading effect is expressed in terms of curvature. For a given axial load level, by assuming different states of deformation, the relationships between the loading effect and the design resistance versus curvature can be plotted. This method was used for the design of a simply supported cylinder subjected to external hydrostatic pressure.

Kristjannsson (1978) and Cervera et al.(1984) carried out material and geometric nonlinear analysis of concrete plates using the finite element method. Their analytically predicted buckling loads agree well with tests by Swartz *et al.*(1974a). Cervera *et al.* (1984) also highlighted in their results the effect of tension stiffening on the intermediate range just after cracking and before final collapse. The conclusion was that a stiffer and more realistic displacement representation is obtained when the tension stiffening effect is taken into account, though this tension stiffening did not influence the ultimate load significantly.

The only analytical method for concrete plates under combined lateral and in-plane loads known to the author is by Aas-Jakobsen (1983). In this analysis the plate is assumed to be simply supported and subjected to uniform in-plane compression and a sinusoidal lateral pressure. The analysis assumes the in-plane load to be applied first and then held constant while lateral pressure is applied until failure. The problem is then to determine the maximum lateral load the plate can carry considering material and geometric nonlinearities. The interaction of in-plane loads and geometric nonlinearities is taken into account by assuming the combined effect equal to an equivalent sinusoidal lateral load. A sinusoidal deflected shape is assumed which reduces the plate problem to a single degree-of-freedom problem similar to the approach used by Toma and Chen(1983a,1983b) for the analysis of tubular steel beam-columns and by Broms and Viest (1961) for the analysis of reinforced concrete columns. The plate equilibrium equation is then solved for the bending and twisting moments assuming constant orthotropic properties. Equilibrium between internal and external moments in the in-plane load direction is then required at the plate center resulting in an equation from which the lateral load-deflection curve can be obtained. The peak of this curve is taken as the ultimate lateral load.

Aas-Jakobsen (1983) also presented a design method for concrete plates under combined in-plane and lateral loads. It is based on representing the interaction of the in-plane load and deflection as an equivalent sinusoidal lateral load. This equivalent load, which is equal to the product of the in-plane load and the curvature at balanced failure, is added to the lateral load to give the design value. The design moments in the x and y directions are obtained using an elastic plate analysis and assuming equal stiffnesses in the x and y directions.

2.4 Summary and Conclusions

From the literature review, the unavailability of experimental results for concrete plates supported on four edges and subjected to combined compressive in-plane and lateral loads is evident, hence the need for an experimental program to provide data against which analytical methods can be verified.

As far as analytical work goes, most of the work has so far been carried out on steel plates. Except for the work by Aas Jakobsen (1983), most previous analyses of concrete plates have been on plates under uniaxial load only or lateral only.

In the analytical methods reviewed so far, four different approaches have been followed:

1. Fourier series method
2. Finite difference and finite element methods
3. Limit analysis (Yield line)
4. Assumed deflection method
5. Ritz energy method.

In approaches 1 and 2, linear elastic and/or elasto-plastic material properties have been used while a rigid-plastic material is assumed in approach 3. In approach 4, nonlinear concrete material properties were used. Applying any of the numerical based methods to concrete plates under combined loads would generally be too complex and too costly for design purposes because of the iterative nature of these solutions and the large numbers of equations to be solved. The application of classical limit analysis (whether lower or upper bound methods) to concrete plates under combined in-plane and lateral loads, unless modified in some way, would appear to be limited to situations where tension steel yields. This will be the case only for small in-plane loads since if in-plane loads are high, the tension steel will not yield at failure, and limit analysis will not be valid.

The analytical and design methods proposed by Aas-Jakobsen (1983) for reinforced concrete plates under combined loads is truly valid only for sinusoidal lateral loads and has not been verified by tests.

In conclusion therefore, the need is felt for analytical and design methods for reinforced concrete plates under combined in-plane and uniform lateral loads. The research efforts in this thesis will be directed at developing a method of analysis and a simple design procedure which will be verified by comparison to results of tests of eight simply supported reinforced concrete plates under uniaxial uniform compressive in-plane and uniform lateral loads.

3. EXPERIMENTAL PROGRAM

3.1 Introduction

The experimental program consisted of tests of nine simply supported reinforced concrete plates. Seven of the specimens had an aspect ratio of 1.0 (square), while two had an aspect ratio of 1.50. Various width-to-thickness ratios and reinforcement ratios were considered. A total of eight plates were tested under combined in-plane and lateral loads. One plate was tested under lateral load only, to give an indication of the reduction in lateral load capacity for the plates loaded within the same series. The maximum applied in-plane load was 44.2 % of the uniaxial in-plane load capacity of the plate cross section.

For this experimental program, it was decided not to simulate actual edge conditions for plates in concrete barges as shown in Fig. 1.2. Instead, well defined boundary conditions were provided in order to facilitate the verification of the analytical model.

3.2 Test Specimens

The test program was divided into four series: Series A consisted of three square specimens with side dimensions of 1830 mm. Two of these specimens were tested under combined loads while one was tested under lateral load only. Series B consisted of two rectangular specimens 1830 mm by 2745 mm tested under combined loads with the in-plane loads applied along the shorter edge. Series C consisted of two square specimens with same side dimensions as series A but with different reinforcement ratios. Both specimens were tested under combined loads. Series D consisted of two square specimens having the same side dimensions as series A but with a different width-to-thickness ratio. Both specimens were also tested under combined loads.

The actual plates tested overlapped the side dimensions given above by 152.4 mm all round. This was for supporting the plates and in order to achieve near uniform compressive in-plane load starting at the support line. At the completion of the tests, plate thicknesses were measured at several points on the plate. The average measured thicknesses of all the specimens is shown in Table 3.1. The specimens had two layers of reinforcement in both orthogonal directions with the top and bottom steel cages held in place (to ensure little movement during casting) by using improvised aluminium spacers. The reinforcement positions at the top and bottom of the specimen were measured after the test by chipping out concrete at several points on the plate. The average locations of the top and bottom steel in both orthogonal directions measured from the compressive face of the plate are shown in Table 3.2. The x direction is perpendicular to the direction of the in-plane loads. Typical cross-sections of the specimens showing arrangement of the reinforcement is shown in Fig. 3.1. The top and bottom layers were equally reinforced. The areas of reinforcement for the specimens in both orthogonal directions are shown in Table 3.3. Plate 3.1 shows a reinforcement cage for a square specimen before concrete casting.

All specimens were cast flat on a plywood bed. The sides of the form were 51 mm by 102 mm wood cut to the required thickness of the specimen. Holes, 44.5 mm in diameter were provided for application of lateral loads. These were formed by installing lengths of 38 mm inside diameter thin-walled steel conduits in the formwork. These conduits were covered with steel washers which prevented the holes from been filled with concrete during casting. Screws placed through the washers held the assembly down to the plywood bed. This ensured that the hole positions were not altered during the casting of concrete. The distance between consecutive hole positions was 610 mm which was chosen to line up with the hole positions on the laboratory strong floor. The square plates had nine holes while the rectangular specimens had twelve. Concrete was cast in two stages with six specimens cast in the first stage and three in the second stage. After casting, finish screeding was accomplished with several passes of a long aluminium channel section screed. Some hours after screeding the surface of the specimens was worked with a steel trowel. Polyethylene plastic cover sheets were applied to all exposed surfaces approximately five hours after casting was completed.

Lift hooks were provided at four points on the surface of the specimens at such points as to prevent cracking due to lifting of specimens into storage or from storage into the test frame. Before lifting the specimens, split tensile tests were carried out to determine the concrete tensile strength at that stage. When it was found that the stresses during lifting due to the weight of the specimen would be less than the concrete tensile strength, the specimens were lifted into storage. The specimens were stored by stacking on top of each other with bricks separating one specimen from the other.

In the first concrete cast, the strain gage wire locations were marked and the wires were then pulled out after the concrete was poured after which the surface was screeded. This was done with great difficulty and resulted in the loss of some gage wires. To avoid this problem in the second cast, the gage wires were tied to strings and then stapled to the sides of the formwork. When concrete had been poured these strings were cut with a pair of scissors and the strain gage wires were lifted to a vertical position after which the concrete surface was re-screeded with a trowel.

3.3 Material Properties

3.3.1 Reinforcing Steel

The reinforcement for the specimens were 6.35 mm diameter deformed bars obtained from Sweden. The bars were tested in the MTS 1000 KN universal testing machine in accordance with Canadian standard G30.12 M1977. A "snap-on" type extensometer was used to measure strains. A typical stress-strain curve for the reinforcement which had a nominal area of 31.6 mm^2 is shown in Fig. 3.2. The reinforcement has an ultimate strength of 670.3 MPa with no defined yield point.

3.3.2 Concrete

Concrete pouring was done in two phases. Specimens A3, A2, A1, C1, C2, and D1 were cast in the first phase while specimens D2, B1 and B2 were cast in the second phase. A major criterion for the concrete used in casting the plate specimens was the ease of placing the concrete in the form because of the relatively small thicknesses of the specimens. The concrete used was ordered from a ready mix supplier and had a specified 28 day strength of 25 MPa. The maximum aggregate size was 14 mm. Some water had to be added to the ready mixed concrete to increase its workability. The concrete was shoveled into the form and vibrated with an electric vibrator in an attempt to remove any trapped air. Excess concrete was screeded off and the surface was worked with a steel trowel. Twenty five cylinders 150 mm x 300 mm were cast in each phase of concrete pouring. The concrete cylinder strength (f'_c), the static modulus of elasticity in compression (E_c) and the splitting tensile strength (f'_t) were recorded at intervals during the testing program. The values for cylinder strength and the modulus of elasticity in compression were obtained in accordance with CAN3 A23.2-9C (CSA, 1977). Splitting tensile strengths were obtained from split cylinder tests carried out in accordance with CAN3 A23.2-13C (CSA, 1977). The data were fitted with regression lines of the form $f'_c(t)=a+bt$ by the method of least squares and these are shown in Figs. 3.3 and 3.4. Table 3.4 gives the age at which each specimen was tested while Table 3.5 gives the modulus of elasticity, and the compressive and tensile strength for each specimen at the day of testing. These were obtained from the regression lines in Figs. 3.3 and 3.4 and similar figures figures for modulus of rupture and tensile strength.

3.4 Test Set-Up

A schematic drawing of the testing frame is shown in Fig. 3.5. The frame was designed to accomodate a maximum compressive in-plane load of 1000 KN/m and a uniform lateral load (pressure) of 115 KPa. The specimens were tested in a horizontal position. The in-plane load was applied using four 500 KN capacity hydraulic jacks that reacted against back-to-back channels which were held in position by W150 x 22 beam passing on top of the specimen and 25.4 mm diameter high strength rods passing underneath the specimens. The load was applied to the specimen by attaching the cylinders of the four 500 KN hydraulic jack to four 125 mm diameter high strength steel half rounds along one edge of the plate. The jacks and the half rounds were placed in a slotted round hollow steel section which was welded to C230 x 30 back-to-back channels. At the opposite edge of the specimen, four 125 mm diameter high strength half rounds were bolted to four C230 x 30 back-to-back channels to provide the reaction for the applied in-plane load. At each loaded edge of the plate, the half rounds, 125 mm long, reacted against 381 mm long clamps (four at each end of the plate) located 444 mm center to center as shown in Plate 3.2. Special consideration was given to the contact stresses at the half round/clamp interface resulting in the use of high strength steel for the clamps. Discrete clamps spaced along the loaded edges were used instead of one clamp along an entire edge as used by Ernst *et al.* (1952), to allow the plate to warp during the test. The in-plane loading frame was a self contained system and was designed to move vertically with the edge of the specimen as the edges rotated due to the application of lateral load. The direction of application of in-plane load was in the y direction for all specimens. A manifold system was used which supplied equal oil pressure to the four jacks and a fifth hydraulic jack of the same capacity which reacted against a 500 KN capacity load cell in a closed frame. The jack loads were measured in this way and checked by oil pressure measurements.

The uniformly distributed lateral load was simulated by the application of nine concentrated loads to the square specimen and twelve to the rectangular specimens. The concentrated loads were applied by means of 19 mm diameter threaded mild steel rods passed through 125 mm by 125 mm by 12.7 mm thick steel plates resting on 3 mm thick plaster as shown in Fig. 3.5 and Plate 3.3. The threaded rods passed through 38.1 mm diameter holes on the specimen, through the laboratory floor and through 120 KN hollow hydraulic jacks beneath the laboratory floor. A manifold system was used to supply equal oil pressure to all the jacks and to an extra jack that reacted against a 100 KN load cell in a closed frame. This enabled the pressure to each lateral load jack to be determined. An overview of the test frame is shown in Plate 3.4.

The theoretical support and load requirements for the test frame were:

1. Minimum deflection normal to the plate surface along the support center lines.
2. Free rotation (no moment) along the supports.
3. No in-plane restraints along the unloaded plate edges.
4. The in-plane load was to be as nearly uniform as possible in the area between the support lines at the loaded edges of the plate.

All the above requirements were satisfied by the test frame. The frame was set up so as to accommodate the square as well as the rectangular specimens. Simple support conditions without in-plane restraint was achieved by using the rocker-roller arrangement shown Fig. 3.6. Consideration was given to the contact stresses and coefficient of static rolling friction in the 1~~2.5 mm~~ diameter ball bearings used as rollers. The manufacturers stated that these ball bearings had a tensile strength of 2225 MPa. Each support point consisted of 25 balls guided by a 125 mm by 125 mm by 9.5 mm thick plywood template with 25, 16 mm diameter holes drilled ~~in~~ it. The maximum contact stresses (calculated from Hertzian theory) were approximately 60-percent of the tensile strength. The use of several small diameter rollers (as opposed to a few of larger diameter) gave an economical and efficient solution to the problem of limiting rolling friction effects. The coefficient of static rolling friction calculated from simple rolling theory was about 4 percent, for the maximum vertical load expected. This value seems high, but as noted by O'Flynn (1987), the Hertzian theory gives much higher values than the actual coefficient of rolling friction. The distance between each support point was chosen such that the maximum vertical deflection of the concrete plate between these points was less than about 0.5 mm. Twelve support points were used for the square specimens, except specimen A3 and the rectangular specimens where sixteen supports were used. No supports were provided under the plate at the corners except for specimen A3 since the plate corners would tend to lift up from the supports once the lateral loads were applied. To simulate a true simple support condition, the corners of the specimens were not allowed to lift up during the test. Each corner was held down by a frame consisting of a rocker-roller assembly as shown in Fig. 3.7.

3.5 Instrumentation

3.5.1 Displacement Measurement

The displacements were recorded electronically using linear variable displacement transducers (LVDTs). The vertical deflections were measured with LVDT's with a range of 152 mm, while the in-plane deflections were measured with LVDT's with a range of 50 mm. The edge rotations were measured using a special device shown in Fig. 3.8 and the LVDT's had a range of 100 mm. The location of LVDT's for the square and rectangular specimens are shown in Figs. 3.9 and 3.10, respectively. Measurements were considered reliable within the middle 80% of this range. The following displacements were recorded:

- in-plane deflections of one edge of the plate relative to the other in the x and y directions.
- vertical surface deflections of the plate.
- rotation of the plate edges along the center lines in the x and y- directions.

3.5.2 Steel Strains

All steel strains were measured using electrical resistance strain gages. The gages employed were Showa foil strain gages, type N11-FA-5-120-11, with the following characteristics: gage length: 5 mm, nominal resistance: 120 ohms, gage factor: 2.11 ± 1%, and temperature compensation for steel. These gages give meaningful results up to 1.5% strain.All gages were installed using the three wire system to minimize the effect of lead wire resistance. The strain gage layout for the specimens are given in Figs. 3.11 through 3.13. These gages were sealed from wet concrete by means of a 3 mm thick epoxy coating.

The strain gages and LVDTs were powered by a common power supply producing output in the range of ±6 volts. The load cells were powered by a 10 volt source. The analog signals from the devices were converted into digital form by a digital voltmeter controlled by an interactive Fortran program in a Data General computer in the Structures Laboratory. This allowed measurements to be monitored and read into storage during testing. At any particular load level, all output was read and recorded automatically. The interactive program allowed for monitoring the deformation and control of loading during the test. After completion of a test, the data were printed on a hard copy terminal, stored on a magnetic disk and later transferred to an Amdahl 470 computer for further processing.

Strain gages adjacent to loading holes were affected by strain concentrations in those regions. These strains were not used in the analysis of the test results.

3.6 Test Procedure

For specimen C1, the in-plane and lateral loads were applied simultaneously from zero load until the peak loads were reached. Thereafter the lateral load was allowed to drop while keeping the in-plane load constant until failure. For the other specimens except specimen A3, the in-plane load was applied incrementally up to the predetermined value and maintained at a constant value as the lateral load was applied monotonically and incrementally from zero to a maximum value and then allowed to drop off steadily beyond the maximum point. During each load increment, crack inspection, deflection and strain readings were carried out. Testing time for the specimens was between two to three hours.

Table 3.1 Average Measured Thickness of Specimens

Specimen #	Average Thickness, mm
A3	65.3
A2	64.2
A1	67.0
C1	64.7
C2	63.7
D1	55.5
D2	57.0
B1	64.5
B2	64.8

Table 3.2 Average Locations of Top and Bottom Reinforcement From Compressive Face

Specimen #	X Direction		Y Direction	
	Distance of Top Rebar From Top Face, mm	Distance of Bottom Rebar From Top Face, mm	Distance of Top Rebar From Top Face, mm	Distance of Bottom Rebar From Top Face, mm
A3	18.6	49.8	12.2	56.1
A2	18.1	47.0	11.7	53.3
A1	17.0	51.3	10.6	57.6
C1	16.7	47.4	10.3	53.7
C2	17.5	46.6	11.1	52.9
D1	18.5	39.9	12.1	46.2
D2	18.2	41.7	11.9	48.0
B1	17.1	49.3	10.7	55.6
B2	17.1	51.1	10.8	57.4

Table 3.3 Area of Reinforcement in x and y Directions

Specimen #	X Direction		Y Direction	
	Area of Top Rebar, mm^2/m	Area of Bottom Rebar, mm^2/m	Area of Top Rebar, mm^2/m	Area of Bottom Rebar, mm^2/m
A3	225.0	225.0	260.0	260.0
A2	225.0	225.0	260.0	260.0
A1	225.0	225.0	260.0	260.0
C1	157.0	157.0	329.3	329.3
C2	157.0	157.0	329.3	329.3
D1	225.0	225.0	260.0	260.0
D2	225.0	225.0	260.0	260.0
B1	324.0	324.0	381.0	381.0
B2	324.0	324.0	381.0	381.0

Table 3.4 Age at Testing for Each Specimen

Specimen #	Age at Testing, days
A3	98
A2	111
A1	113
C1	122
C2	117
D1	126
D2	112
B1	119
B2	118

Table 3.5 Modulus of Elasticity, Compressive and Tensile Strength of Specimens

Specimen #	Modulus of Elasticity MPa	Compressive Strength MPa	Tensile Strength MPa
A3	23151.0	32.24	2.80
A2	23010.0	32.25	2.80
A1	22975.0	32.25	2.80
C1	22904.0	32.26	2.80
C2	22939.0	32.25	2.80
D1	22833.0	32.26	2.80
D2	25487.0	40.00	2.96
B1	25580.0	40.27	2.97
B2	25553.0	40.23	2.97

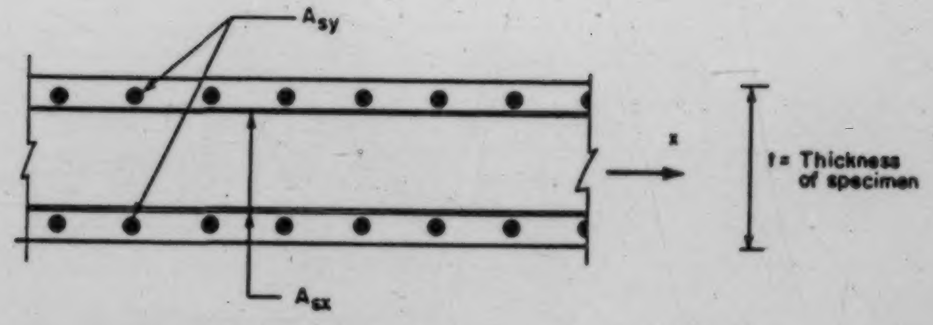
A_{sy}
x
t = Thickness of specimen
A_{sx}

NOTE : The in-plane load is applied along the y direction.

Figure 3.1 Placement of Reinforcement

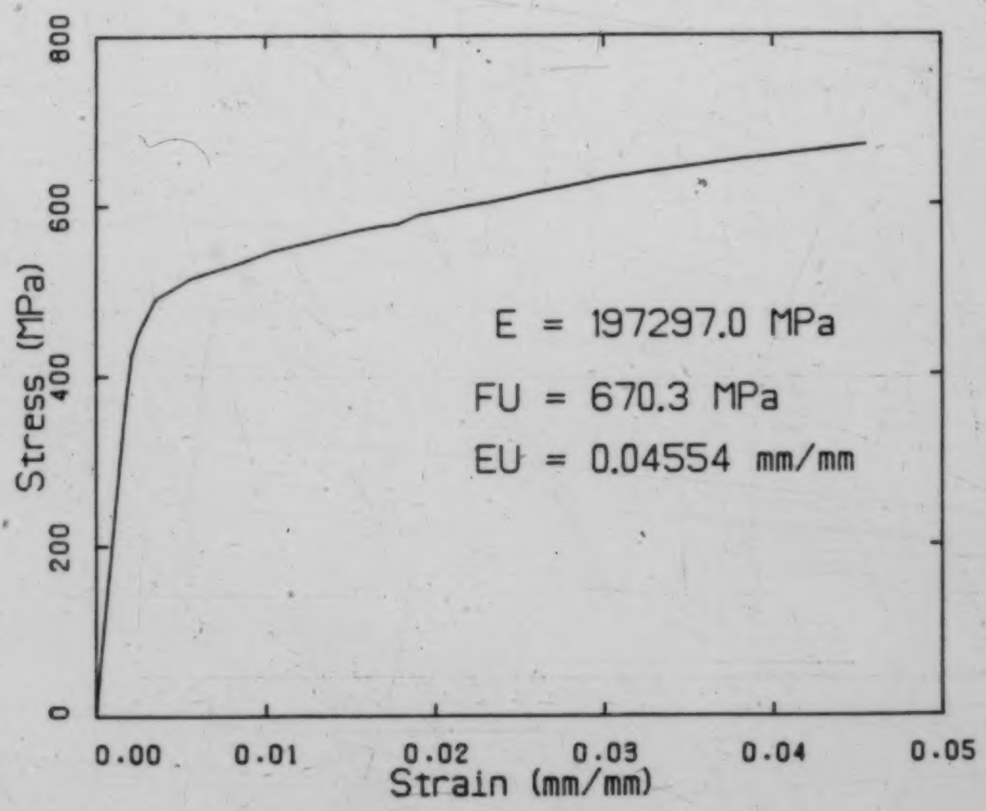

Figure 3.2 Stress Strain Curve for Reinforcement

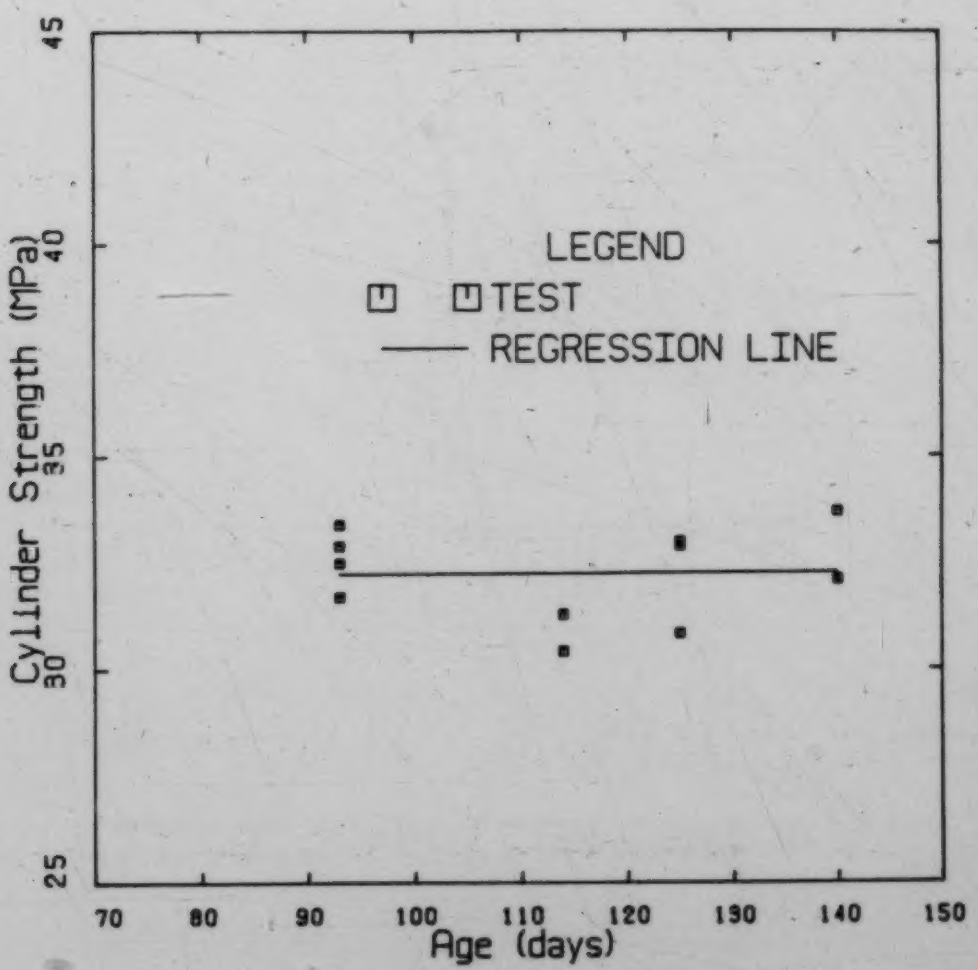

Figure 3.3 Least Squares Estimate of Cylinder Strength/Time Curve for First Concrete Cast

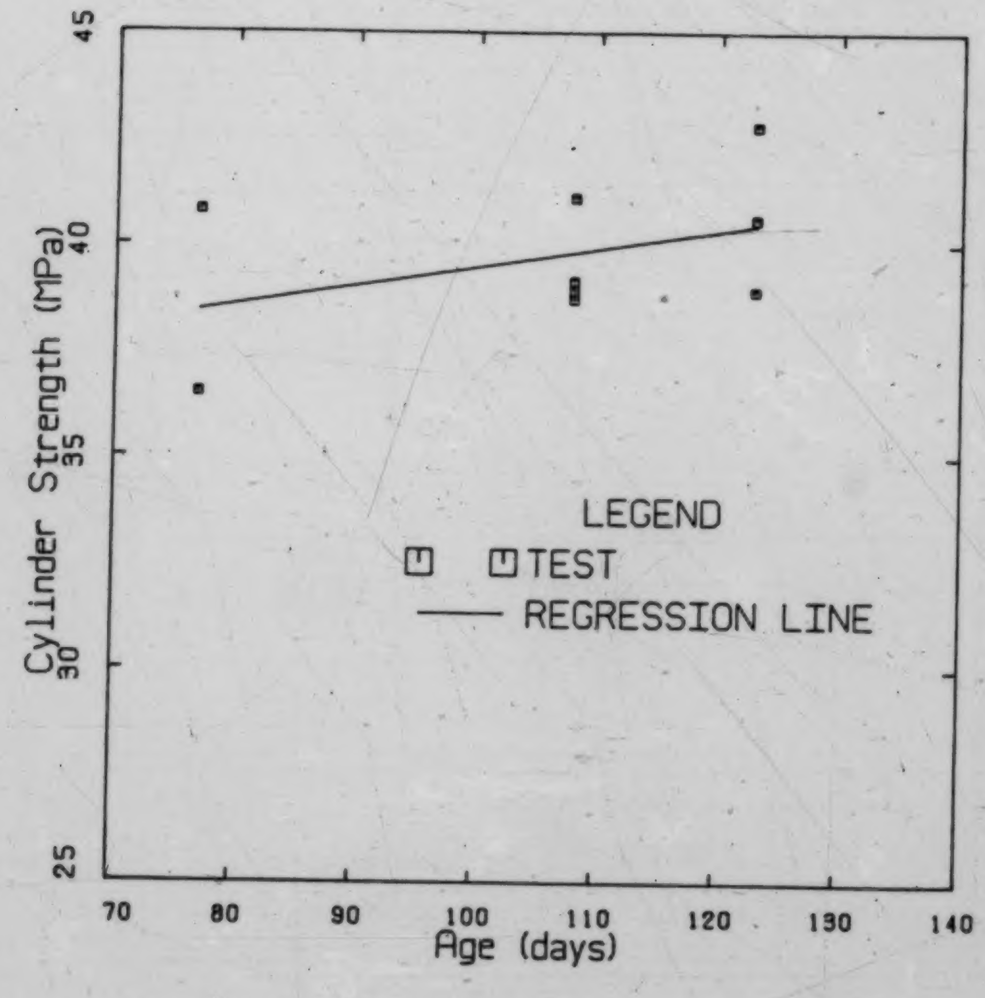

Figure 3.4 Least Squares Estimate of Cylinder Strength/Time Curve for Second Concrete Cast

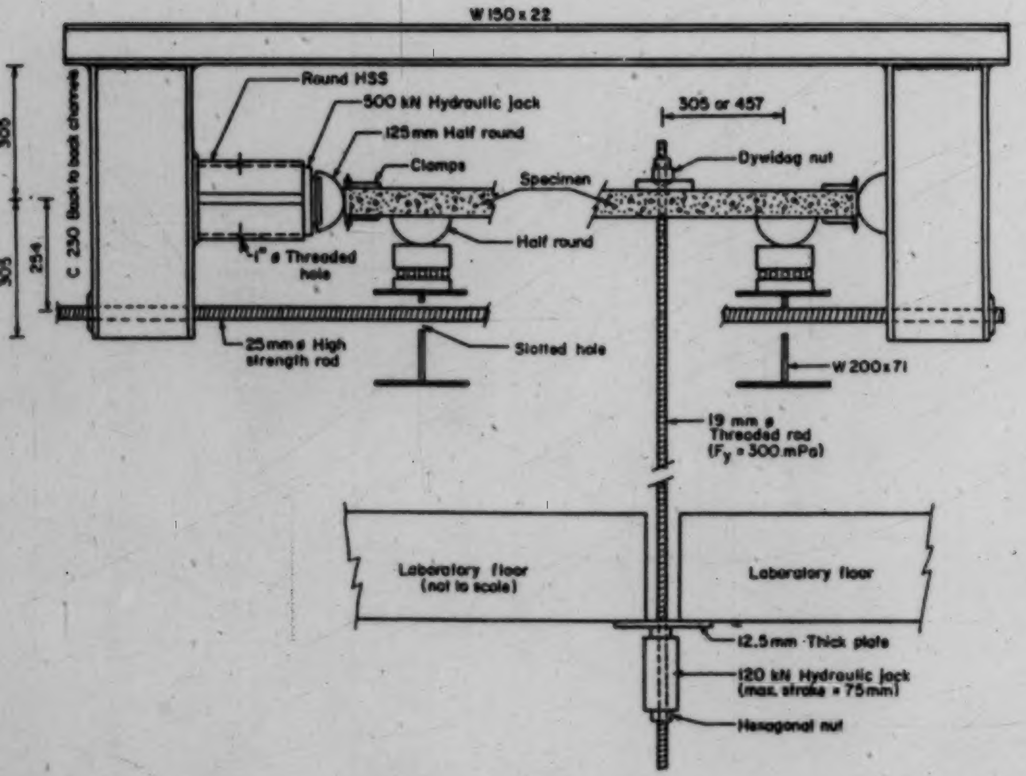
W 150 x 22
305
305
254
C 230 Back to back channels
Round HSS
500 kN Hydraulic jack
125 mm Half round
Clamps
Specimen
305 or 457
Dywidag nut
1" ø Threaded hole
Half round
25 mm ø High strength rod
Slotted hole
W 200 x 71
19 mm ø Threaded rod (F_y = 300 mPa)
Laboratory floor (not to scale)
Laboratory floor
12.5 mm Thick plate
120 kN Hydraulic jack (max. stroke = 75 mm)
Hexagonal nut

Figure 3.5 Schematic of Test Frame

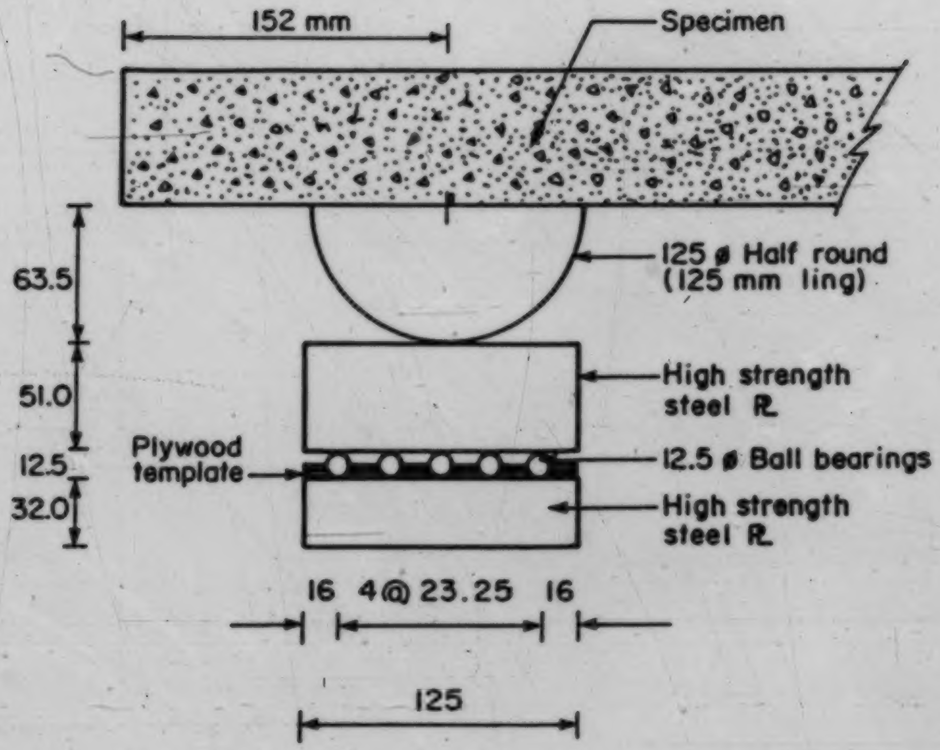
152 mm
Specimen
63.5
51.0
12.5
32.0
125 ø Half round
(125 mm ling)
High strength
steel PL
Plywood
template
12.5 ø Ball bearings
High strength
steel PL
16
4@ 23.25
16
125

Figure 3.6 Schematic of Rocker-Roller Assembly

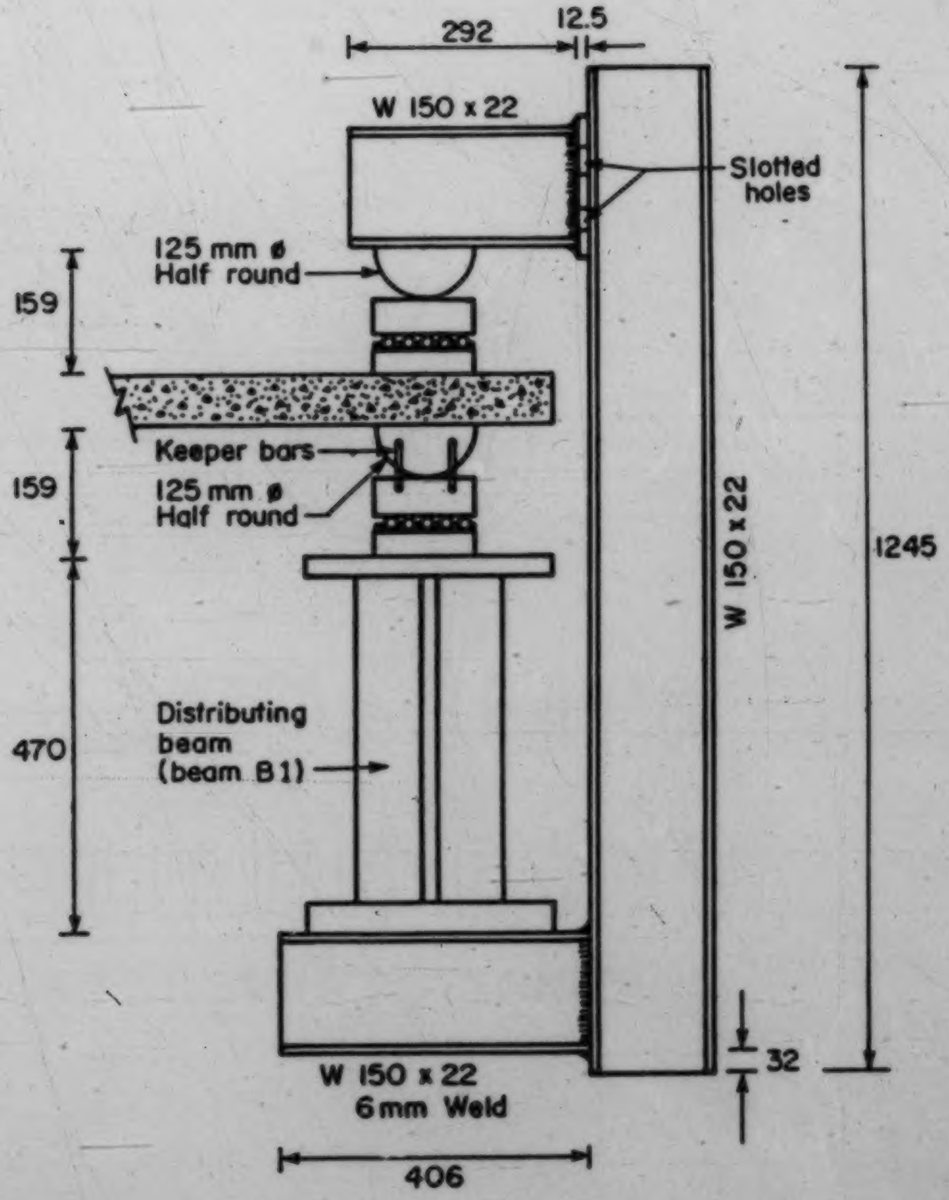
292
12.5
W 150 x 22
Slotted holes
125 mm ø Half round
159
Keeper bars
159
125 mm ø Half round
W 150 x 22
1245
Distributing beam (beam B1)
470
W 150 x 22
6 mm Weld
32
406

Figure 3.7 Schematic of Corner Support Frame

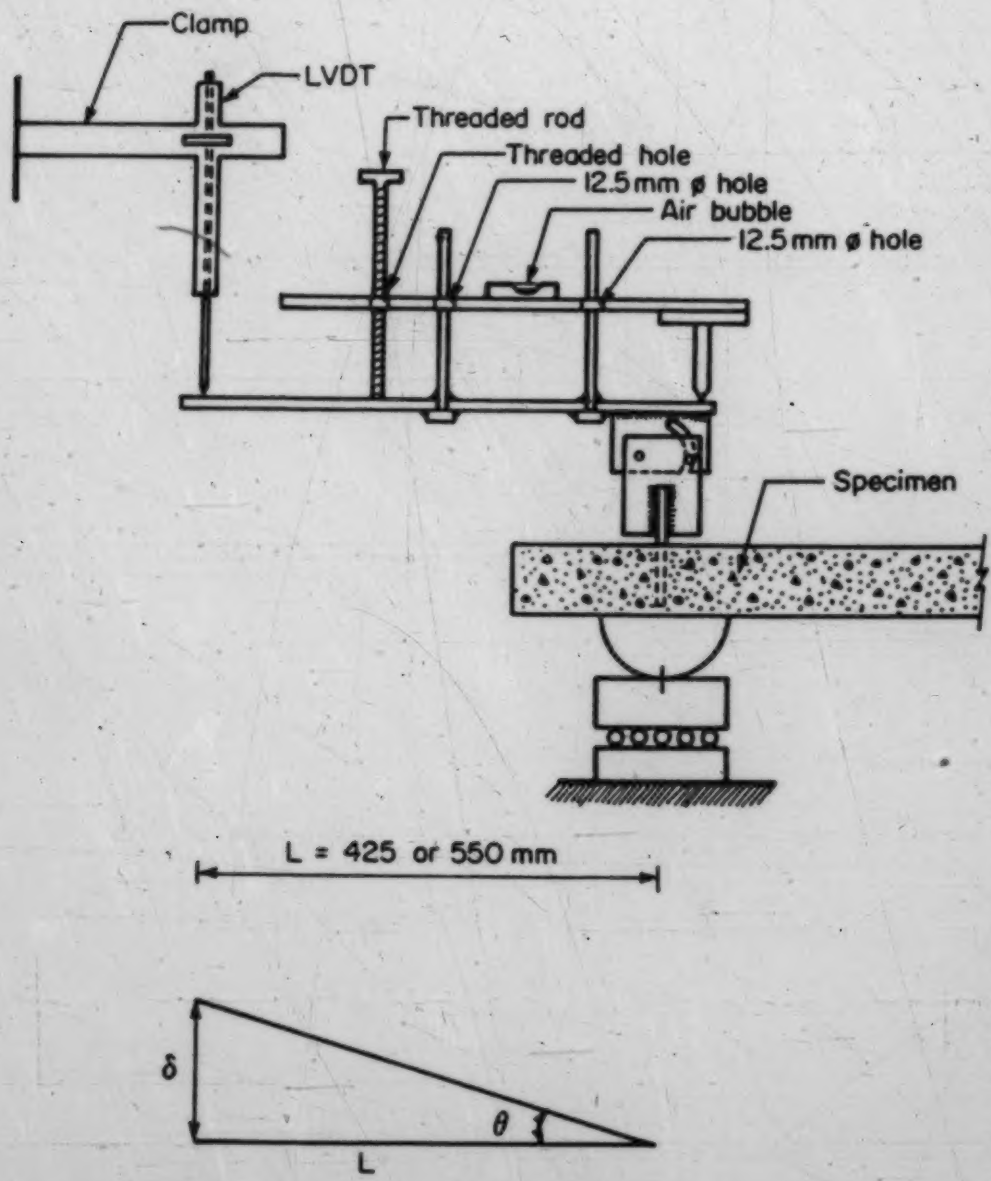
Clamp
LVDT
Threaded rod
Threaded hole
12.5 mm ø hole
Air bubble
12.5 mm ø hole
Specimen
L = 425 or 550 mm
δ
θ
L

Edge Rotation, $\theta = \delta / L$ radians (for small angles)

Figure 3.8 Edge Rotation Measuring Device

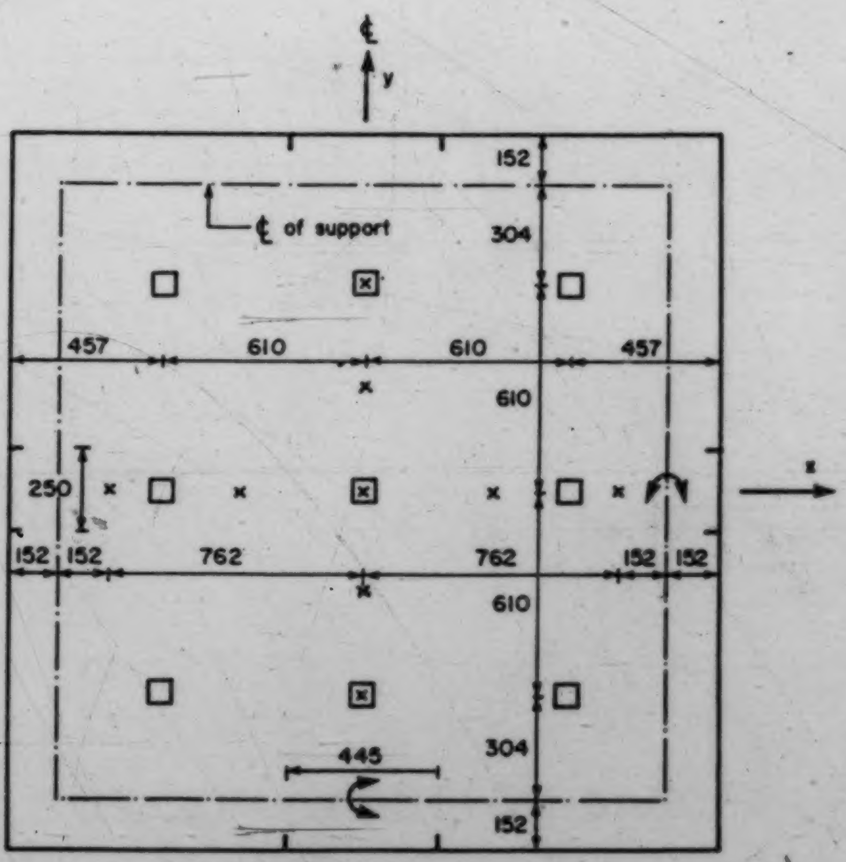
℄
y
x
℄ of support
152
304
457
610
610
457
610
250
152
152
762
762
152
152
610
304
445
152

LEGEND
× Vertical deflection point
– Relative in-plane deflection point
Edge rotation point
□ Lateral load point

Figure 3.9 LVDT Locations for Square Specimens

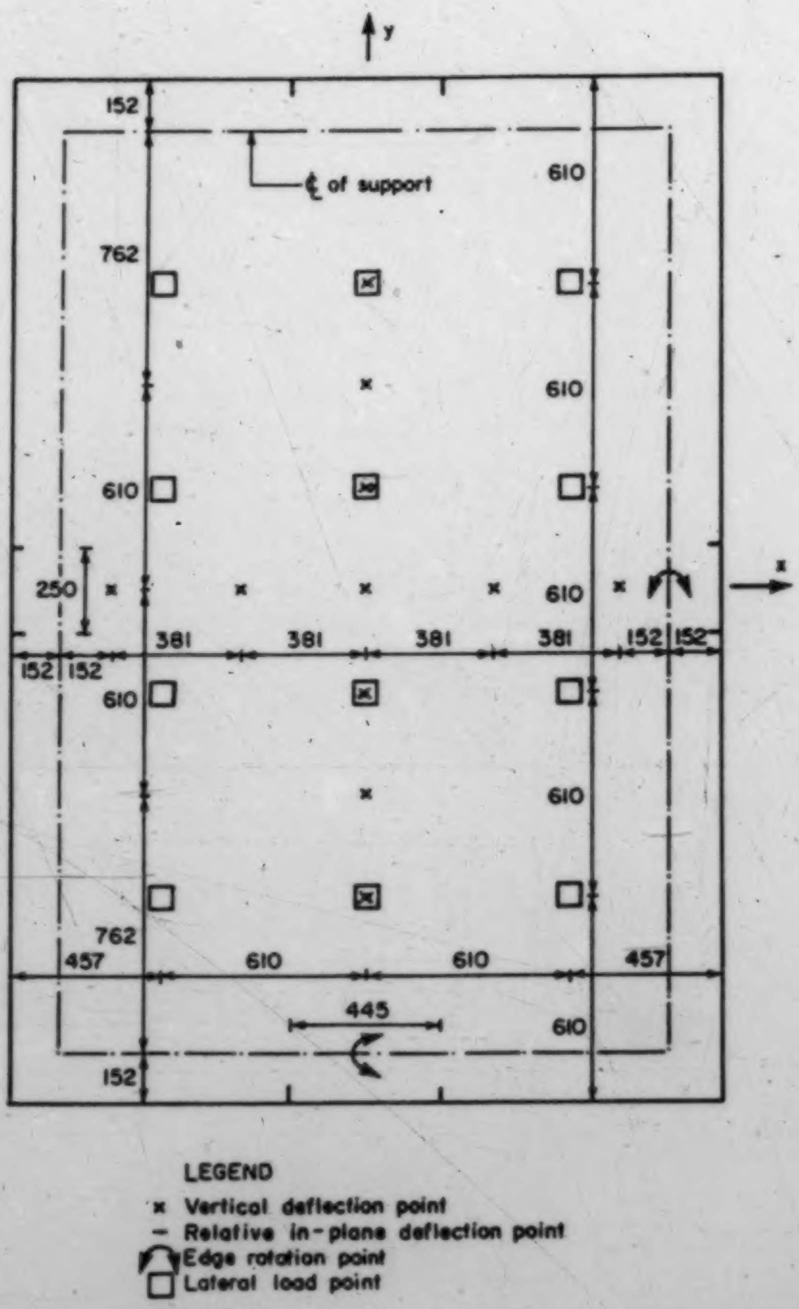
y
x
152
℄ of support
610
762
610
610
250
610
381
381
381
381
152
152
152
152
610
610
762
457
610
610
457
445
610
152
LEGEND
× Vertical deflection point
– Relative in-plane deflection point
Edge rotation point
☐ Lateral load point

Figure 3.10 LVDT Locations for Rectangular Specimens

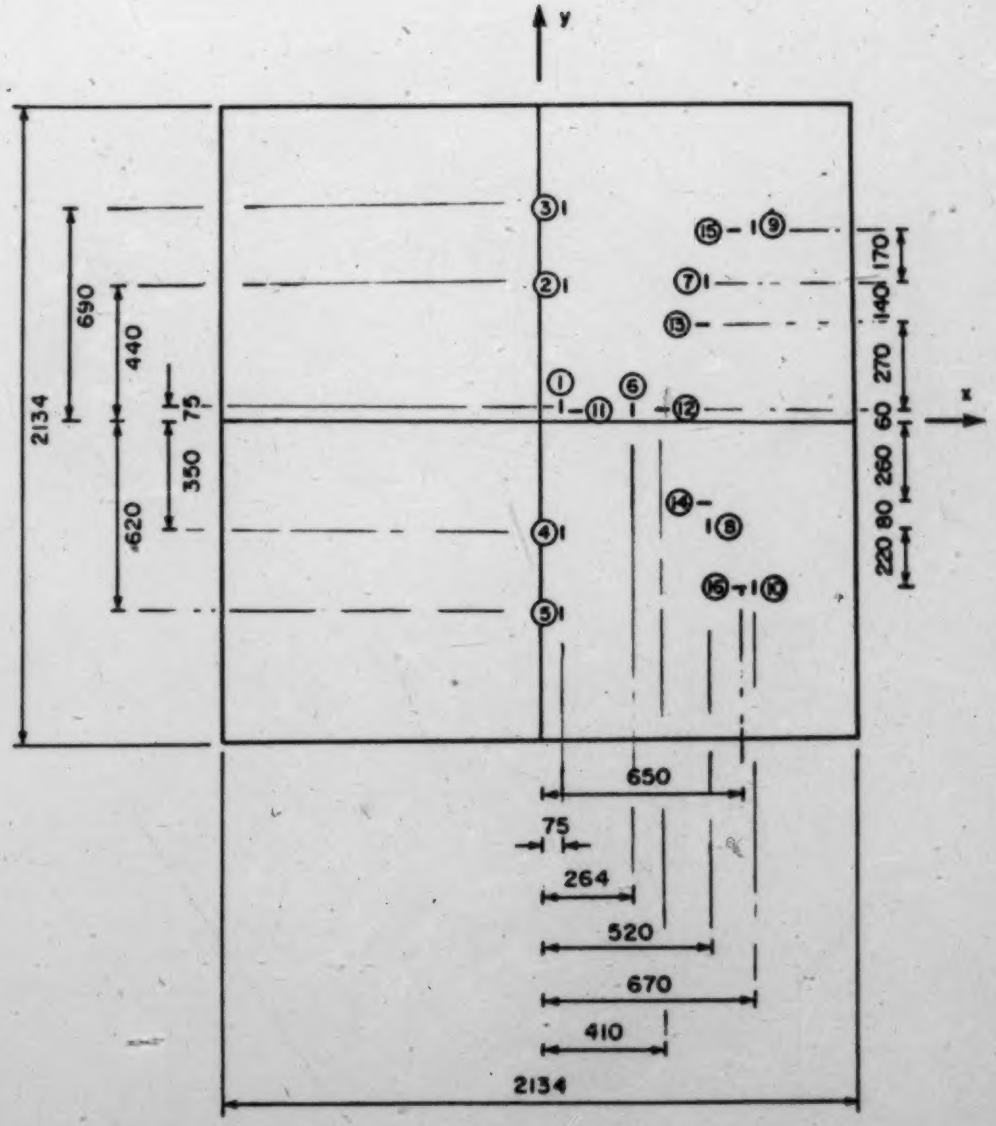
y
x
①
②
③
④
⑤
⑥
⑦
⑧
⑨
⑩
⑪
⑫
⑬
⑭
⑮
⑯
2134
690
440
75
350
620
170
140
270
60
60
260
80
220
650
75
264
520
670
410
2134

Figure 3.11 Strain Gage Layout for A Series

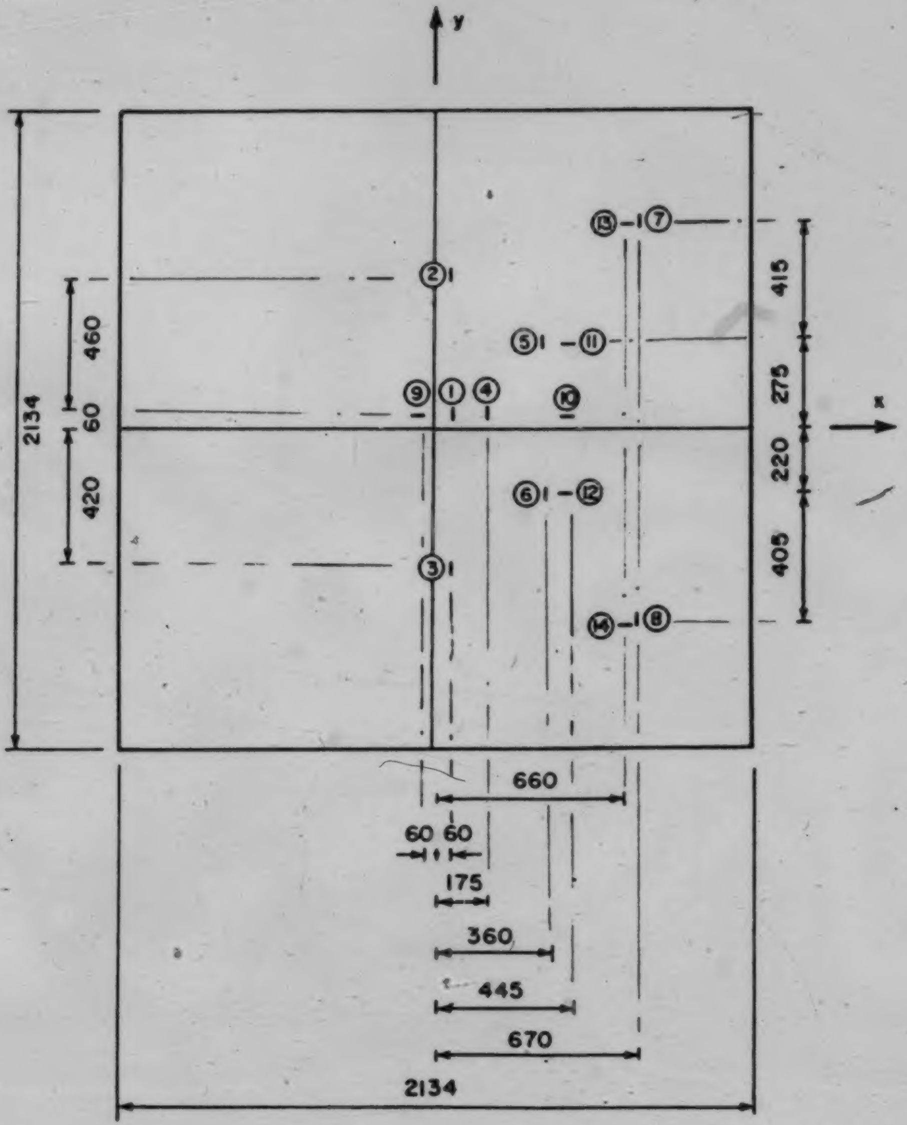
y
x
①
②
③
④
⑤
⑥
⑦
⑧
⑨
⑩
⑪
⑫
⑬
⑭
2134
460
60
420
415
275
220
405
660
60 60
175
360
445
670
2134

Figure 3.12 Strain Gage Layout for C and D Series

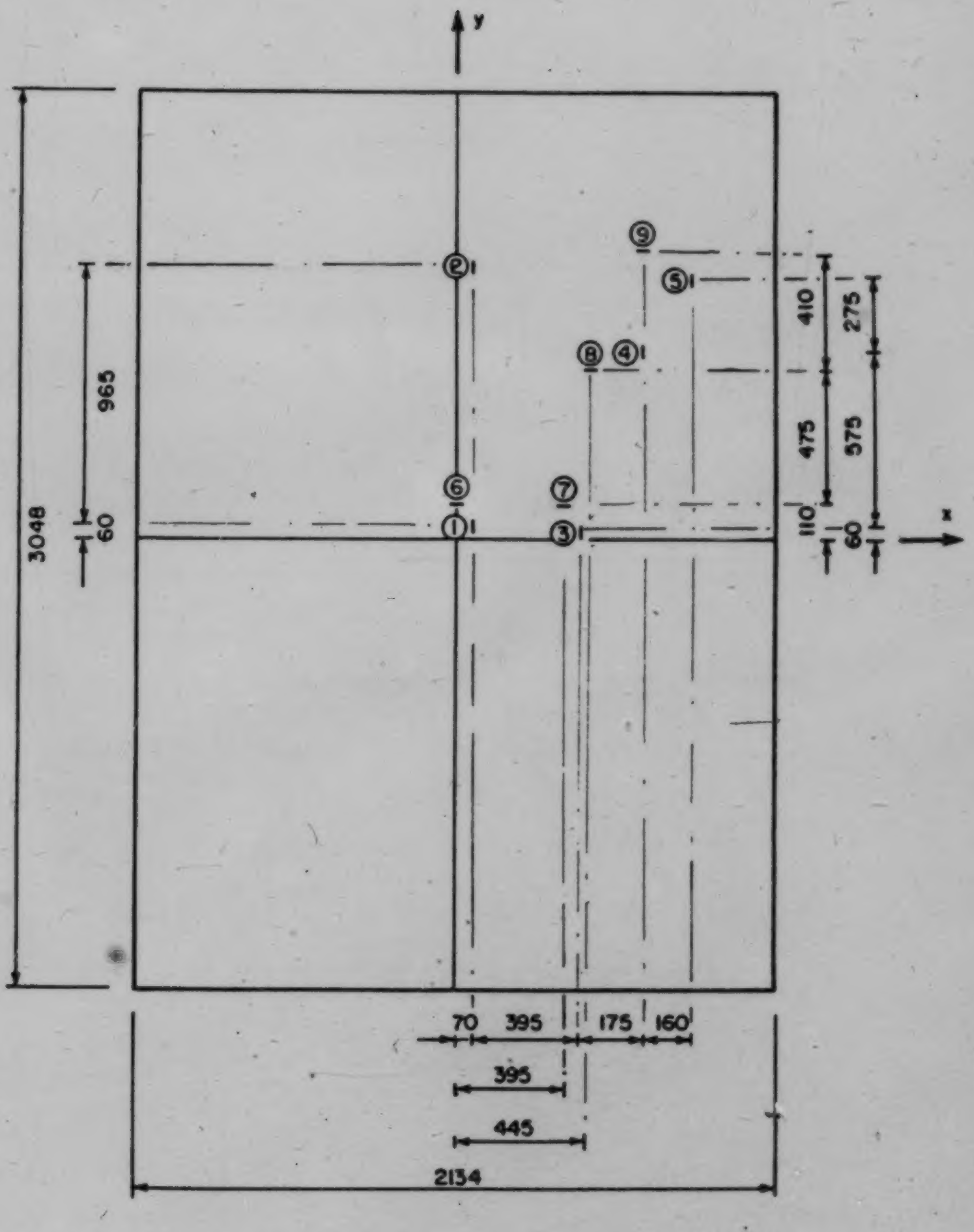
y
x
①
②
③
④
⑤
⑥
⑦
⑧
⑨
3048
965
60
410
475
110
275
575
60
70
395
175
160
395
445
2134

Figure 3.13 Strain Gage Layout for B Series

Plate 3.1 Reinforcement Cage for Square Specimen

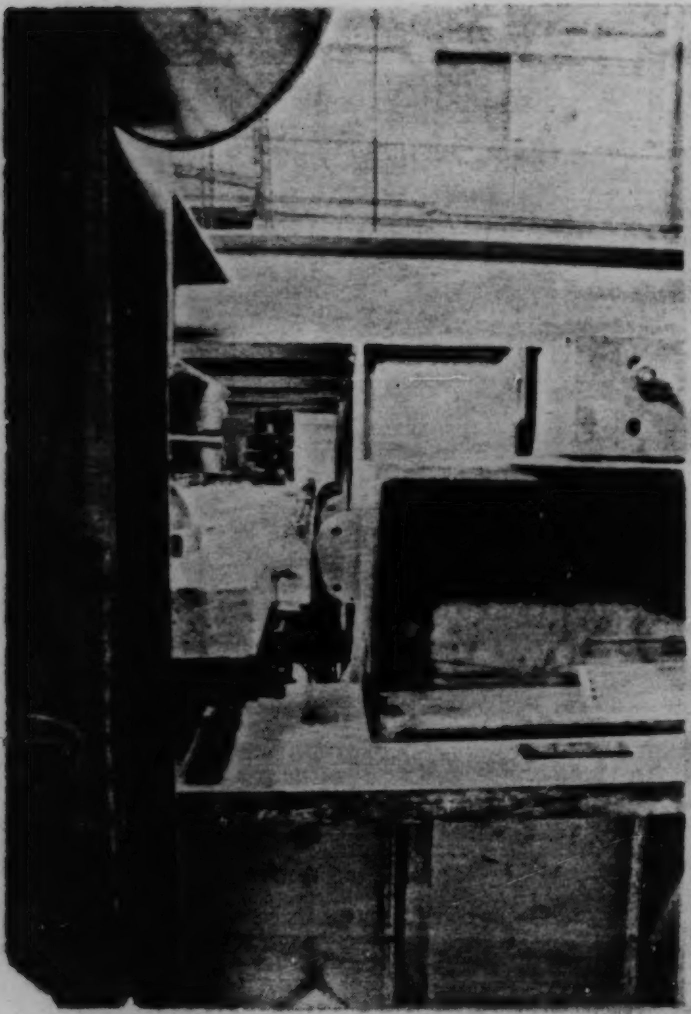

Plate 3.2 In-plane Loading Frame Showing Clamps

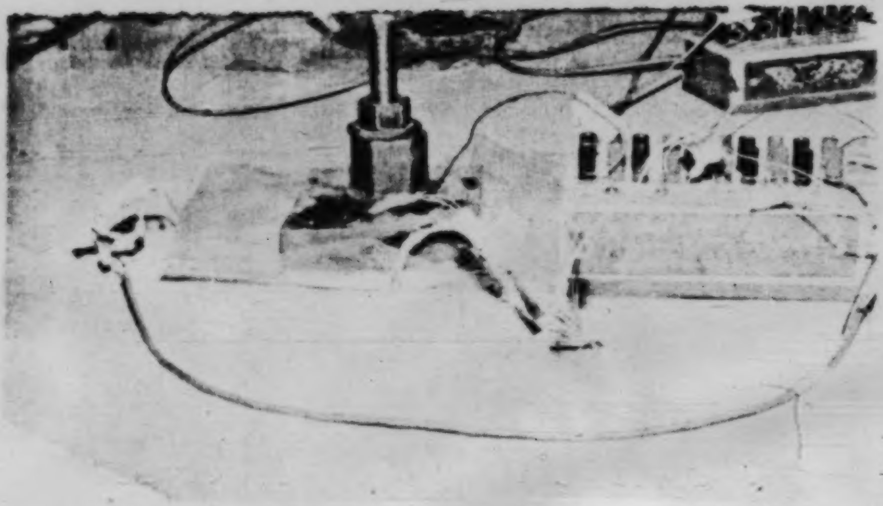

Plate 3.3 Load Spreading Plate for Lateral Loading

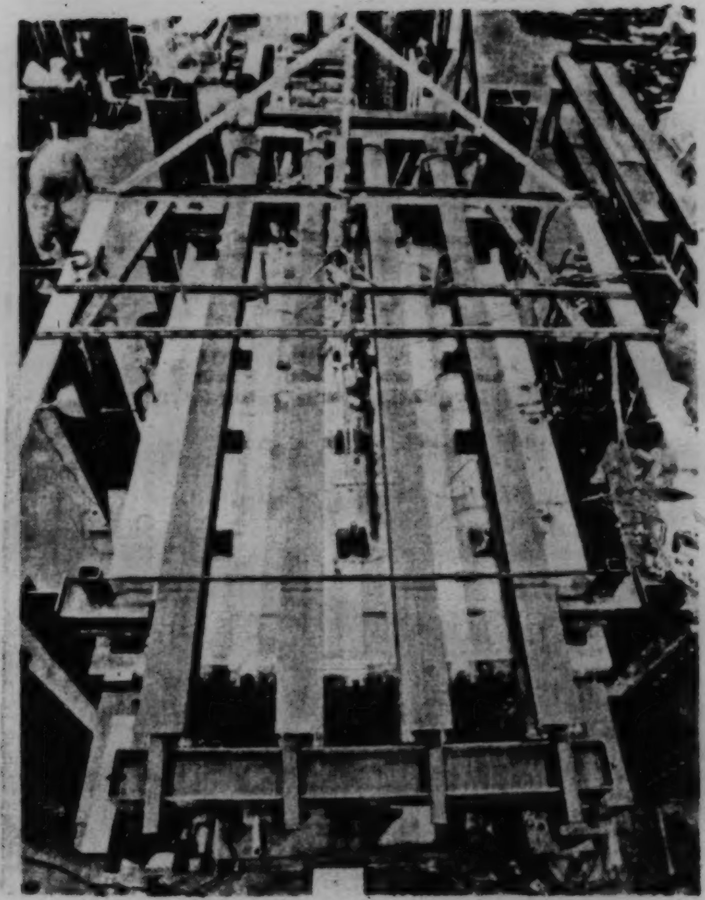

Plate 3.4 An Over View of Test Frame

4. TEST RESULTS

4.1 Introduction

The following quantities were recorded at regular intervals for each test:

1. Applied in-plane and lateral loads
2. Vertical (out-of-plane) deflections of the plate surface
3. In-plane deflections at the plate center lines
4. Edge rotations at the plate center lines in the x and y directions
5. Top and bottom steel strains in both orthogonal directions.

Items (1) and (2) are necessary for comparisons with the analytical model developed in Chapter 5. These comparisons are performed in Chapter 5. Item (5) gave an idea of the strain distributions in the plate. Items (3) and (4) were recorded for future correlation with a finite element analysis.

4.2 General Test Observations

4.2.1 Maximum Loads and Modes of Failure

Table 4.1 shows for each specimen the maximum lateral load per unit area and the constant uniform in-plane load per unit width applied in the y direction. The variation of the in-plane load during the application of the lateral load was less than one percent. The lateral load is given in KPa as the sum of the nine or twelve point loads divided by the area of the plate within the center-lines of the supports, while the in-plane load is given in KN/m as the sum of the four horizontal point loads divided by the width of the plate.

Specimen A3 was subjected to lateral load only to give an indication of the reduction in capacity for specimens within the same series. Cracks were first observed on the flexural tension (bottom) face at a lateral pressure of 16 KPa. Yield lines formed on the tension face of the specimen at maximum load. Cracks were observed along the diagonal on the bottom face near the corners and at failure crushing of concrete occured on the top face of the specimen above these cracks. In addition, cracks developed perpendicular to the diagonal on the top surface. These cracks resulted from the holding down of the plate corners permitting the development of anticlastic corner surfaces. The twisting moment near the corners caused "torsional cracks" on the edges of the plate near the corners. It should be noted that Specimen A3 was not tested to final failure. The test was stopped several load steps after the peak load due to excessive deflections and rotations of the supports. The maximum deflection obtained at the center of the plate was 95 mm.

In Specimen A1, cracks were first observed at the bottom face of the specimen in the direction of the in-plane load at a lateral load of 21.5 KPa. The tension and compression faces of this plate are shown in Plates 4.1 and

4.2. Final failure which occurred at a center deflection of 34 mm was explosive and concrete crushing lines were observed at the top of the specimen. Cracks were more prevalent in the y direction. The outer layer of rebar was in this direction.

Failure of specimen A2 was also explosive with cracks first observed at the bottom face in the in-plane load direction at a lateral load of 21.5 KPa. The deflection at the center of the plate at final failure was 40 mm.

In Specimen C2, cracks were first observed at the bottom face in the y direction at an in-plane load of 765 KN/m before any lateral load was applied. With further load, cracking similar to that observed in specimen A1 occurred on the tension face of the plate. Final failure which occurred at a center deflection of 37 mm was similar to specimen A1.

The in-plane and lateral loads were applied simultaneously in the test of specimen C1. The in-plane load was applied in 31 KN/m steps and the lateral load in steps of 1.35 KPa up to the peak loads. Beyond the peak loads, the lateral load was allowed to drop off as the deflection increased, while keeping the in-plane load constant at the peak value. Cracks were first noticed in the y direction on the tension face at in-plane and lateral loads of 398 KN/m and 17.5 KPa, respectively. The tension and compression faces of this plate are shown in Plates 4.3 and 4.4. Final failure occurred at a center deflection of 38 mm.

In Specimens D1 and D2, cracks were first noticed in the y direction on the tension face at lateral loads of 16 KPa and 13.5 KPa, respectively and the failure modes were similar to Specimen A1. Final failure for Specimens D1 and D2 occurred at center deflections of 48 mm and 39 mm, respectively.

In Specimen B1, cracks were first noticed in the y direction on the tension face at a lateral load of 12 KPa. The maximum lateral load was reached at a center deflection of 48 mm while the final failure occurred at a deflection of 53 mm. The tension and compression faces of specimen B1 are shown in Plates 4.5 and 4.6.

In Specimen B2, cracks were first observed in the y direction at a lateral load of 7 KPa. The maximum lateral load was reached at a center deflection of 44.5 mm, while the deflection at final failure was 49 mm.

In most specimens, buckling of the compression reinforcement took place at failure as shown in Plate 4.7 and all failures were compression failures due to crushing of the concrete. For all specimens, the cracks in the tension face tended to propagate in an orthogonal pattern coinciding with the reinforcement layout. This same behavior was observed by Nawy (1968) in slabs with closely spaced reinforcements of the order of 100 mm to 200 mm. This behavior is due to the local stress concentrations, caused in particular by the presence of reinforcing steel. The crack patterns for the axially loaded specimens approached that of a similar plate under lateral loads only.

4.2.2 Load Deflection Response

Typical lateral load versus out-of-plane deflection plots at the center of the plate for the square and rectangular specimens are shown in Figs. 4.1 through 4.3. It was observed that the square specimens continued to carry a decreasing lateral load after the maximum load had been reached indicating a stability type of failure. The rectangular specimens failed almost immediately after reaching the peak lateral load indicating a material type of failure. A small out-of-plane deflection occured in several specimens during the application of the in-plane loads. This deflection was less than 7 percent of the deflection at maximum lateral load.

The lateral load versus in-plane deflections in both the x and y directions along the plate center lines for typical square and rectangular specimens are shown in Figs. 4.4 through 4.7. The horizontal offsets at zero lateral pressures indicate the shortening of the plates as the in-plane loads were applied. Plots of the lateral load versus edge rotations in the x and y directions along the plate center lines are shown in Figs. 4.8 through 4.11.

4.2.3 Deflected Shapes

Vertical deflections of the plate surface were measured at 9 and 11 points for the square and rectangular specimens, respectively. From these, the deflected shapes at various lateral load levels in both the x and y directions were obtained. Typical deflection profiles for the square and rectangular specimens are shown in Figs. 4.12 through 4.15.

The deflected shapes across square plates and in the x direction of the rectangular plates approach a half sine wave shape. The deflected shape in the long direction of plate B1 in Fig. 4.15 suggests there may have been a region of one-way load transfer in the middle of the plate.

4.2.4 Strain Distribution

To measure the uniformity of the applied in-plane loads, strains were measured on the top and bottom reinforcements in the direction of the applied in-plane load during the application of the in-plane load. The average of top and bottom strains at a point was computed and plotted. Typical strain distributions across half of the plate width are shown in Figs. 4.16 and 4.17. The position of the strain gages are given relative to the center-line of the plate. The plots indicate that the in-plane load was fairly uniform across the width of the specimens.

When the lateral load was applied at constant in-plane load, the strains in the transverse top reinforcement increased (became more tensile) rather than decreasing. A typical plot of the strains in the transverse top and bottom reinforcement is shown in Fig. 4.18. The offset at zero lateral load was due to Poisson's ratio.

Attempts have been made here to explain the reason for this increase in strain but none of these was successful. The analysis of the roller supports by Hertzian theory showed the maximum friction force to be much less than the net transverse tensile force indicated by the strain readings. The analysis of the strips bounding the specimens showed that only very small in-plane restraint was present due to these strips. Kordina *et al.* (1973) have also observed this same phenomenon in their tests but were unable to explain it.

Specimen	Aspect Ratio a/b	$\frac{b}{h}$	$\rho_x = A_{sx}/bh$	$\rho_y = A_{sy}/bh$	Applied In-plane Load N_y kN/m	$\frac{N_y}{f'_c bh}$	Maximum Lateral Load, q kPa	Failure Mode
A3	1.0	28.0	0.00344	0.0040	0.0	0.0	58.6	Material failure
A2	1.0	28.5	0.00350	0.0040	765.0	0.37	37.7	Instability
A1	1.0	27.3	0.00336	0.0039	962.0	0.45	45.7	Instability
C1	1.0	28.3	0.00240	0.0050	822.5	0.394	34.8	Instability
C2	1.0	28.7	0.00246	0.0052	765.0	0.372	32.8	Instability
D1	1.0	33.0	0.00405	0.0047	524.6	0.293	26.8	Instability
D2	1.0	32.1	0.00395	0.0046	852.6	0.374	27.0	Instability
B1	1.5	28.4	0.00500	0.0059	874.3	0.337	28.3	Material failure
B2	1.5	28.2	0.00500	0.0059	63.9	0.243	36.4	Material failure

Note: In all tests except C1 the full in-plane load was applied first, before lateral loading was commenced. In C1 the in-plane and lateral loads were applied proportionally.

Table 4.1 Maximum Lateral Load and Applied In-plane Load

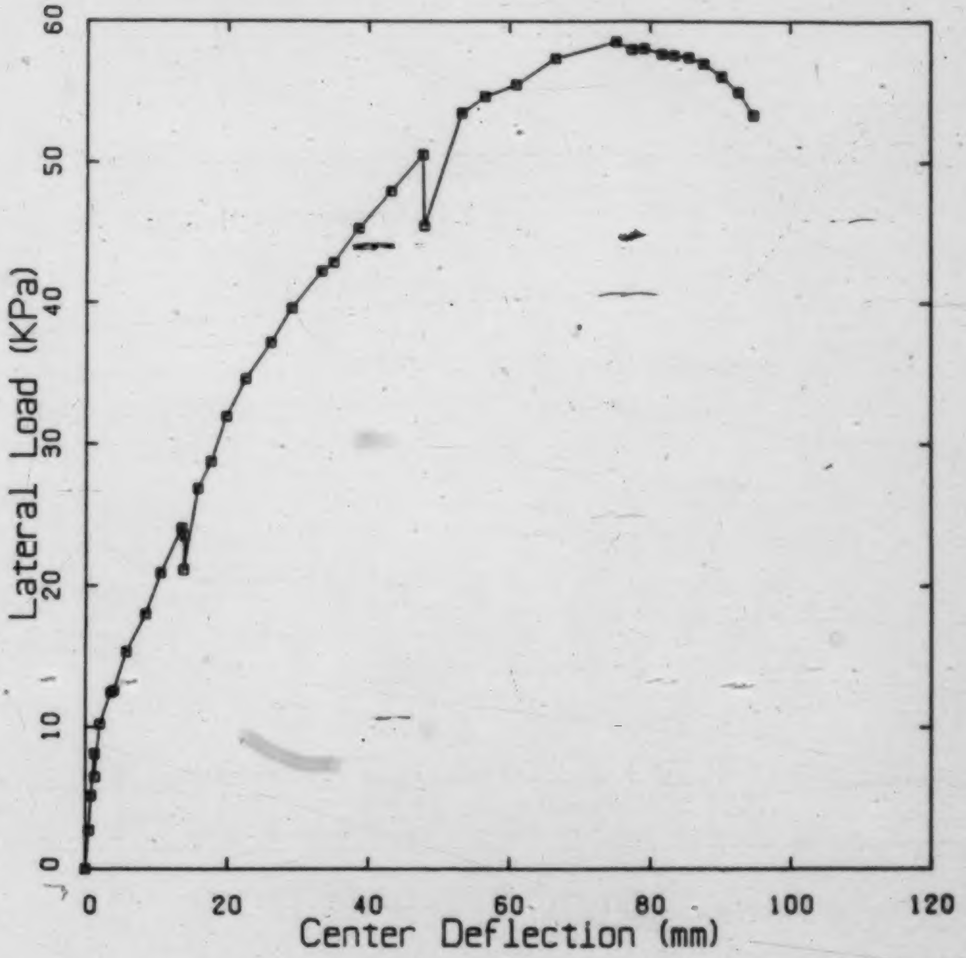

Figure 4.1 Lateral Load versus Out-of-Plane Center Deflection for Specimen A3

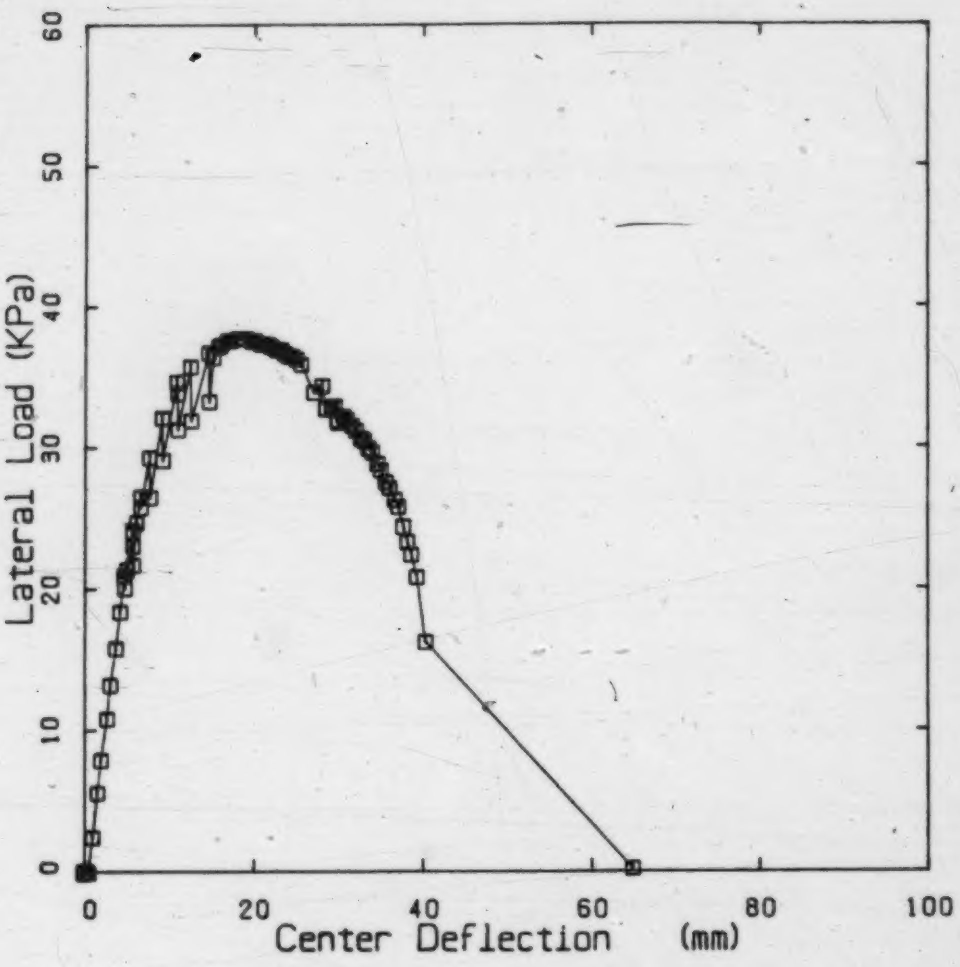

Figure 4.2 Lateral Load versus Out-of-Plane Center Deflection for Specimen A2

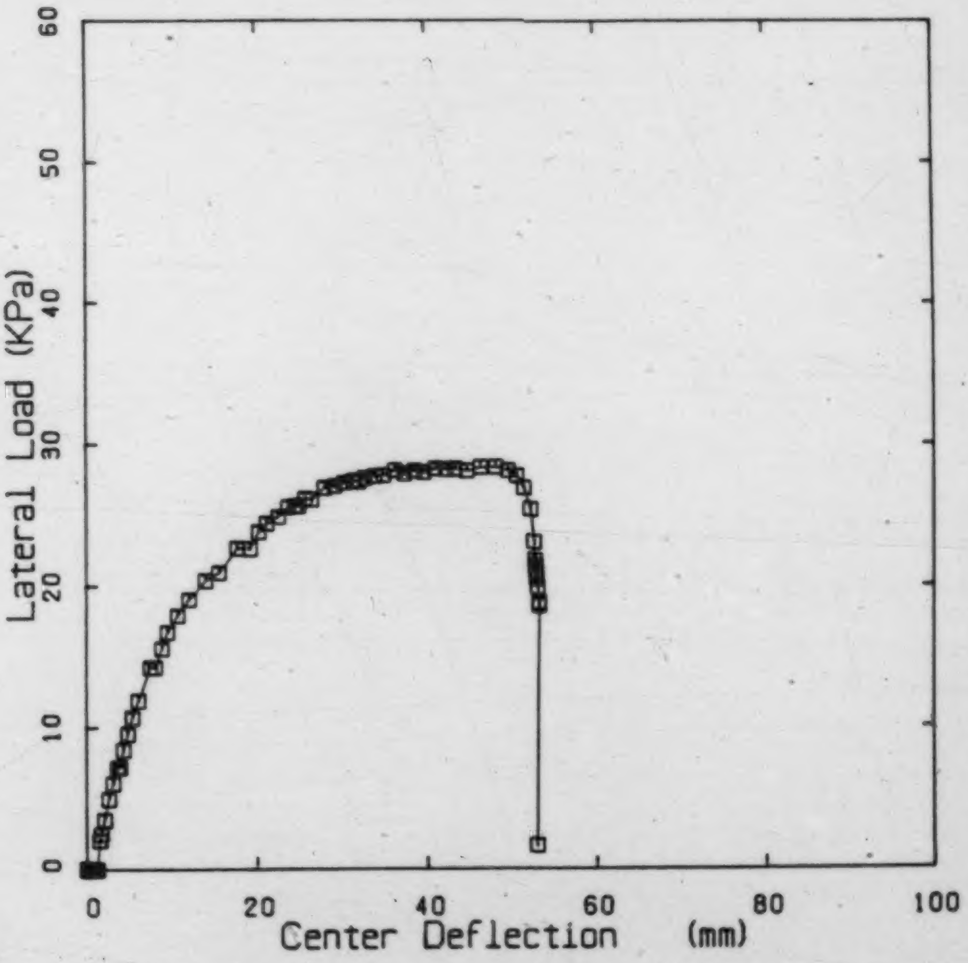

Figure 4.3 Lateral Load versus Out-of-Plane Center Deflection for Specimen B1

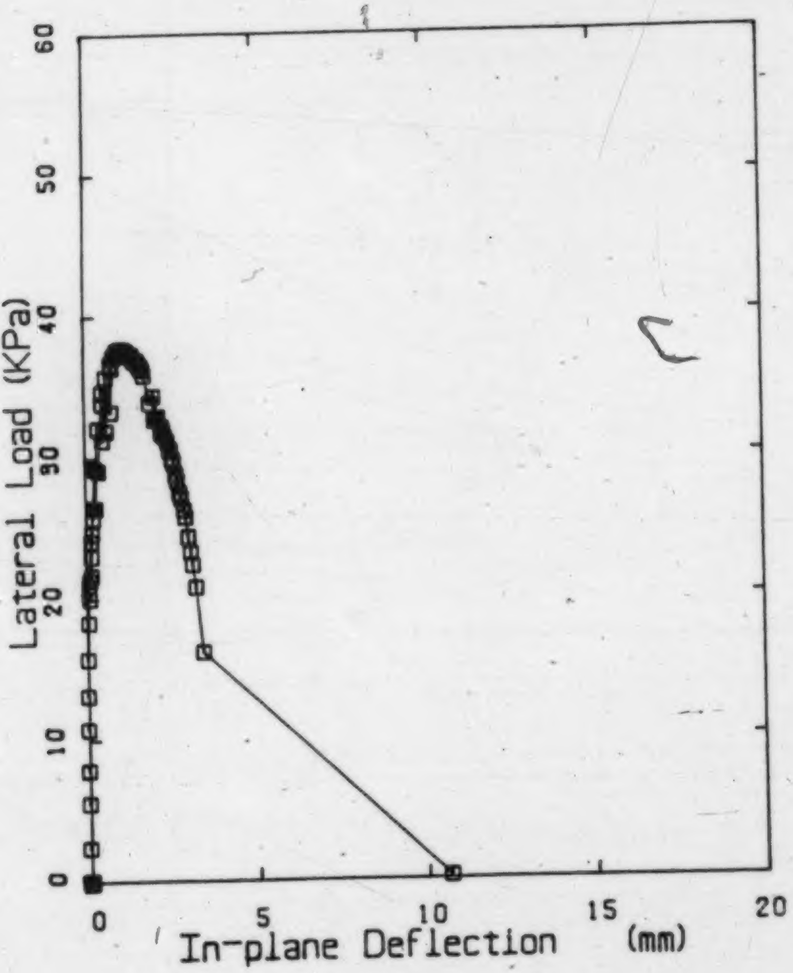

Figure 4.4 Lateral Load versus In-plane Deflection in the x Direction for Specimen A2

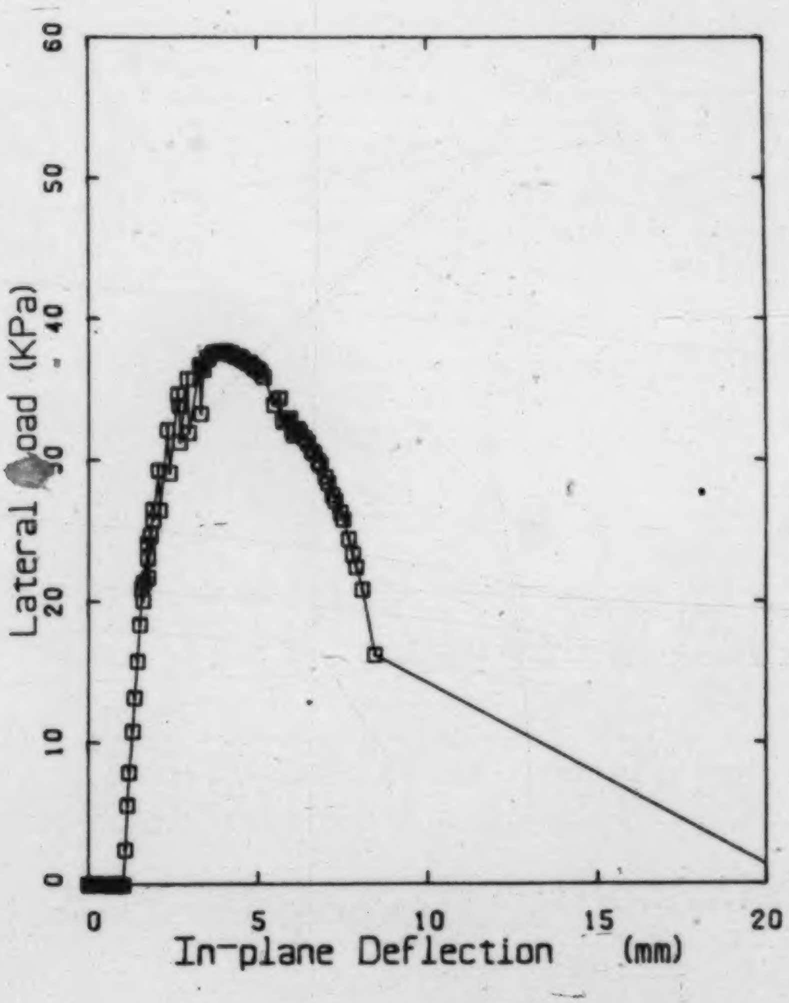

Figure 4.5 Lateral Load versus In-plane Deflection in the y Direction for Specimen A2

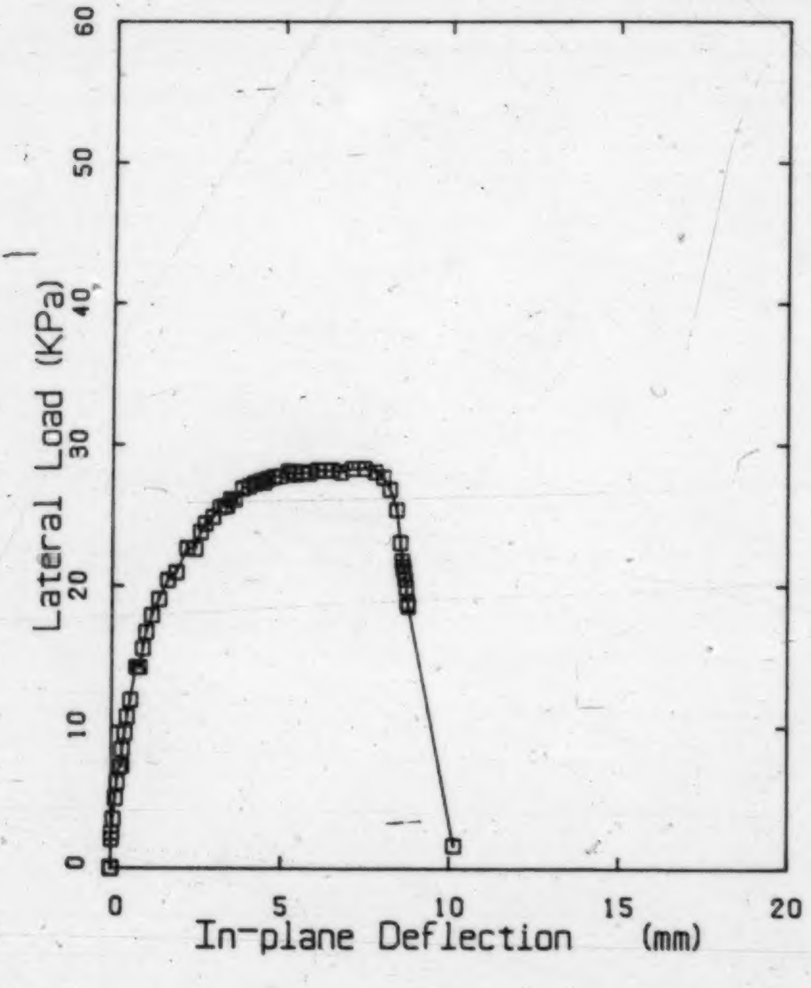

Figure 4.6 Lateral Load versus In-plane Deflection in the x Direction for Specimen B1

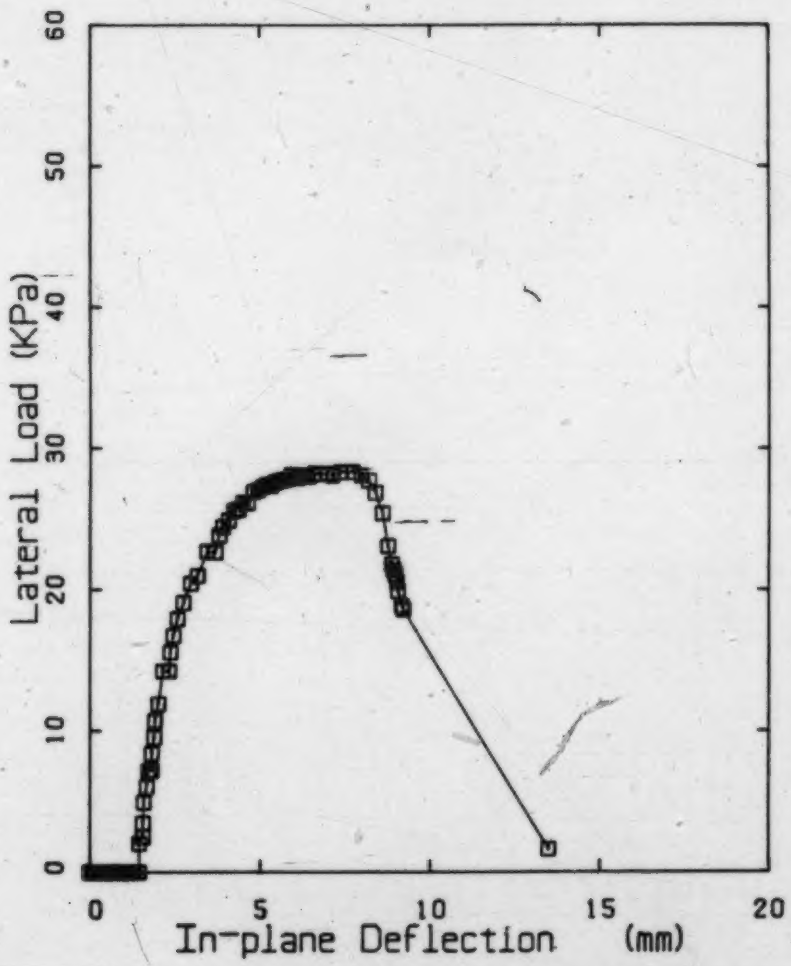

Figure 4.7 Lateral Load versus In-plane Deflection in the y Direction for Specimen B1

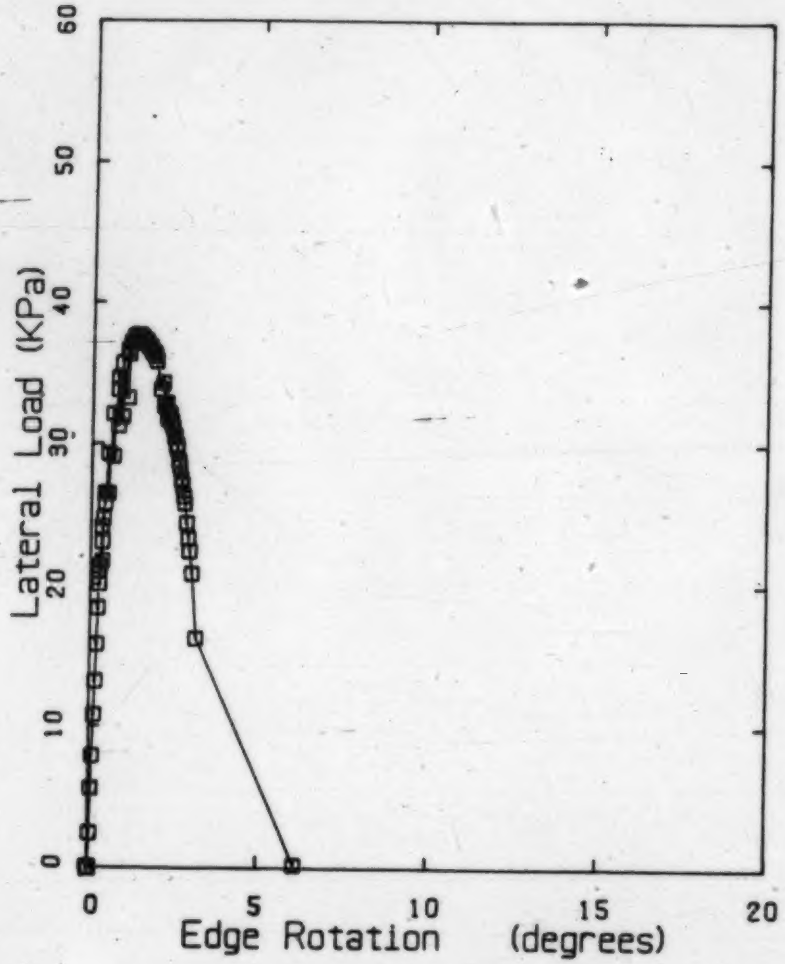

Figure 4.8 Lateral Load versus Edge Rotation in the x Direction for Specimen A2

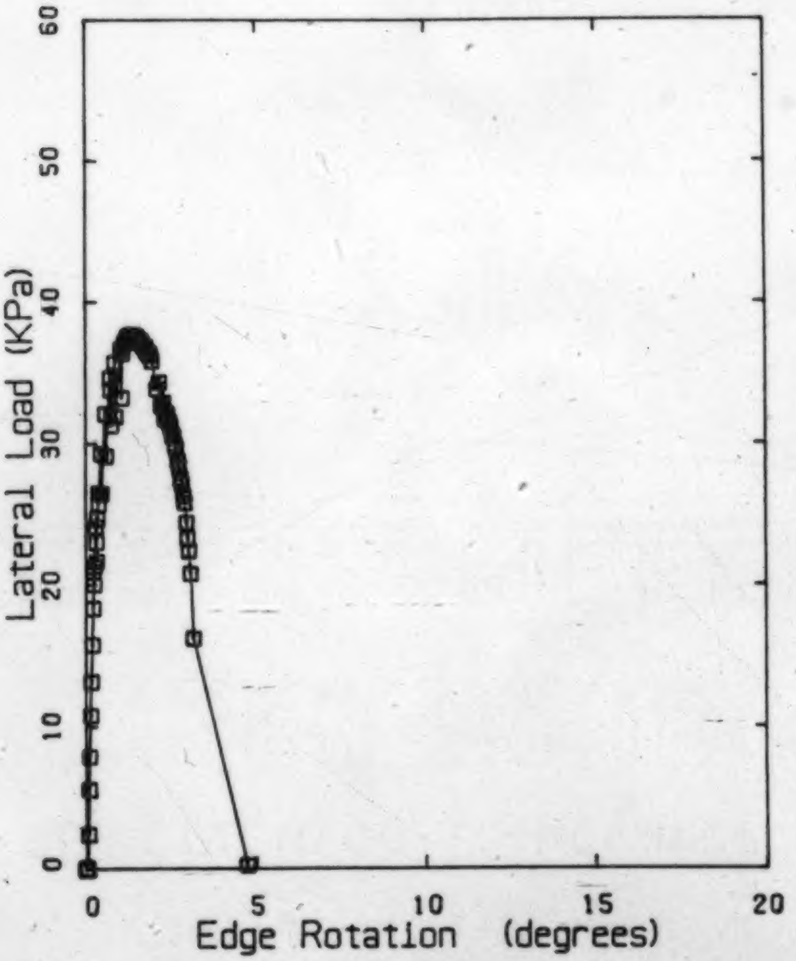

Figure 4.9 Lateral Load versus Edge Rotation in the y Direction for Specimen A2

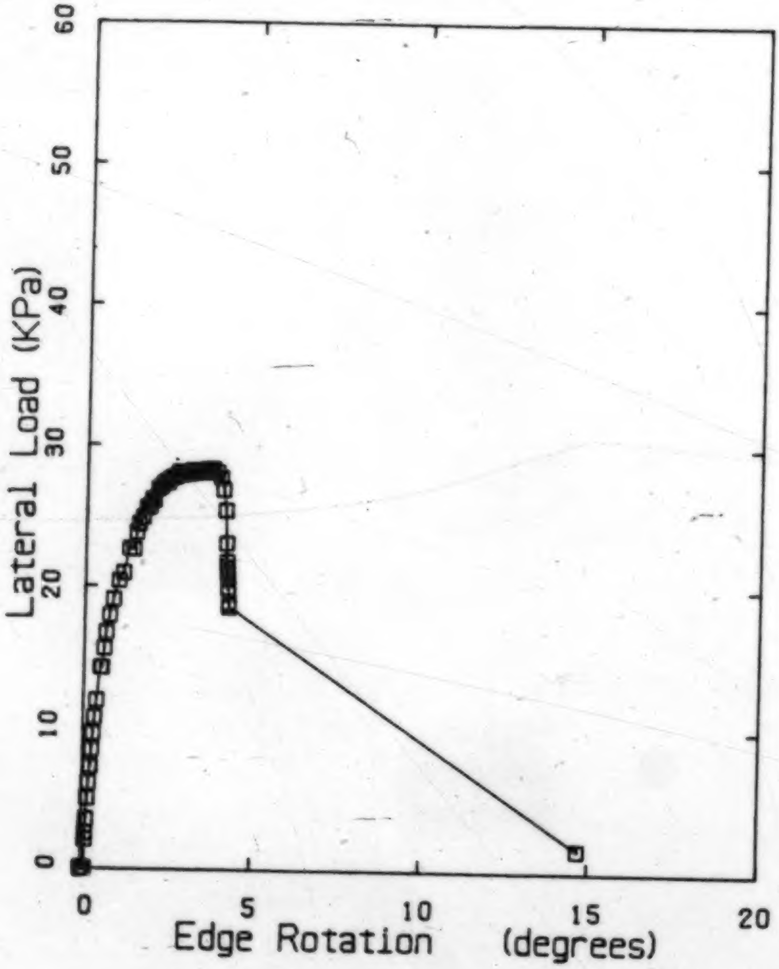

Figure 4.10 Lateral Load versus Edge Rotation in the x Direction for Specimen B1

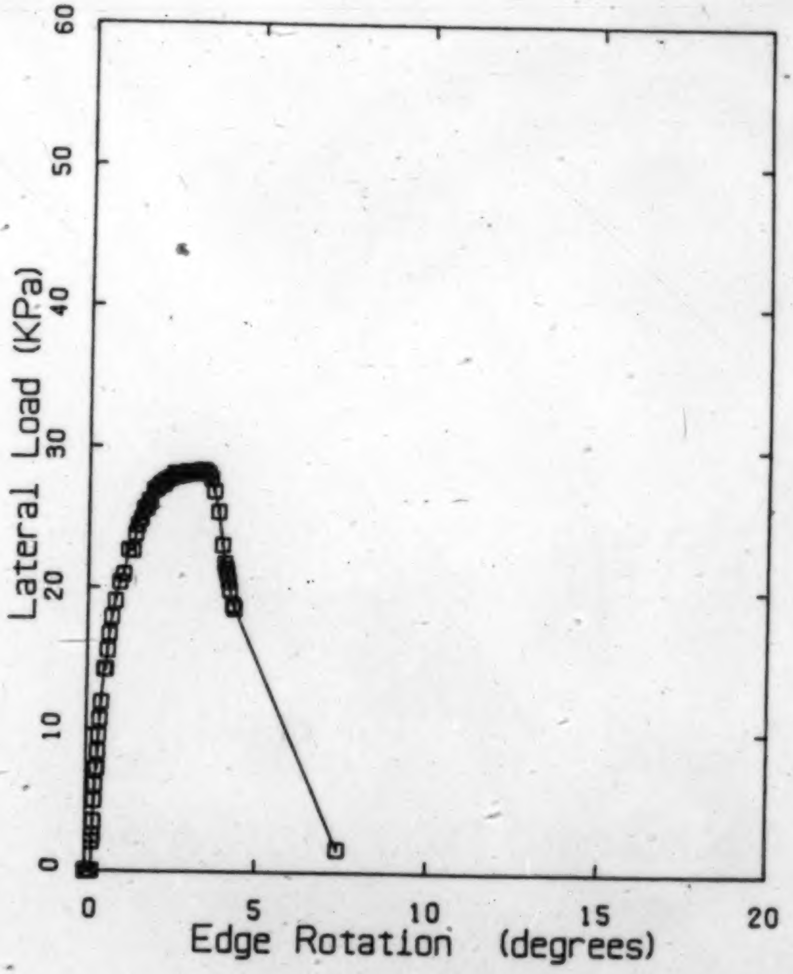

Figure 4.11 Lateral Load versus Edge Rotation in the y Direction for Specimen B1

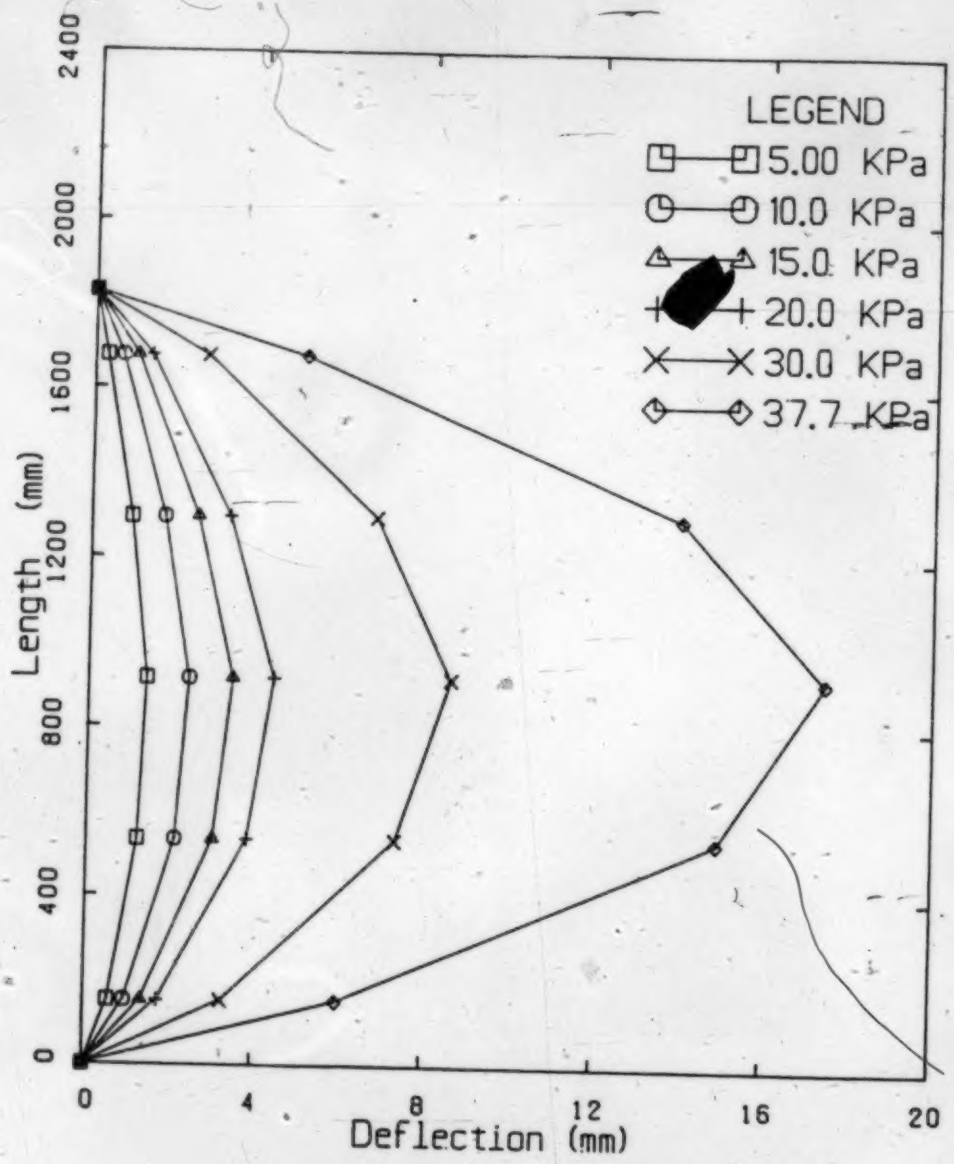

Figure 4.12 Deflection Profiles in the x Direction for Specimen A2

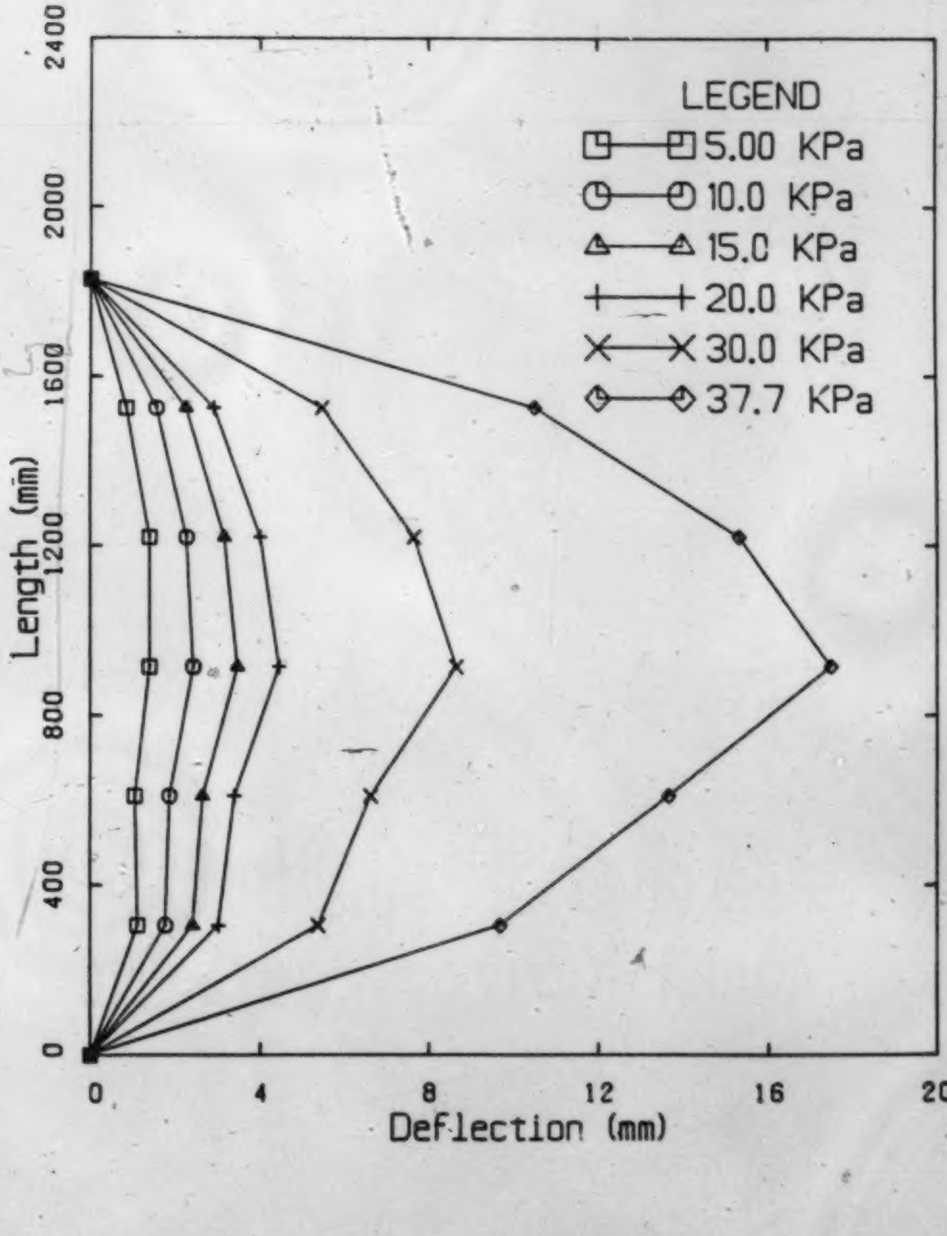

Figure 4.13 Deflection Profiles in the y Direction for Specimen A2

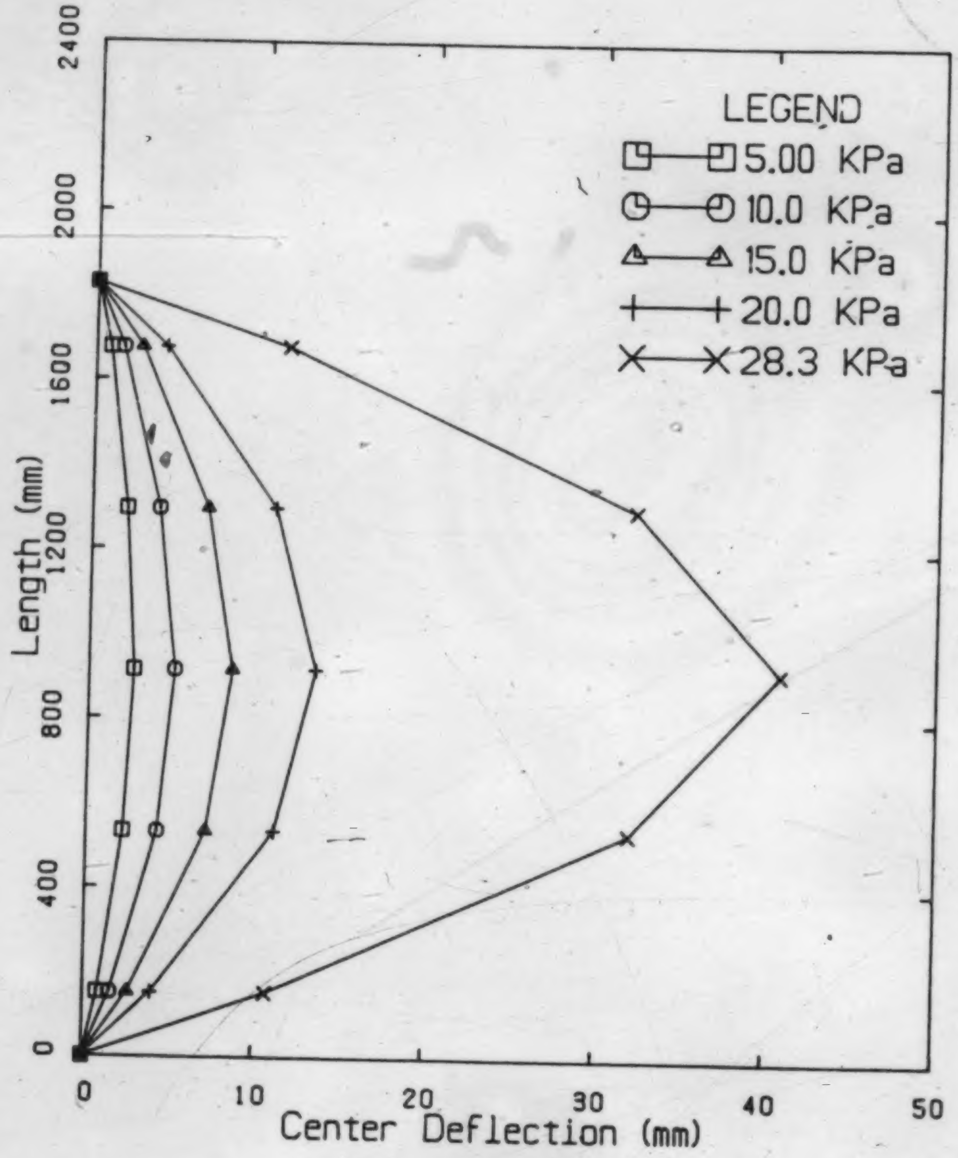

Figure 4.14 Deflection Profiles in the x Direction for Specimen B1

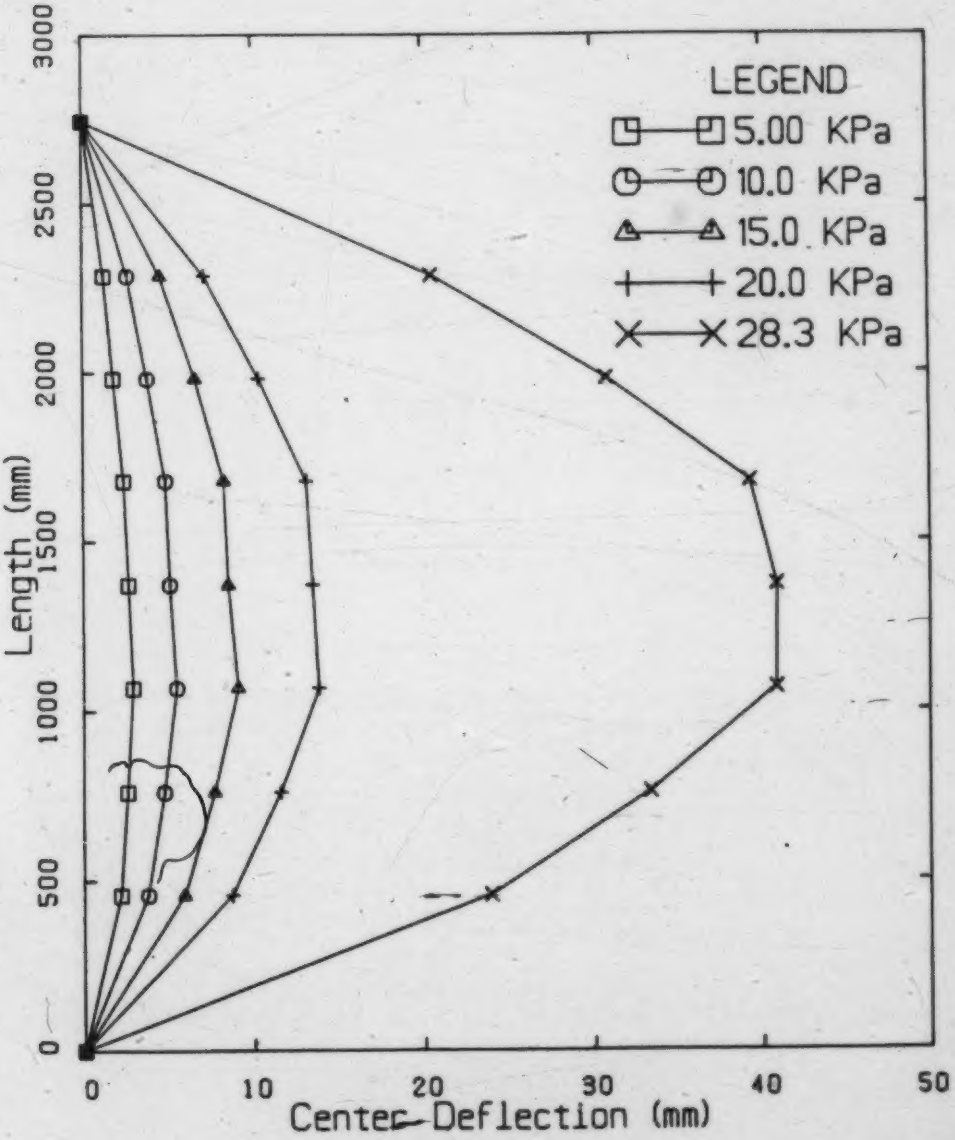

Figure 4.15 Deflection Profiles in the y Direction for Specimen B1

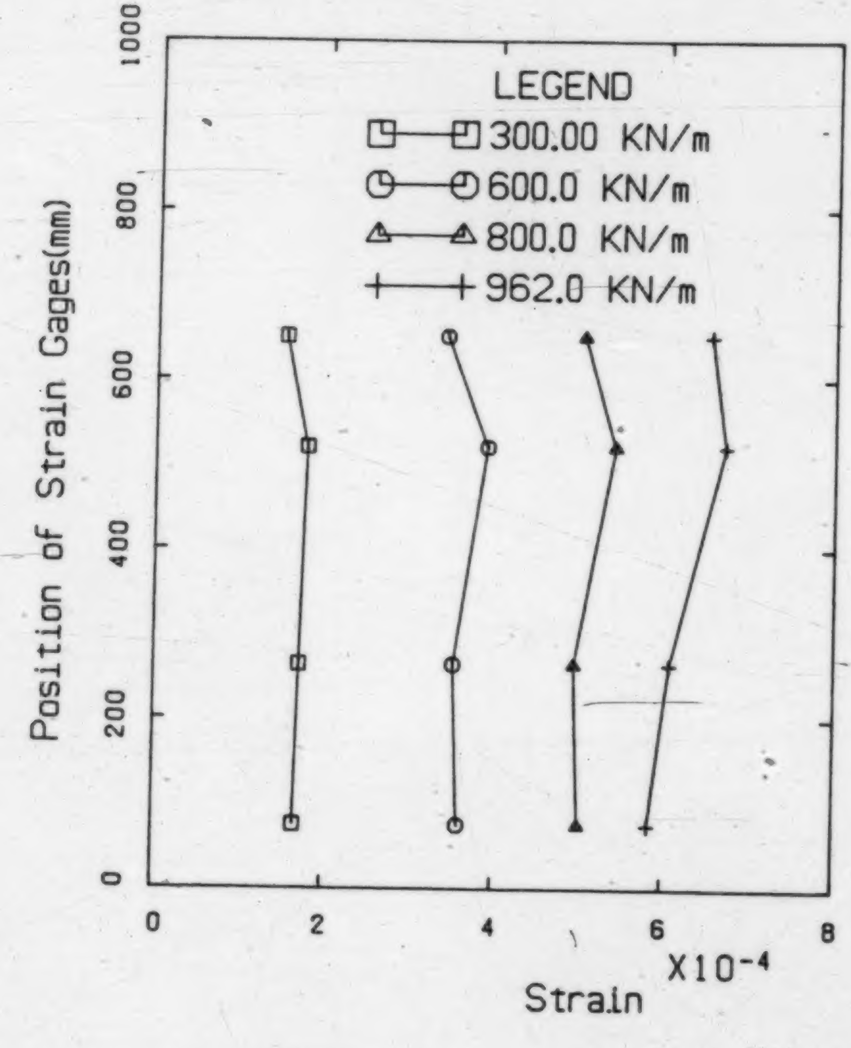

Figure 4.16 In-plane Strain Distribution for Specimen A1

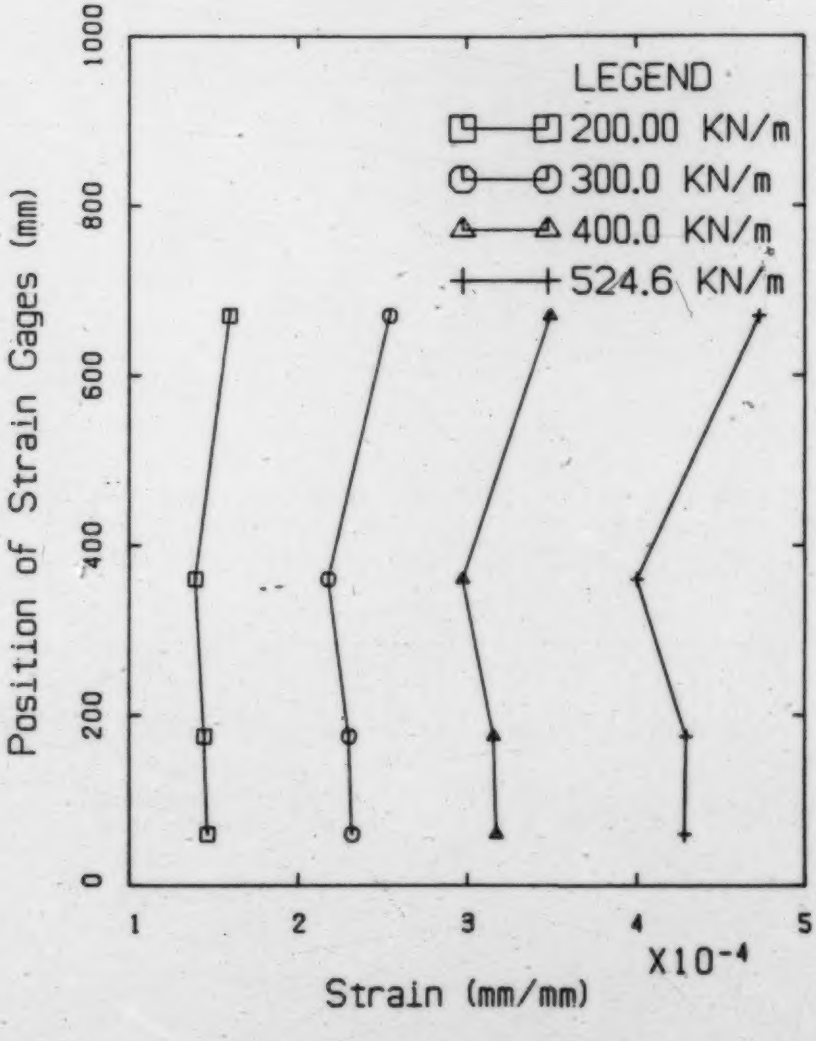

Figure 4.17 In-plane Strain Distribution for Specimen D1

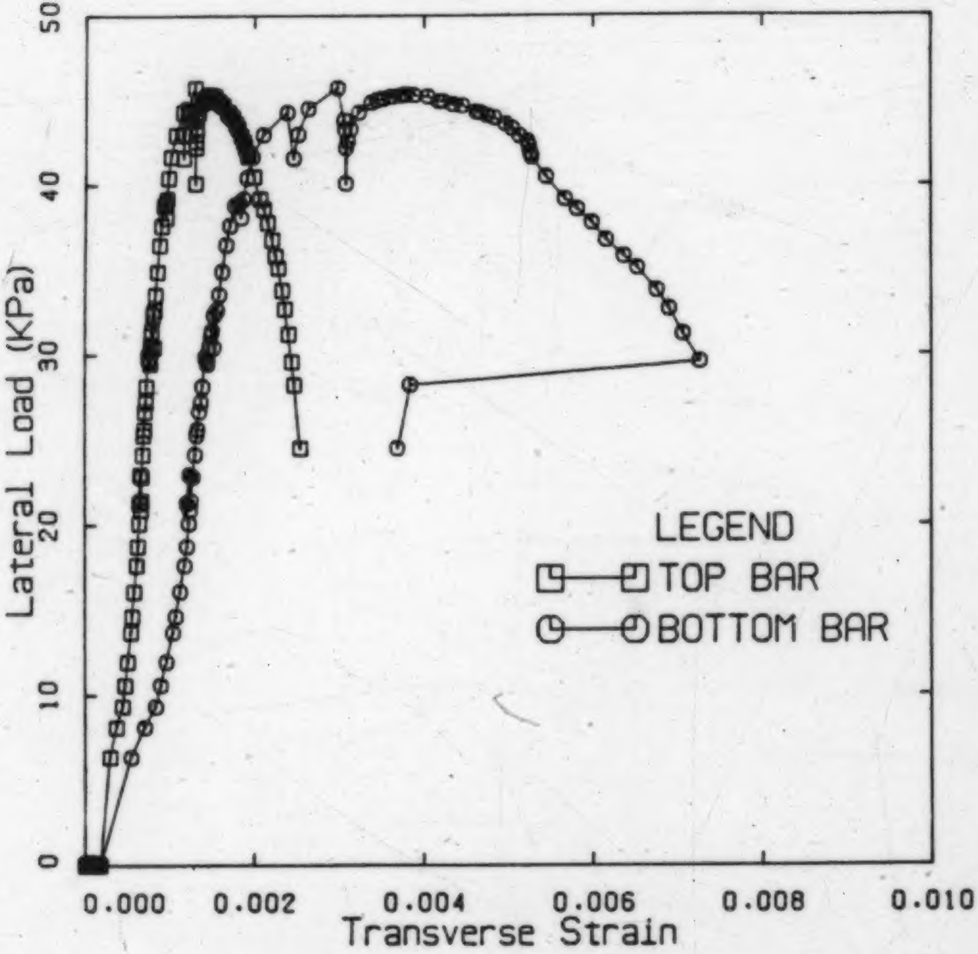

Figure 4.18 Lateral Load vs Transverse Steel Strains

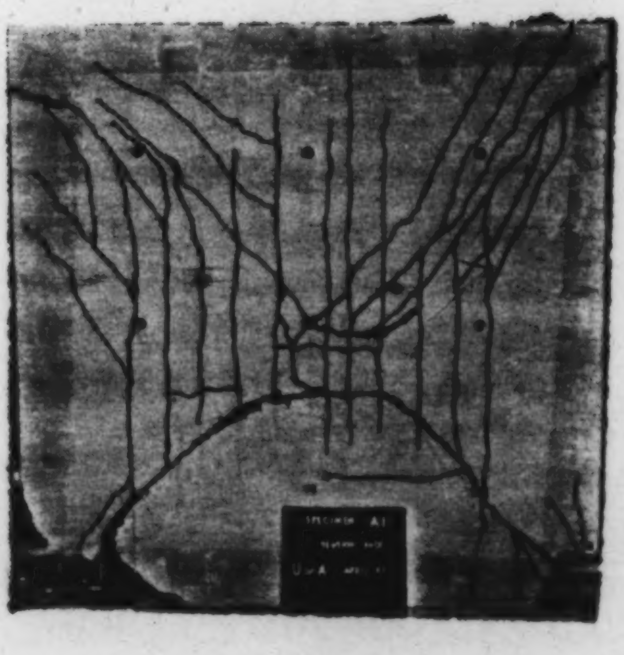
SPECIMEN A1
U of A

Plate 4.1 Tension Face of Specimen A1 After Failure, y Direction vertical

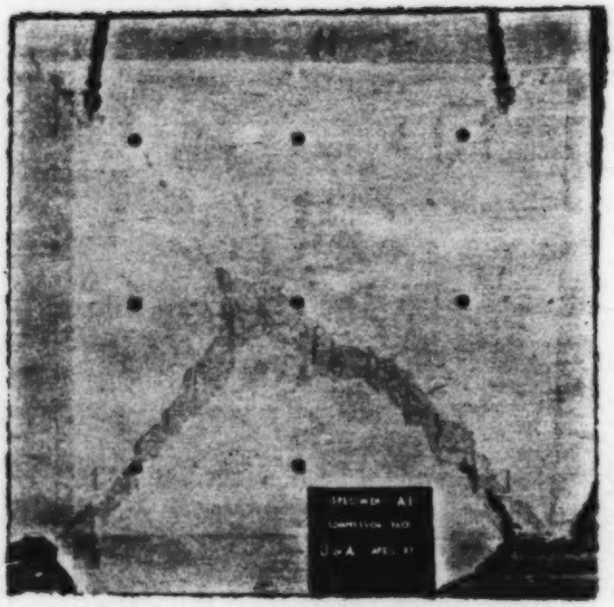
SPECIMEN A1
COMPRESSION FACE

Plate 4.2 Compression Face of Specimen A1 After Failure, y Direction vertical

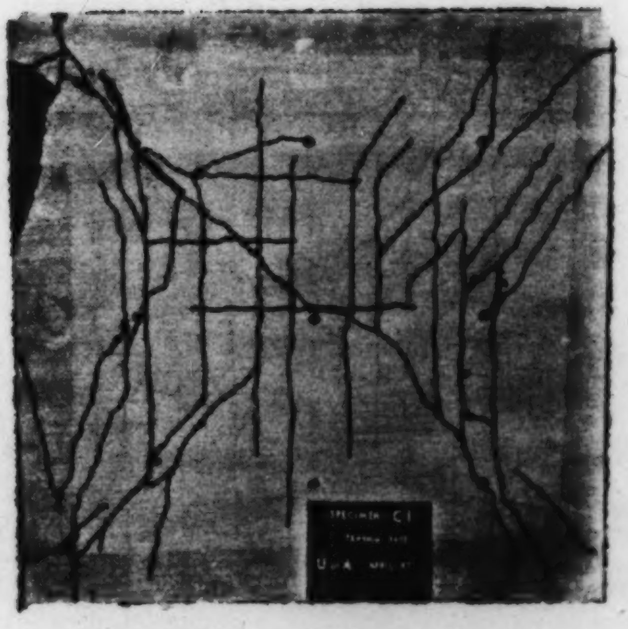
SPECIMEN C1

Plate 4.3 Tension Face of Specimen C1 After Failure, y Direction vertical

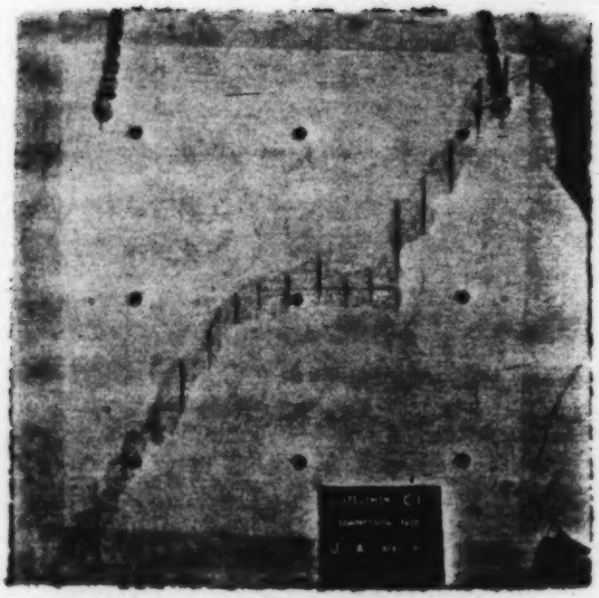

Plate 4.4 Compression Face of Specimen C1 After Failure, y Direction vertical

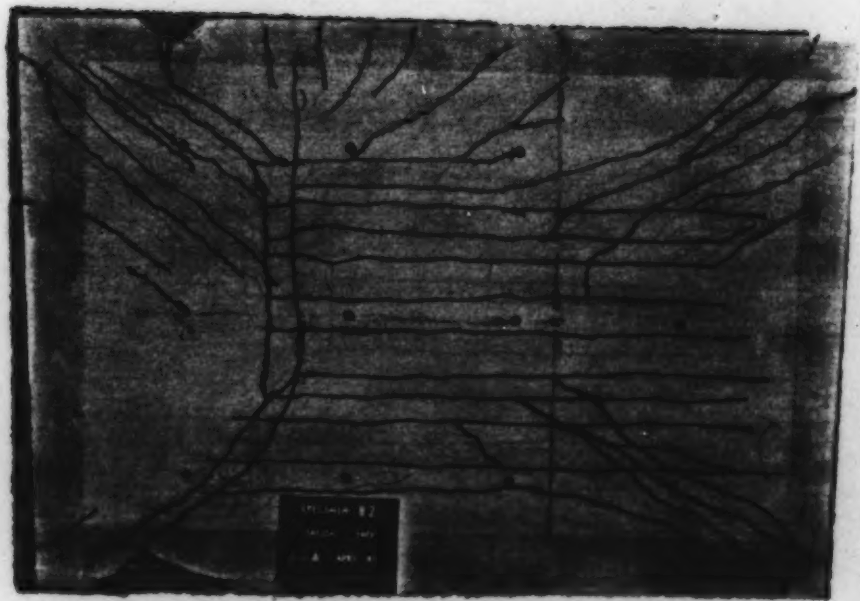

Plate 4.5 Tension Face of Specimen B2 After Failure, y Direction horizontal

Plate 4.6 Compression Face of Specimen B2 After Failure, y Direction horizontal

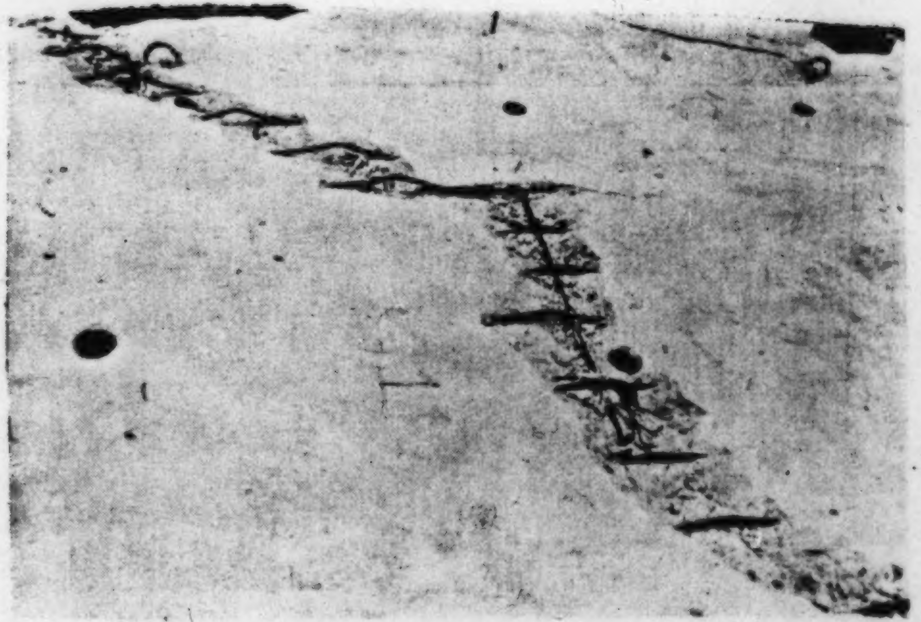

Plate 4.7 Buckling of Compression Reinforcement after Failure, y Direction horizontal

5. ANALYSES, DESIGN AND DISCUSSION OF RESULTS

5.1 Introduction

There are a number of possible approaches for the analysis of concrete plates under combined in-plane and lateral loads. These are :

1. Classical Methods-

   Classical elastic theory analysis applies to plates which are sufficiently thin for shear deformations to be insignificant. The distributions of moments and shears found by elastic theory are such that:

   - The equilibrium conditions are satisfied at every point in the plate.
   - The boundary conditions are complied with.
   - Stress is proportional to strain; that is bending moments are proportional to curvature.

   The governing equation is a fourth order partial differential equation in terms of the deflection at a general point (x,y) on the plate, and flexural/torsional rigidity of the plate section.

   Several analytical techniques such as the Levy and Fourier series methods (Timoshenko and Woinowsky-Krieger, 1959) have been used to solve this differential equation. To use this method for the analysis of a reinforced concrete plate would require some modifications to include the effects of material nonlinearities.

2. Lower Bound Limit Analysis.

A valid lower bound solution should satisfy equilibrium, the boundary conditions, and the strength of the plate section should not be exceeded anywhere in the plate. Several lower bound methods have been proposed for simply supported reinforced concrete plates under lateral loads only (Kemp,1962; Holmes and Steel,1964; Nielsen,1971). These involved expressions for the moment field and substituting these into the equilibrium equation for the plate. Subba Rao *et al.*(1977) developed a rational solution for laterally loaded rectangular orthotropic slabs for any combination of clamped and simply supported edge conditions.

This method can be extended to the analysis of plates under combined lateral and compressive in-plane loads by including the effect of in-plane load in the equilibrium equation and using moment curvature relationships for the plate sections in the two orthogonal directions.

3. Numerical Methods

The bending and torsional moments and deflections of a reinforced concrete plate with given dimensions, steel content, and material properties at any stage of loading from zero to ultimate load, can be determined numerically by finite elements, finite difference and grillage methods using conditions of static equilibrium and geometric compatibility if the moment-deformation characteristics and the yield criteria for bending and torsional moments of the plate elements are known. In such an analysis of the complete behavior of plates, difficulties are caused by the nonlinearity of the moment curvature relationships of the plate elements at high stress levels and the geometric nonlinearities which result from the influence of deformations on the total moments in the presence of in-plane loads. As a result a step-by-step procedure with the load increased incrementally is generally necessary.

At low levels of load, the plate elements are uncracked and the actions and deformations can be computed from elastic theory using the uncracked flexural rigidity of the plate elements. The plate elements are searched at each load increment to ascertain whether cracking of concrete has taken place. When it is found that the cracking moment has been reached, the flexural rigidity of the element is recomputed using the moment curvature relationship of the element. This requires the computation to be repeated at each load level until the flexural rigidity of each element has stabilized. The ultimate load is reached when deflections occur without further increase in load and hence further load cannot be carried.

It is evident that the analysis of reinforced concrete plates under combined lateral and in-plane loads using numerical based methods is lengthy and very costly and can only be successfully carried out with the aid of a computer with large storage capabilities.

In this thesis, a simple analytical model based on a modified lower bound limit analysis approach is developed. Material nonlinearities are taken into account using moment curvature relationships which include tension stiffening effects.

5.2 Moment-Load-Curvature Relationships

The moment-load-curvature (M-N-ϕ) relationships are calculated using a method similar to that of Pfrang *et al.*(1964) except that tension stiffening is included. The following assumptions were made in deriving the M-N-ϕ relationships for the reinforced concrete sections:

1. The section is rectangular.
2. For the purpose of defining the stress-strain response of concrete, the stress-strain curves defined by Eqns. 5.1 and 5.2 are assumed to define the behavior in compression and tension respectively, in members loaded in flexure or combined axial load and bending (Todeschini, *et al.* 1964). A typical stress-strain curve in compression is shown in Fig. 5.1.

$$f_c = f'_c \left(\frac{2\,X}{1 + X^2}\right) \qquad [5.1]$$

$$f_t = f'_t \left(\frac{\varepsilon}{\varepsilon_{ult}}\right) \qquad [5.2]$$

where,

$$X = \frac{\epsilon}{\epsilon_o} \qquad [5.3]$$

and the concrete strain at maximum stress is

$$\epsilon_o = \frac{2\ f'_c}{E_c} \qquad [5.4]$$

The ultimate tensile strain is given as:

$$\epsilon_{ult} = \frac{f'_t}{E_c} \qquad [5.5]$$

3. The stress strain curve for steel is as shown in Fig 3.2.
4. At all loads, plane sections remain plane.
5. The in-plane load is assumed to be applied first and held constant while the moments are increased to their failure values.
6. The maximum concrete stress f'_c is taken as 85 percent of the cylinder strength of the concrete, f'_c.
7. Concrete loaded in combined bending and compression is assumed to fail at a limiting strain of 0.0038.
8. The stress of reinforcing bars in compression is taken as $f_s - f_c$.
9. There is perfect bond between steel and concrete.
10. Creep and shrinkage strains are neglected.

11. The measured modulus of elasticity E_c of each specimen is used.
12. The measured tensile strength f'_t of each specimen is used.
13. The moment-curvature relationship for bending about one axis is independent of moments about an orthogonal axis.
14. The in-plane load is assumed to act through the mid-depth of the section.

Several of these assumptions are discussed in Section 5.5.1.

The M-N-ϕ relationship can be established using the following procedure, illustrated in Fig. 5.2. A curvature ϕ is assumed and a strain corresponding to this curvature is assumed at the top edge of the section. The neutral axis depth is given as

$$c = \frac{\epsilon 1}{\tan\phi} \qquad [5.6]$$

For small values of curvatures, Eqn. 5.6 then becomes

$$c = \frac{\epsilon 1}{\phi} \qquad [5.7]$$

The distribution of stresses across the depth of the section is then determined using appropriate stress-strain relationships for the concrete and the reinforcement. From this stress distribution, the resultant forces M and N are obtained. The procedure is repeated until the computed in-plane force is equal to the applied in-plane load. The curvature ϕ is varied and the iterative procedure repeated until the strain at the top edge is equal to 0.0038.

In this report the moment curvature relationships are obtained for a section of one meter width in both the x and y directions. In the procedure described above, the tension stiffening effect of concrete between cracks has not yet been included. A method for considering this effect in the moment curvature relationship will now be discussed.

5.2.1 Tension Stiffening

Consider a reinforced concrete member shown in Fig 5.3 subjected to a moment and in-plane load. When the stress in concrete has not exceeded its tensile strength, the member is free from cracks. The reinforcement and concrete undergo compatible strains. This is referred to as State 1. Analysis of stress and strain in State 1 is accomplished using the transformed section or modular ratio method to calculate the uncracked transformed gross stiffness and for a given moment M, the curvature ϕ_1 in State 1 can be computed.

When the tensile strength of concrete is exceeded, cracks occur. At the location of a crack, the tensile stress is assumed to be resisted completely by the reinforcement as shown in Fig. 5.3 c. The tensile zone is assumed to be fully cracked and this is referred to as State 2. The moment curvature relationship computed in the previous section corresponds to State 2. In both States 1 and 2, plane sections are assumed to remain plane after deformation and cracking. The curvature, ϕ_2 in State 2 corresponding to the moment M is known from the previously derived moment curvature relationship.

At a section situated between cracks, bond between the concrete and the reinforcing bars restrains the elongation of the steel and thus a part of the tensile force in the reinforcement at a crack is transmitted to the concrete situated between the cracks. The stress and strain or moment and curvature in the section will be in an intermediate condition between States 1 and 2. Thus, the strain in a reinforcing bar varies from a maximum value at the cracks to a minimum value midway between the cracks. The stiffness and curvature varies between consecutive cracks in a similar way. A method for computing the average curvature given by Ghali and Favre(1986) will be used here. The average curvature is:

$$\phi_m=(1-\gamma)\phi_1 + \gamma\phi_2 \qquad [5.8]$$

where ϕ_1 and ϕ_2 are the curvatures in States 1 and 2 and

$$\gamma=1.0-\beta_1\beta_2\left(\frac{M_{cr}}{M}\right)^2 \qquad [5.9]$$

M_{cr} is the cracking moment and M is the moment in State 2. β_1 equals 1.0 and 0.5 for deformed and plain bars, respectively, while β_2 equals 1.0 and 0.5, respectively, for first loading and for cyclic or sustained loads. A moment-curvature plot for a typical cross section with $\beta_1=1$ and $\beta_2=1$ is shown in Fig. 5.4.

5.3 Analytical Model

Equations for orthotropic plates derived in most text books on the theory of plates (Timoshenko,1959 ; Szilard,1974) from equilibrium and strain compatibility considerations, are needed for use in the proposed analytical model. For elastic plates, the relationships between moments and deformations are given as:

$$M_x=-D_x\left(\frac{\partial^2 w}{\partial x^2} + \nu_y\frac{\partial^2 w}{\partial y^2}\right) \tag{5.10}$$

$$M_y=-D_y\left(\frac{\partial^2 w}{\partial y^2} + \nu_x\frac{\partial^2 w}{\partial x^2}\right) \tag{5.11}$$

$$M_{xy}=2D_t\,\frac{\partial^2 w}{\partial x\partial y} \tag{5.12}$$

where,

$$2D_t=(1-\sqrt{\nu_x\nu_y})\sqrt{D_xD_y} \tag{5.13}$$

represents the torsional rigidity of the plate while D_x and D_y are the bending rigidities in the x and y directions, respectively. M_x, M_y and M_{xy} are moments per unit width. Moment M_x is taken about the y axis, while M_y is taken about the x axis. These moments are considered positive when they create a compression surface at the top of the member.

The equilibrium equation for an elastic orthotropic plate under combined lateral load $q(x,y)$ per unit area and compressive in-plane loads N_x and N_y per unit width in the x and y directions, respectively, is given as:

$$\frac{\partial^2 M_x}{\partial x^2} - 2\frac{\partial^2 M_{xy}}{\partial x \partial y} + \frac{\partial^2 M_y}{\partial y^2}$$

$$= -q(x,y) + N_x \frac{\partial^2 w}{\partial x^2} + N_y \frac{\partial^2 w}{\partial y^2} \qquad [5.14]$$

The governing differential equation for the deflection will be:

$$D_x \frac{\partial^4 w}{\partial x^4} + 2H \frac{\partial^4 w}{\partial x^2 \partial y^2} + D_y \frac{\partial^4 w}{\partial y^4}$$

$$= q(x,y) - N_x \frac{\partial^2 w}{\partial x^2} - N_y \frac{\partial^2 w}{\partial y^2} \qquad [5.15]$$

where,

$$H = 0.5\nu_x D_y + 0.5\nu_y D_x + 2D_t \qquad [5.16]$$

is called the "effective torsional rigidity" of the plate while ν_x and ν_y are the Poisson's ratios in the x and y directions, respectively.

These equations were derived based on the following assumptions:

1. Small lateral deflections are assumed. This means membrane action is neglected.
2. Plane sections remain plane after bending. This implies that the vertical shear strains are negligible and the strain ϵ_z normal to the mid-plane is omitted.
3. The stress normal to the midplane, σ_z is small compared with the other stress components and may be neglected.

4. The plate is initially flat.
5. The material is elastic and orthotropic.

Since there are material nonlinearities in a concrete plate, to use the above equations, the bending stiffness at any level of loading is taken as the moment from the M-N-ϕ relationship, divided by the corresponding curvature where the Poisson's ratio is assumed to be zero.

5.3.1 Modified Limit Analysis Method

A typical rectangular plate as considered in the analysis is shown in Fig. 5.5. The plate is of length a, width b, and uniform thickness t. The x, y, and z axes are longitudinal, transverse, and lateral respectively, where z is zero at mid-thickness. A uniform in-plane compressive force per unit length N_x is applied in the x direction to the sides of length a at an eccentricity e_x and a force per unit length N_y is applied in the y direction to the sides of length b, at an eccentricity e_y. In addition, there is a uniform lateral pressure q and at any point (x,y), w represents the total lateral displacement from the flat state. It is assumed in the analysis that the in-plane loads will be applied first and maintained at a constant value as the lateral load is applied monotonically from zero to a maximum value and then allowed to drop off steadily beyond the maximum point.

From Eqn. 5.14 the equilibrium equation for a plate under combined loads with zero in-plane shear force is:

$$\frac{\partial^2 M_x}{\partial x^2} - 2\,\frac{\partial^2 M_{xy}}{\partial x \partial y} + \frac{\partial^2 M_y}{\partial y^2}$$

$$= -q(x,y) + N_x \frac{\partial^2 w}{\partial x^2} + N_y \frac{\partial^2 w}{\partial y^2} \qquad [5.17]$$

To obtain a possible lower bound solution using the above equation, the loads on the right hand side can be arbitrarily proportioned between the terms on the left hand side as follows (Subba Rao *et al.*, 1977):

$$\frac{\partial^2 M_x}{\partial x^2} = -q_x + N_x \frac{\partial^2 w}{\partial x^2} \qquad [5.18]$$

$$\frac{\partial^2 M_y}{\partial y^2} = -q_y + N_y \frac{\partial^2 w}{\partial y^2} \qquad [5.19]$$

$$-2\,\frac{\partial^2 M_{xy}}{\partial x \partial y} = -q_{xy} \qquad [5.20]$$

where,

$$q = q_x + q_y + q_{xy} \qquad [5.21]$$

Integrating Eqns. 5.18 through 5.20 give,

$$M_x = -0.5 q_x x^2 + N_x w + A(y)x + Rx + B(y) + T \qquad [5.22]$$

$$M_y = -0.5 q_y y^2 + N_y w + C(x)y + Vy + D(x) + Z \qquad [5.23]$$

$$2M_{xy} = q_{xy} x.y + E(x) + F(y) + G \qquad [5.24]$$

where C(x), D(x) and E(x) are arbitrary functions of x while A(y), B(y) and F(y) are arbitrary functions of y and G, R, T, V and Z are integration constants. Their values depend on the boundary conditions. Simple support conditions without in-plane restraints will be considered. Mathematically these conditions are:

At $x=\pm\frac{b}{2}$,

$$M_x=N_x e_x \qquad [5.25]$$

$$w= 0 \qquad [5.26]$$

At $y=\pm\frac{a}{2}$,

$$M_y= N_y e_y \qquad [5.27]$$

$$w= 0 \qquad [5.28]$$

At x=0 and y=0,

$$M_{xy};\ \frac{\partial M_x}{\partial x};\ \frac{\partial M_y}{\partial y}= 0 \qquad [5.29]$$

The condition of zero shear along the axes gives

At x=0,

$$\frac{\partial M_{xy}}{\partial y}= 0 \qquad [5.30]$$

At y=0,

$$\frac{\partial M_{xy}}{\partial x}= 0 \qquad [5.31]$$

Satisfaction of these boundary conditions in Eqns. 5.22 through 5.24 give

$$M_x= -0.5\ q_x x^2 + N_x w + 0.125\ q_x b^2 + N_x e_x \qquad [5.32]$$

$$M_y= -0.5\ q_y y^2 + N_y w + 0.125\ q_y a^2 + N_y e_y \qquad [5.33]$$

$$2M_{xy} = q_{xy}x.y \qquad [5.34]$$

Assume a deflection function for the lateral deflection that satisfies the boundary conditions as:

$$w = w_0 \cos\frac{\pi x}{b} \cos\frac{\pi y}{a} \qquad [5.35]$$

where, w_o is the maximum lateral deflection and occurs at the center of the plate. The maximum bending moments occur at x=0 and y=0, while the maximum twisting moments occurs at the plate corners. These maximum moments are:

$$M_{xm} = N_x w_o + 0.125\ q_x b^2 + N_x e_x \qquad [5.36]$$

$$M_{ym} = N_y w_o + 0.125\ q_y a^2 + N_y e_y \qquad [5.37]$$

$$M_{xym} = 0.125\ q_{xy} a.b \qquad [5.38]$$

The curvatures can be approximated by the second derivative of the deflection function. In concrete members, material failure will occur long before this assumption is invalidated (Alcock and Nathan, 1977). Thus the curvatures in the x and y directions, respectively, are

$$\phi_x = -\frac{\partial^2 w}{\partial x^2} \qquad [5.39]$$

$$\phi_y = -\frac{\partial^2 w}{\partial y^2} \qquad [5.40]$$

and the twist is,

$$\phi_{xy} = \frac{\partial^2 w}{\partial x \partial y} \qquad [5.41]$$

Using Eqns. 5.35 and 5.39 through 5.41, we obtain,

$$\phi_{xo} = \frac{w_o \pi^2}{b^2} \qquad [5.42]$$

$$\phi_{yo} = \frac{w_o \pi^2}{a^2} \qquad [5.43]$$

$$\phi_{xyo} = \frac{w_o \pi^2}{ab} \qquad [5.44]$$

where ϕ_{xo} and ϕ_{yo} are the maximum curvatures in the x- and y-directions, respectively, and occur at the center of the plate. ϕ_{xyo} is the maximum twist in the plate and occurs at the corners. From Eqns. 5.42 to 5.44:

$$\phi_{xo} = \frac{a^2 \ \phi_{yo}}{b^2} \qquad [5.45]$$

$$\phi_{xyo} = \frac{a \ \phi_{yo}}{b} \qquad [5.46]$$

To satisfy equilibrium between the maximum external and maximum internal resisting moments, Eqns. 5.36 to 5.38 become, after rearranging and using Eqns. 5.42 and 5.43,

$$q_x = \frac{8}{b^2}\left(M_{xi} - \frac{N_x b^2 \phi_{xo}}{\pi^2} - N_x e_x\right) \qquad [5.47]$$

$$q_y = \frac{8}{a^2}\left(M_{yi} - \frac{N_y a^2 \phi_{yo}}{\pi^2} - N_y e_y\right) \qquad [5.48]$$

$$q_{xy} = \frac{8 \ M_{xyi}}{ab} \qquad [5.49]$$

where M_{xi}, M_{yi} are the internal resisting bending moments at the center of the plate in the x and y directions, respectively, and M_{xyi} is the internal resisting twisting moment at the plate corners. Eqns. 5.10 through 5.13 and 5.42 through 5.46 while assuming Poisson's ratio to be zero, which is rational for a cracked reinforced concrete plate (Park and Gamble, 1980), give,

$$M_{xi} = D_x \ \phi_{xo} \qquad [5.50]$$

$$M_{yi} = D_y \ \phi_{yo} \qquad [5.51]$$

$$M_{xyi} = \sqrt{D_x D_y} \ \phi_{xyo} \qquad [5.52]$$

From the above equations, we obtain

$$M_{xyi} = \sqrt{M_{xi} M_{yi}} \qquad [5.53]$$

Eqn. 5.53 is identical to the twisting resistance obtained from Johansen's normal moment yield criterion (Park and Gamble, 1980) for the case where the x and y moments are zero as in the corners of a simply supported plate. Substituting Eqns. 5.53 into 5.49 and using Eqn. 5.21 we obtain the total lateral load versus curvature relationship as given in Eqn. 5.54.

$$q = \frac{8}{b^2}\left(M_{xi} - \frac{N_x b^2 \phi_{xo}}{\pi^2} - N_x e_x\right) +$$

$$\frac{8}{a^2}\left(M_{yi} - \frac{N_y a^2 \phi_{yo}}{\pi^2} - N_y e_y\right) +$$

$$\frac{8\sqrt{M_{xi}M_{yi}}}{ab} \qquad [5.54]$$

For zero in-plane loads Eqn. 5.54 is identical to the equations derived for slabs under lateral loads only by Kemp (1962) and Subba Rao *et al.* (1977).

Up to this point the plate has been assumed to be perfectly flat. Since initial imperfections are always present, a method for including the effects of initial deflections in the analysis will now be discussed. Assume the initial deflections are of the form

$$w_i = w_{io}\cos\frac{\pi x}{b}\cos\frac{\pi y}{a} \qquad [5.55]$$

where w_{io} is taken as positive if the initial deflection is in the same direction as the final deflected shape and negative otherwise. The effect of the interaction between. the in-plane load and the initial deflection is equivalent to the effect of a fictitious lateral load (Timoshenko, 1959) given as

$$q_{eqiv} = -N_x\frac{\partial^2 w_i}{\partial x^2} - N_y\frac{\partial^2 w_i}{\partial y^2} \qquad [5.56]$$

This equivalent lateral load is added to the lateral load q(x,y) in Eqn. 5.17 and the procedures from Eqns. 5.18 through 5.55 will yield the final equation given as

$$q = \frac{8}{b^2}\left(M_{xi} - \frac{N_x b^2(\phi_{xo}+\phi_{xio})}{\pi^2} - N_x e_x\right) +$$

$$\frac{8}{a^2}\left(M_{yi} - \frac{N_y a^2(\phi_{yo}+\phi_{yio})}{\pi^2} - N_y e_y\right) +$$

$$\frac{8\sqrt{M_{xi}M_{yi}}}{ab} \qquad [5.57]$$

where,

$$\phi_{xio} = \frac{w_{io}\pi^2}{b^2} \qquad [5.58]$$

and

$$\phi_{yio} = \frac{w_{io}\pi^2}{a^2} \qquad [5.59]$$

are the maximum initial curvatures in the x and y directions, respectively.

The procedure for obtaining the total lateral load, q, for a given set of in-plane loads N_x and N_y per unit width is as follows:

1. Obtain the M-N-ϕ relationships for a section of unit width at the center of the plate in the x and y directions for the given values of N_x and N_y as done in Section 5.2.
2. Obtain maximum initial deflection and hence maximum initial curvatures in the x and y directions, respectively from Eqns. 5.58 and 5.59.
3. Assume a value for ϕ_{yo}.
4. From Eqn. 5.45 determine ϕ_{xo}.
5. From the M-N-ϕ relationship derived in step (1) obtain M_{xi} and M_{yi} corresponding to ϕ_{xo} and ϕ_{yo}, respectively.

6. Compute the lateral load for a given ϕ_{yo} using Eqn. 5.57.
7. Increment ϕ_{yo} and repeat steps (3) through (5).

This gives a plot of lateral load, q versus the maximum curvature in the y direction, ϕ_{yo}. The peak of this curve is taken as the lateral load capacity.

5.4 Design Method

Though a nonlinear stability analysis such as presented in the previous section is desirable for plates under combined loads as a final step in the design process, there remains a need for a simple design procedure. This is useful for the initial selection of the reinforcement and dimensions of the plate. The ACI code presents a moment magnifier method for analysing the effects of slenderness on the strength of columns. For braced columns with lateral loads acting between the ends of the column, and assuming the member resistance factor as 1.0, the magnified moment is given as

$$M_c = \delta_b \, M_2/\phi \qquad [5.60]$$

where the magnification factor

$$\delta_b = \frac{1.0}{1.0 - P_f/\phi P_{cr}} \qquad [5.61]$$

where ϕ is the capacity reduction factor. This is normally used to account for such things as variability of the material, construction tolerances and design assumptions. A value of 0.9 is used for zero axial loads and 0.7 for axially loaded columns. M_1 is the first order moment due to lateral loads and in-plane load eccentricity while P_{cr} is the critical load of the column and P_f is the factored axial load.

Design equations similar to Eqn. 5.60 will now be derived for simply supported concrete plates under combined loads using the Fourier series approach.

5.4.1 Formulation

In the following development it is convenient to use a set of axes different from that shown in Fig. 5.5. Assume a Fourier series expansion for the lateral deflection and lateral load as

$$w=\sum_{m=1}^{\infty}\sum_{n=1}^{\infty} A_{mn}\sin m\pi\bar{x}/b \sin n\pi\bar{y}/a \qquad [5.62]$$

and

$$q(\bar{x},\bar{y})=\sum_{m=1}^{\infty}\sum_{n=1}^{\infty} \frac{16q}{\pi^2 mn}\sin m\pi\bar{x}/b \sin n\pi\bar{y}/a \qquad [5.63]$$

The relationship between the two sets of axes is

$\bar{x}= x + b/2$, and

$\bar{y}= y + a/2$.

Substituting Eqns. 5.62 and 5.63 into Eqn. 5.15 and simplifying gives

$$A_{mn}=\frac{16q}{\pi^2 mnD^*(1.0 - N_x m^2\pi^2/b^2D^* - N_y n^2\pi^2/a^2D^*)} \qquad [5.64]$$

where

$$D^*=\frac{D_x m^4\pi^4}{b^4}+\frac{2Hm^2n^2\pi^4}{a^2b^2}+\frac{D_y n^4\pi^4}{a^4} \qquad [5.65]$$

The effective torsional rigidity H is obtained from Eqn. 5.16 where Poisson's ratio is assumed to be zero. Substituting Eqn. 5.64 into Eqn. 5.62 gives

$$w=\sum_{m=1}^{\infty}\sum_{n=1}^{\infty}\frac{1.621qAMPF}{\pi^2 mnD^*}\sin m\pi\bar{x}/b \sin n\pi\bar{y}/a \qquad [5.66]$$

where AMPF is a moment amplification factor for the plate. The maximum moment in the y direction is given as

$$M_{ym}=D_y\sum_{m=1}^{\infty}\sum_{n=1}^{\infty}\frac{16qnAMPF}{ma^2D^*}\sin m\pi/2 \sin n\pi/2 \qquad [5.67]$$

where

$$\frac{1}{AMPF}=1-\frac{N_x}{D^*b^2/m^2\pi^2}-\frac{N_y}{D^*a^2/n^2\pi^2} \qquad [5.68]$$

Comparing Eqns. 5.67 and 5.68 with Eqn. 5.60, we can rewrite the former equations as

$$M_{ym}=\text{AMPF } M_{y1}/\phi \qquad [5.69]$$

$$\text{AMPF}=\frac{1.0}{\lambda} \qquad [5.70]$$

and

$$\lambda=1.0-\frac{N_x}{\phi N_{xcr}}-\frac{N_y}{\phi N_{ycr}} \qquad [5.71]$$

where ϕ is the capacity reduction factor while N_{xcr} and N_{ycr} are the plate buckling loads per unit width in the x and y directions, respectively. These are obtained using the method of Swartz and Rosebraugh (1974). M_{y1} is the maximum moment in the y direction due to lateral loads. This is expressed as

$$M_{y1}= C_y\, qa^2 \qquad [5.72]$$

The coeficient C_y is tabulated by Timoshenko and Woinowsky-Krieger (1959) for given values of θ, where

$$\theta=\frac{b}{a}\left(\frac{D_y}{D_x}\right)^{0.25} \qquad [5.73]$$

In the proposed design method, the quantity $\alpha = D_y/D_x$ is required in order to calculate M_{y1}. The values of α at maximum lateral loads obtained with the developed analytical model were computed. These values were found to be reasonably predicted as shown in Table 5.1 by

$$\alpha = \frac{M_{yb} a^2}{M_{xb} b^2} \qquad [5.74]$$

where M_{xb} and M_{yb} are the moments at balanced failure in the x and y directions, respectively. In calculating these balanced moments, the area of compression reinforcement can be neglected for simplicity. The yield stress of the reinforcement used in the tests was assumed as the stress at a strain of 0.0035 as recommended by the ACI code. Having obtained the design moment in the y direction, M_{ym}, the moment in the x direction and the twisting moments are obtained from

$$M_{xm} = \frac{a^2}{b^2 \alpha} M_{ym} \qquad [5.75]$$

$$M_{xym} = \sqrt{M_{xm} M_{ym}} \qquad [5.76]$$

The recommended design procedure is as follows:

1. Assume dimensions for the plate.
2. Compute the applied factored in-plane and lateral loads.
3. Assume areas of reinforcement in the x and y directions.

4. Compute α from Eqn. 5.74

5. Compute θ from Eqn. 5.73

6. Compute M_{y1} from Eqn. 5.72

7. Calculate the buckling loads N_{xcr} and N_{ycr} neglecting the effect of reinforcement as shown below (Swartz and Rosebraugh, 1974):

$$R_y = \frac{\pi^2(1+p^2)^2t^2}{6\epsilon_o p^2 b^2}$$

$$R_x = \frac{\pi^2(1+z^2)^2t^2}{6\epsilon_o z^2 a^2}$$

where

$p = a/b$, if a/b is less than or equal to 1.0

$p = 1$, if a/b is greater than or equal to 1.0

$z = b/a$, if b/a is less than or equal to 1.0

$z = 1$, if b/a is greater than or equal to 1.0

$$N_{xcr} = 0.425tf'_cR_x\{-R_x + (4 + R_x^2)^{0.5}\}$$

$$N_{ycr} = 0.425tf'_cR_y\{-R_y + (4 + R_y^2)^{0.5}\}$$

where t is the plate thickness while a and b are the lengths of the plate in the y and x directions, respectively.

8. Calculate the magnified moment M_{ym} using Eqns. 5.69

through 5.71, assuming a ϕ value of 0.9 for zero in-plane loads and 0.70 otherwise.

9. Calculate M_{xm} and M_{xym} from Eqns. 5.75 and 5.76.
10. Calculate the section capacities in the x and y directions using the assumed areas of reinforcement. These are M_{xu} and M_{yu} while the twisting moment capacity capacity, M_{xyu} is taken as the square root of the product of the section capacities in the x and y directions.
11. If the magnified moments M_{xm}, M_{ym} and M_{xym} are less than the section capacities M_{xu}, M_{yu} and M_{xyu}, respectively, then the design is safe.

5.5 DISCUSSION AND ANALYSIS OF RESULTS

In this section, test results are discussed in relation to the proposed analytical model and design method. The assumptions made in the model are discussed followed by a treatment of initial imperfections. Finally, comparisons are made between the measured maximum lateral loads and those obtained from the analytical model and the design method.

5.5.1 Assumptions in Analytical Model

5.5.1.1 Small Deflection Theory

The proposed model assumes small deflection theory. If the edges of a plate are restrained in the in-plane directions, membrane action becomes significant when the lateral deflection exceeds approximately half the plate thickness. If the edges are free from in-plane restraints, membrane action becomes significant typically at a deflection larger than the plate thickness. Small deflection theory is applicable if the maximum deflection is not greater than 75 percent of the plate thickness (Hughes, 1983). Since the maximum deflection obtained at maximum lateral loads, for the combined loaded specimens was not greater than 75 percent of the plate thickness (Table 5.2), it is considered reasonable to neglect membrane effects in the analysis of these specimens. However, for specimen A3 large deflection behavior was observed as the maximum load was approached.

5.5.1.2 Deflected Shape

In the analysis, a double cosine function was used to represent the vertical deflection of the plate surface. Figs. 5.6 through 5.9 show comparisons between measured deflected shapes and the cosine function assumed in the analysis. A reasonably good agreement is indicated by these figures for the square and rectangular specimens.

5.5.1.3 Poisson s Ratio

In the analysis, Poisson's ratio was assumed to be zero. The effect of Poisson's ratio on a cracked reinforced concrete plate will be less than that of a homogeneous plate, because the tensile stress elements in the plate consist of crossing, discrete reinforcing bars which are not connected together. Therefore, the stress in the steel in the x direction can affect the stress in the steel in the y direction only by being transmitted through the concrete. Due to cracking and the large differences in the modulus of elasticity for steel and concrete, this would not be an efficient transfer. The true value of Poisson's ratio actually varies over the area of the plate depending on the extent of cracking. The value of 0.15 sometimes used, would apply only to an uncracked plate and should approach zero as the plate approaches the fully cracked state.

5.5.1.4 Independence of Moment Curvature Diagrams For Two Axes

In computing the moment curvature diagrams, it was assumed that the moments about the x axis did not affect the load-moment-curvature diagram for moments about the y axis and vice-versa. The concrete in the compression zone is stressed in biaxial compression. The effect of Poisson's ratio has been discussed in the preceeding section. Biaxial compressive stresses lead to an increase of up to 20 percent in the compressive strength in each direction (Kupfer *et al.*, 1969). Vebo and Ghali (1977) presented a method for computing the moment curvature relationship for concrete slab elements orthotropically reinforced with top and/or bottom steel and subjected to a general state of applied moment.

Poisson's ratio and biaxial stress effects were neglected in their analysis. Tension stiffening effects were considered. They reported good agreement between their results and available test results. Park and Gamble (1980) have also shown the effects of biaxial stresses on the moment capacity of a slab to be quite small. Thus in the proposed analytical model, the effects of biaxial stresses was ignored.

5.5.1.5 Initial Imperfections

During application of the in-plane load, deflections were recorded for several points on the plate surface. All readings were relative to zero lateral loaad position, therefore there was no knowledge of actuaal initial deflections. The deflected shape measured at the maximum in-plane load before any lateral load was applied is assumed to be the initial deflected shape of the plate. Initial deflected shapes for specimens A2 and B2 in the x and y directions, respectively are shown in Figs. 5.10 through 5.13. A cosine deflected shape in each direction was assumed in the analysis. The maximum deflection was chosen by equating the areas under the measured and assumed deflected shapes. Table 5.3 gives the maximum computed initial deflections for each specimen. In the tests, the maximum initial deflection never exceeded about 7 percent of the deflection at peak lateral load.

5.5.2 Comparison of Analytical Predictions With Test Results

Table 5.4 compare the maximum lateral loads from the proposed model with the maximum loads obtained from the tests. The measured maximum loads are reasonably well predicted by the analytical model. The average test-to-predicted ratio is 1.033 and the standard deviation is 3.9 percent.

Specimens C1 and C2 are the only values less than 1.0. These specimens differ from the A series in that the areas of steel in the two directions were different. C1 was tested under proportional loading, C2 in the normal fashion. The comparison between the design capacity assuming a ϕ factor of 1.0 and the measured values is shown in Table 5.5. An acceptable prediction was obtained. Figs. 5.14 through 5.22 show comparisons between the analytical and test load-deflection curves. In the ascending branch of the load-deflection curves, the figures indicate a fairly good agreement between test and analysis except in specimens A3, B1 and B2. In Specimens B1 and B2 the deviation between analysis and test results increases as the peak load is approached. These specimens were rectangular with a length parallel to the in-plane loading of 1.5 times the width. As a result the lateral load is resisted more by bending in the x direction. However, the second order effect of the in-plane load is more in the y direction. Since the maxima of these effects did not occur in the same direction, there was a tendency towards a material failure mode in these specimens as opposed to the instability failure mode predicted by the analysis.

5.5.3 Lateral load capacity of specimens for zero in-plane load

To estimate the reduction in load capacity due to the presence of in-plane loads, the proposed model was used to analyze the specimens for the case of zero in-plane load. Table 5.6 shows the percentage reduction in capacity due to the presence of in-plane loads. For all the plates tested, the presence of in-plane loads led to a reduction in the lateral load capacity, the highest reduction being 45.3 percent in specimen D2.

5.5.4 Effects of Various Parameters

- Effect of width-to-thickness ratio, b/t

All specimens except D1 and D2 had b/t ratios in the range of 28. These two specimens had b/t values about 33. They had same reinforcement as A1 to A3. The test results and analytical predictions indicate that for a given in-plane load, a lower lateral load capacity is obtained with a higher b/t ratio. This is to be expected since, with constant reinforcement the flexural capacity and flexural stiffness decrease as the thickness decreases. As a result the effects of geometric nonlinearities due to in-plane load increase with an increase in the slenderness of the plate.

- Effect of ρ_x/ρ_y ratio.

The A series specimens had approximately the same area of reinforcement in both the x and y directions while in the C series specimens the area in the x direction was about half that in the y direction. Comparing specimens A2 and C2 which had the same in-plane load, it was found that specimen A2 carried about 15 percent more load than specimen C2. From this limited comparison, it seems advantageous to use equal amount of reinforcement in both the x and y directions.

- Effect of Load History.

Two specimens (C1 and C2) were subjected to different load histories in order to study the effect of load history on the load carrying capacity of the plate. For specimen C2, the in-plane load was applied first and held constant while lateral load was applied until failure, while for specimen C1, the in-plane and lateral loads were applied simultaneously. For specimen C1, the ratio of the applied lateral load to in-plane load was chosen equal to the ratio of maximum lateral load to maximum in-plane load for specimen C2 which had been tested earlier. Specimen C1 carried about 6 percent more lateral load and 8 percent more in-plane load than specimen C2. From this limited comparison it appears that there is little difference in the load capacity for these two load histories. A similar behavior has been observed for steel and concrete beam-columns. Galambos and Ketter (1959) carried out a theoretical analysis on steel beam-columns in which bending was applied from zero to the full value while the pre-applied axial load was held constant. The analysis was found to correlate well with test results in which bending and axial loads were applied simultaneously. Nathan (1985) also observed that as long as the loading on a beam-column was monotonic, the ultimate load is not affected by the loading history. It can be expected, that the conclusion for the beam-column problem may be extended to the case of plates. Therefore, the developed method of analysis can be applied to plates under simultaneously applied in-plane and lateral loads.

- Effect of Axial Load Level

Table 5.7 shows the ratio of in-plane load to the balanced failure load for a section of unit width in the y direction for each specimen. Specimen A3 had no in-plane load and specimens A2, D1, D2 and B2 had in-plane loads between 0.78 to 0.95 times the balanced load while specimens A1, B1, C1 and C2 had in-plane loads of 1.08 to 1.25 times the balanced loads. As a result, the load-moment-curvature diagrams for bending about the x axis showed a small amount of ductility for the first group but not for the second. The load-moment-curvature diagrams for bending about the y axis were ductile in all cases.

Comparing the two rectangular specimens tested, the lateral load capacity was found to decrease with an increase in the in-plane load. This is seen also in the lateral load vs in-plane load interaction diagram for specimen B2 obtained using the developed analytical model and shown in

Fig. 5.23. From the interaction diagram for specimen D2 shown in Fig. 5.24, a similar conclusion can be drawn. Plates with high length-to-thickness ratios such as specimens B1 and B2 would tend to have close to a straight line interaction between lateral and in-plane loads. In the tests, specimen A1 had the lowest length-to-thickness ratio with a value of 27.30. The interaction diagram for plates with low length-to-thickness ratios would approach that of specimen A1 shown in Fig. 5.25. The figure indicates that for certain levels of in-plane load, an increase in lateral load capacity is obtained with an increase in the in-plane load. Due to the shape of the interaction curve of a reinforced concrete cross section for low values of axial load, the ultimate moment capacity of a section increases with increasing axial load. Hence axial load may be favorable if the length-to-thickness ratio is not very high.

-Effect of Aspect Ratio, a/b.

The load deflection curve for the square specimens shows a gradually descending branch after the peak load was reached. In the case of the rectangular specimens, failure occurred almost immediately after the peak lateral load was attained. The deflections at maximum lateral load of the rectangular specimens was also much more than that of the square specimens. This is to be expected since the maximum deflection of a plate for a given load increases with an increase in the aspect ratio. A parametric study carried out on rectangular plates loaded axially along the plate width, b shows that as the aspect ratio, a/b, of a plate decreases below 1.0, the lateral load capacity decreases markedly because the middle portion of the plate recieves less support from the short sides and becomes more like a wide beam column under in-plane and lateral loads. As the aspect ratio increases above 1.0, the lateral load capacity also decreases but not as much as in the previous case. This is because the plate becomes more like a wide beam and the P-delta effect becomes minimal as most of the load is carried by bending in a direction perpendicular to the direction of in-plane load.

All plates tested had aspect ratios such that the buckling mode would be one half wave. Further studies are required for aspect ratios greater than 2 which might be expected to develop two or more half waves.

Table 5.1 Comparison of Dy/Dx Ratios

Specimen #	Dy/Dx Analysis	Dy/Dx Design Method	$\frac{\text{Analysis}}{\text{Design}}$
A3	1.137	1.300	0.874
A2	3.880	3.400	1.141
A1	4.090	3.300	1.238
C1	5.100	4.960	1.030
C2	4.820	4.950	0.973
D1	3.310	3.020	1.100
D2	4.300	3.670	1.172
B1	5.230	6.550	0.800
B2	4.700	6.100	0.770

Average = 1.010
Coefficient of Variation = 0.157
Standard Deviation = 0.158

Table 5.2 Ratio of Maximum Plate Deflection at Peak Lateral Load to Plate Thickness

Specimen #	Deflection at Maximum Lateral Load mm	$\frac{\text{Deflection}}{\text{Plate Thickness}}$
A3	75.2	1.15
A2	19.0	0.30
A1	15.8	0.24
C1	15.9	0.25
C2	16.1	0.25
D1	15.1	0.27
D2	14.0	0.25
B1	48.1	0.75
B2	44.4	0.69

Table 5.3 Maximum Calculated Initial Deflections

Specimen #	Maximum Initial Deflections mm
A3	-
A2	0.60
A1	-0.08
C1	-
C2	1.12
D1	-0.01
D2	0.15
B1	1.30
B2	0.28

Table 5.4 Maximum Lateral Loads: Test versus Analytical Predictions

Specimen #	Maximum Lateral Load from Tests KPa	Maximum Lateral Load from Analysis KPa	$\frac{\text{Test}}{\text{Predicted}}$
A3	58.6	55.93	1.048
A2	37.7	36.66	1.028
A1	45.7	42.24	1.082
C1	34.8	36.40	0.956
C2	32.8	33.26	0.986
D1	26.8	25.18	1.064
D2	27.0	26.38	1.024
B1	28.3	27.50	1.029
B2	36.4	33.80	1.077

Average = 1.033
Coefficient of Variation = 0.039
Standard Deviation = 0.038

Table 5.5 Maximum Lateral Loads: Test versus Design Predictions

Specimen #	Maximum Lateral Load from Tests KPa	Maximum Lateral Load from Design Method KPa	$\frac{\text{Test}}{\text{Design}}$
A3	58.6	58.77	0.997
A2	37.7	37.60	1.003
A1	45.7	35.90	1.272
C1	34.8	32.30	0.987
C2	32.8	32.06	1.023
D1	26.8	31.10	0.862
D2	27.0	28.10	0.961
B1	28.3	28.20	1.004
B2	36.4	36.00	1.011

Average = 1.013
Coefficient of Variation = 0.101
Standard Deviation = 0.102

Table 5.6 Reduction in Lateral Load Capacity Due To In-plane Load

Specimen #	Maximum Lateral Load from Tests KPa	Maximum Lateral Load from Analysis (N = 0.0) KPa	Reduction in Lateral Load Capacity Due To In-plane Load %
A2	37.7	52.36	28.0
A1	45.7	56.30	18.8
C1	34.8	51.85	32.9
C2	32.8	51.08	31.3
D1	26.8	44.80	40.2
D2	27.0	49.39	45.3
B1	28.3	49.82	43.2
B2	36.4	51.69	29.6

Table 5.7 Ratio of Applied In-plane Load to Balanced Load

Specimen #	$\frac{\text{Applied In-plane Load}}{\text{Balanced Load}}$
A3	0.000
A2	0.905
A1	1.100
C1	1.246
C2	1.170
D1	0.950
D2	0.940
B1	1.080
B2	0.783

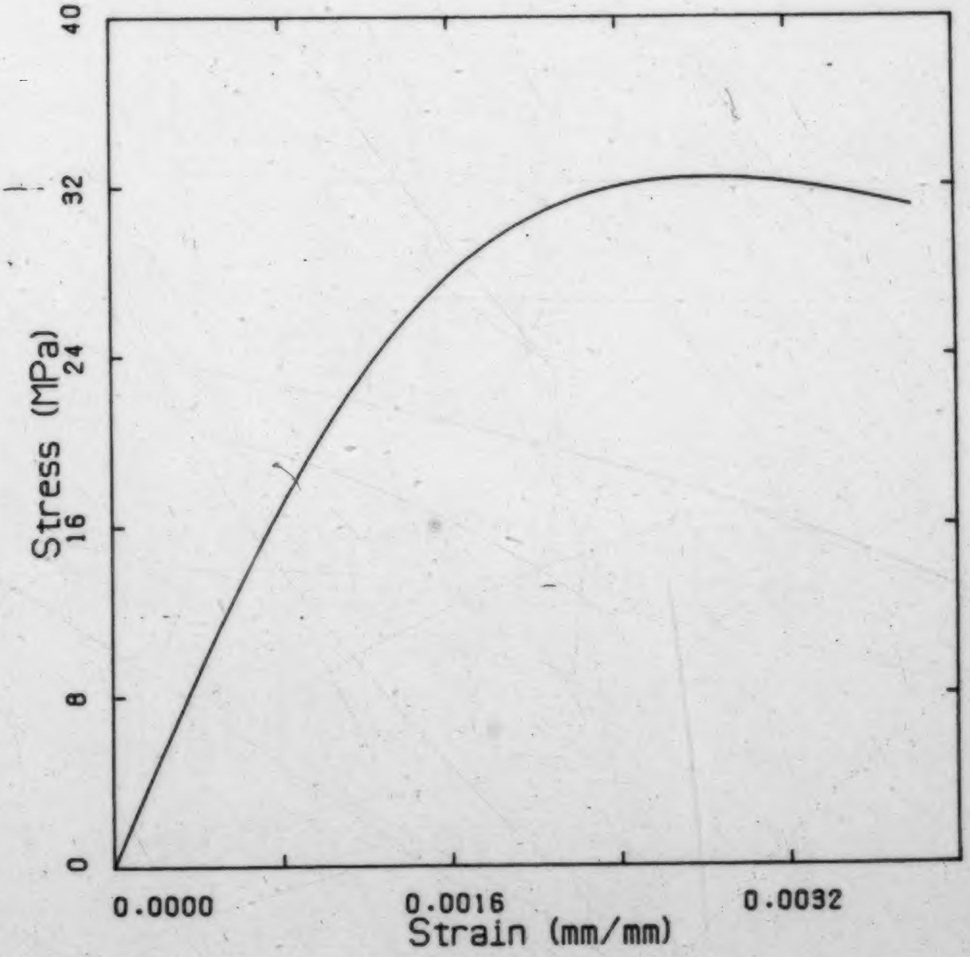

Figure 5.1 Uniaxial Stress-Strain Curve for Concrete

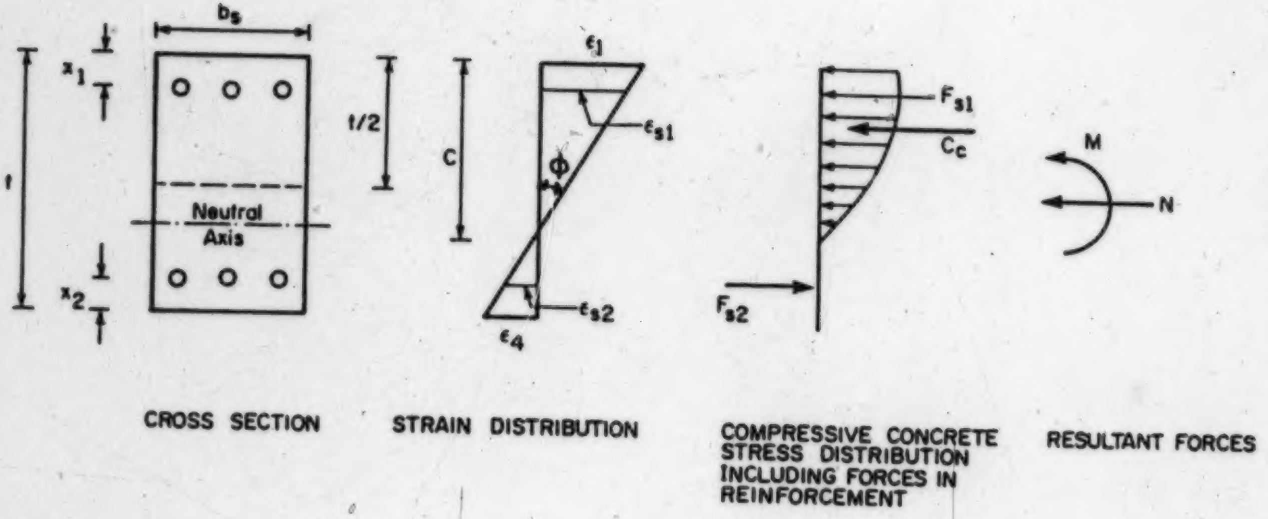
b_s
x_1
t
x_2
Neutral Axis
$t/2$
C
ϵ_1
ϵ_{s1}
ϕ
ϵ_{s2}
ϵ_4
F_{s1}
C_c
F_{s2}
M
N

CROSS SECTION

STRAIN DISTRIBUTION

COMPRESSIVE CONCRETE STRESS DISTRIBUTION INCLUDING FORCES IN REINFORCEMENT

RESULTANT FORCES

Figure 5.2 Derivation of M-N-ϕ Relationship

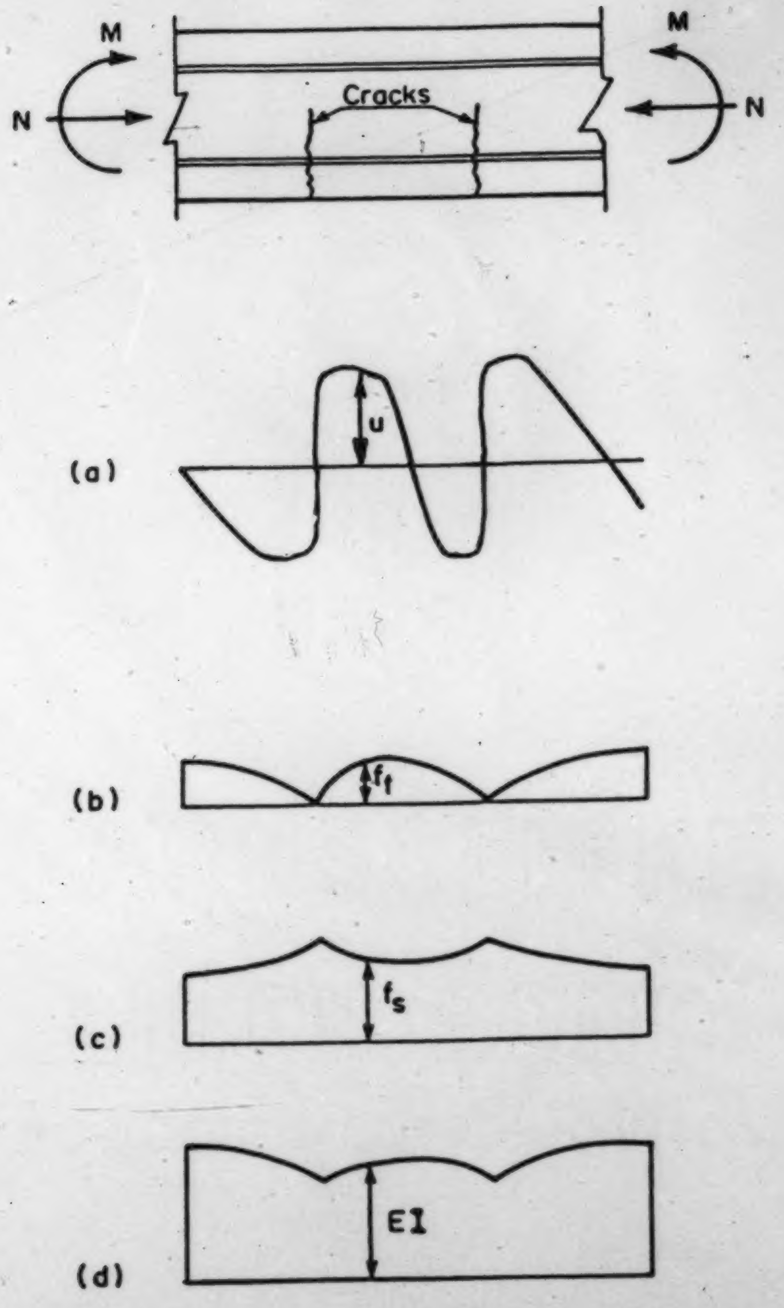
M
M
N
N
Cracks
u
(a)
f_t
(b)
f_s
(c)
EI
(d)

Figure 5.3 Reinforced Concrete Element. Distribution of :(a) Bond Stress. (b)Concrete Tensile Stress. (c) Steel Tensile Stress. (d) Flexural Rigidity.

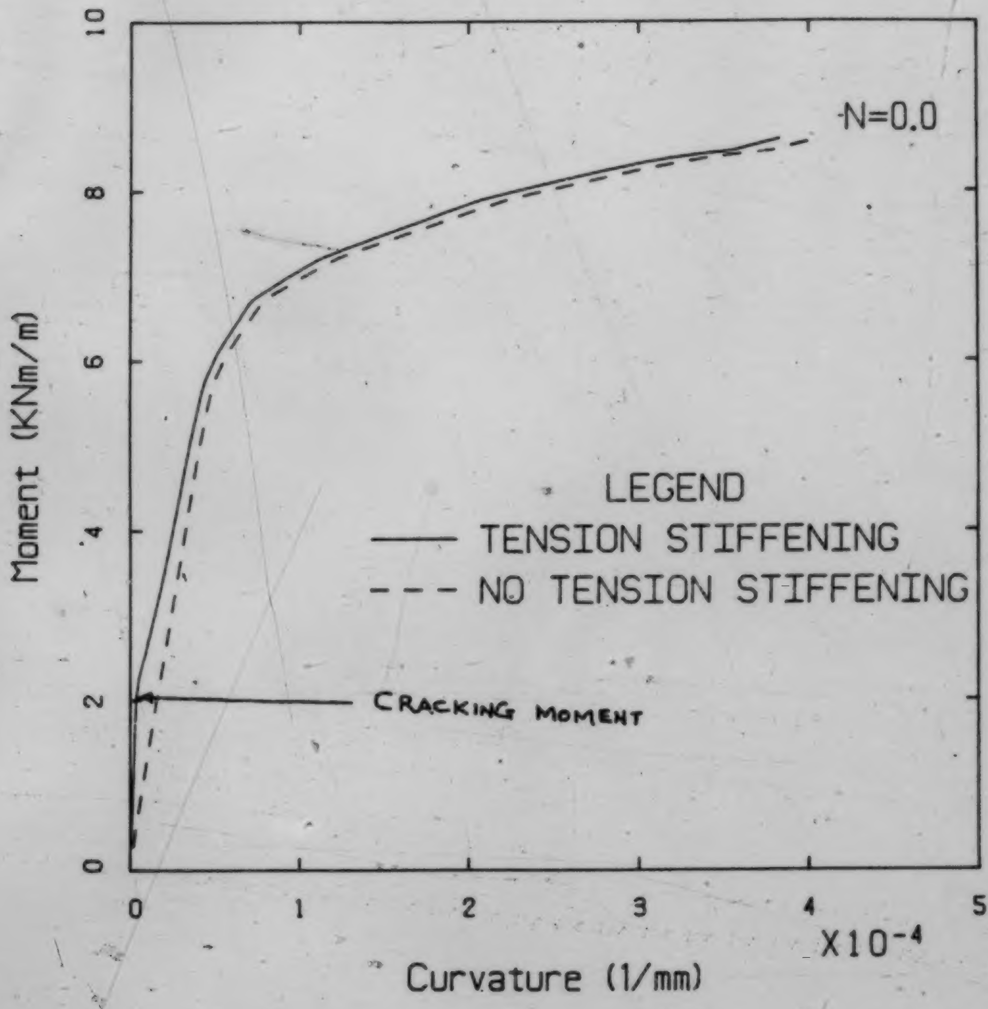

Figure 5.4 Moment-Curvature for a Typical Cross Section

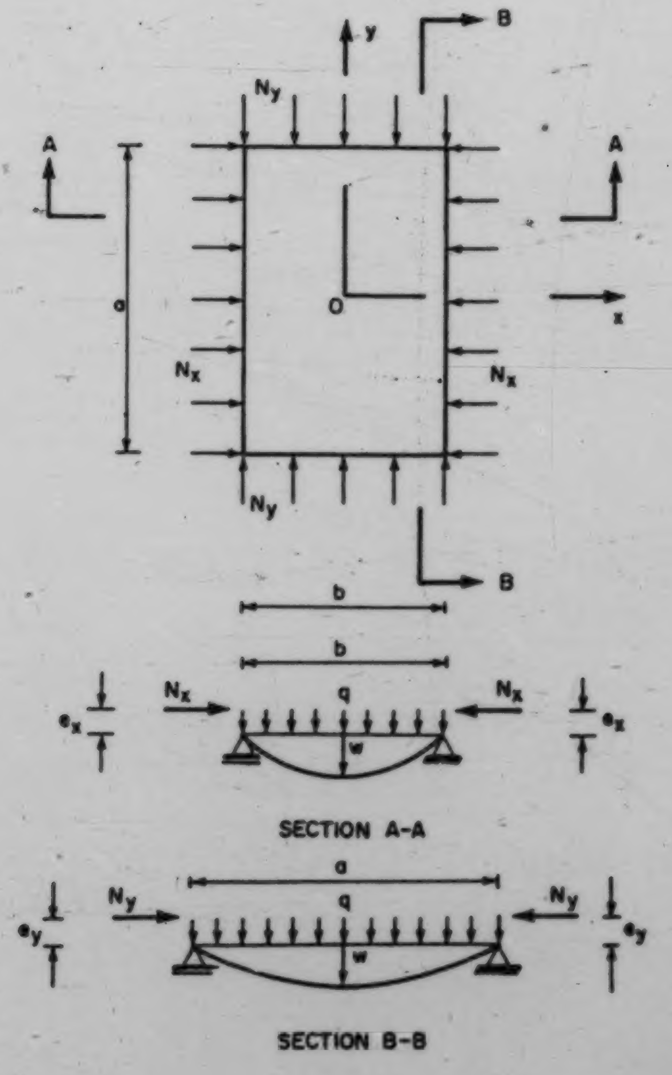
y
B
A
A
a
O
x
N_y
N_x
N_x
N_y
B
b
b
e_x
N_x
q
N_x
e_x
w
SECTION A-A
a
e_y
N_y
q
N_y
e_y
w
SECTION B-B

Figure 5.5 Plate Dimensions, Coordinate axes and Loading.

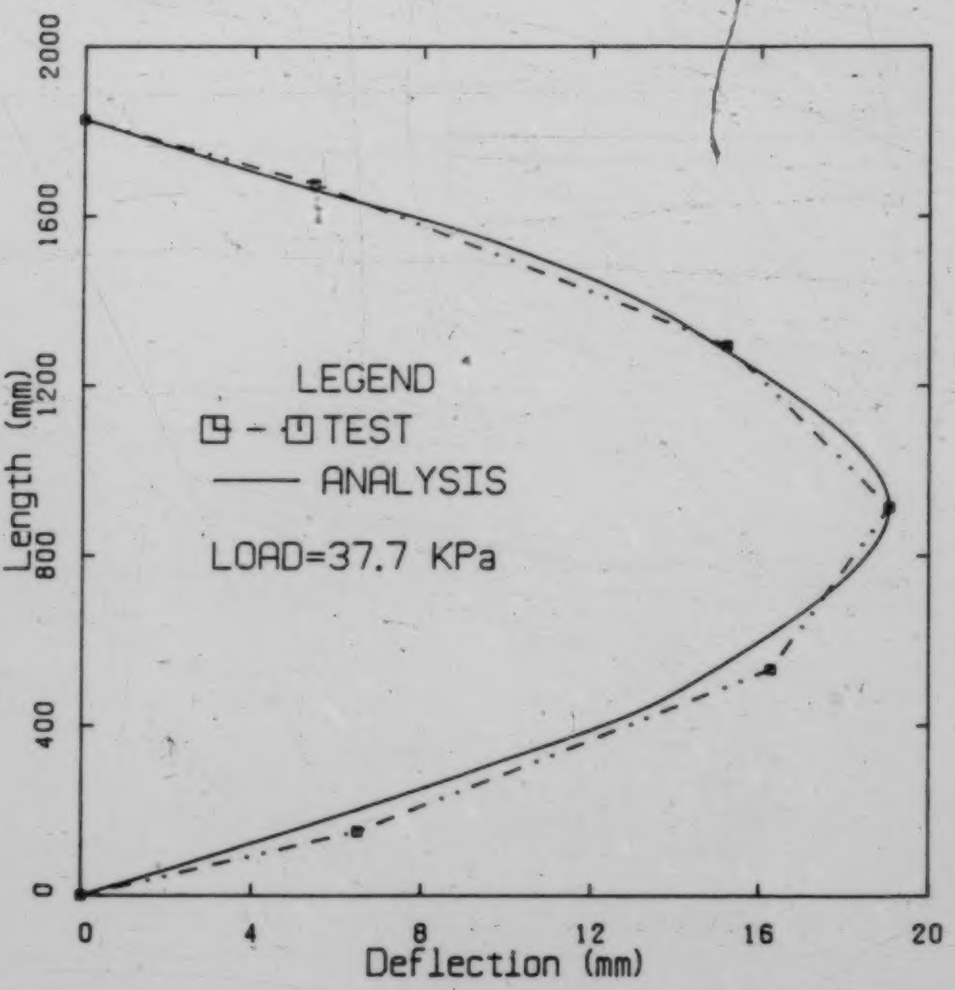

Figure 5.6 Comparison of Deflected Shapes: Specimen A2 - x Direction

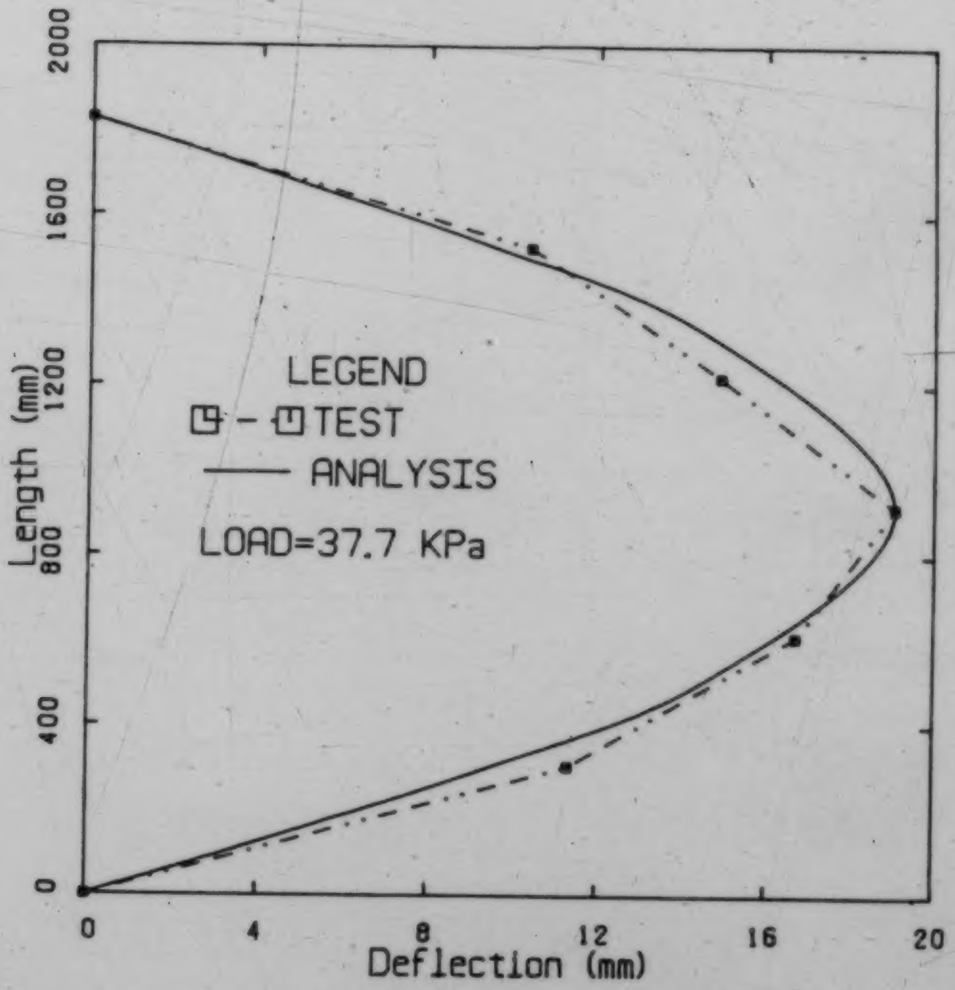

Figure 5.7 Comparison of Deflected Shapes: Specimen A2 - y Direction

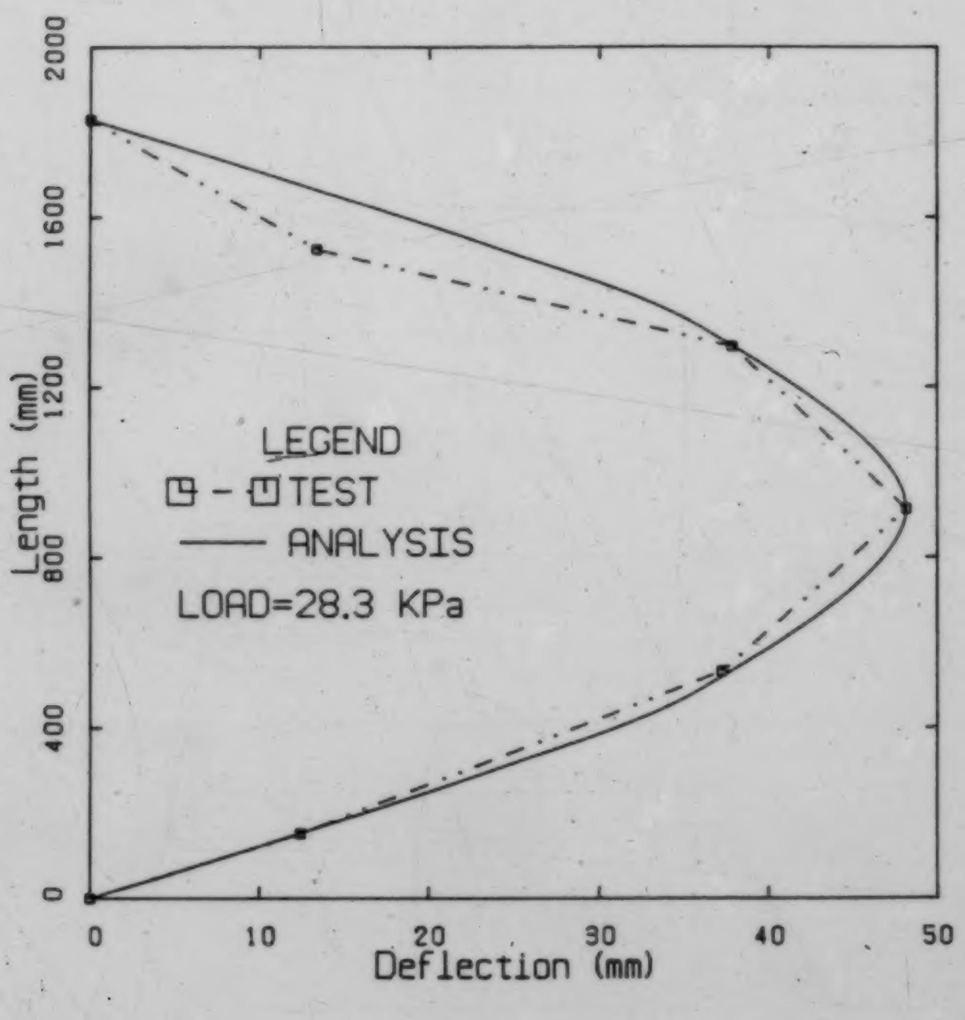

Figure 5.8 Comparison of Deflected Shapes: Specimen B1- x Direction

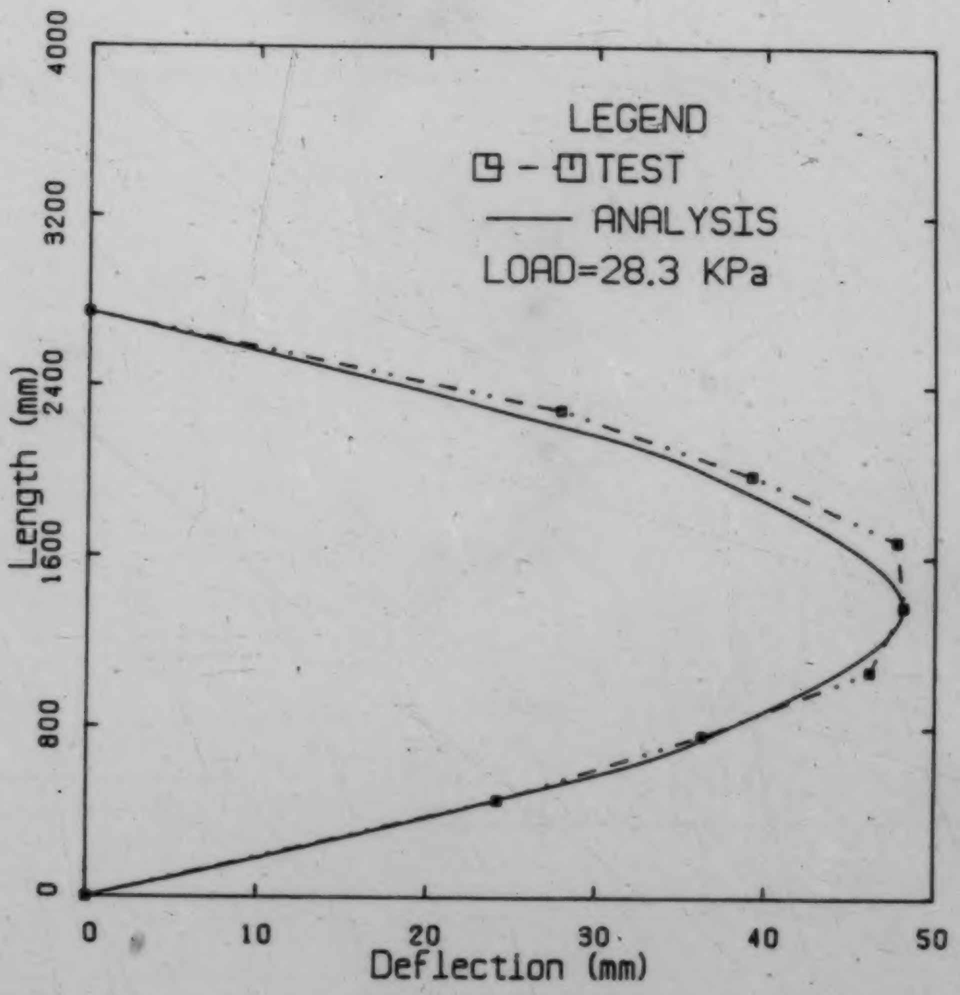

Figure 5.9 Comparison of Deflected Shapes: Specimen B1- y Direction

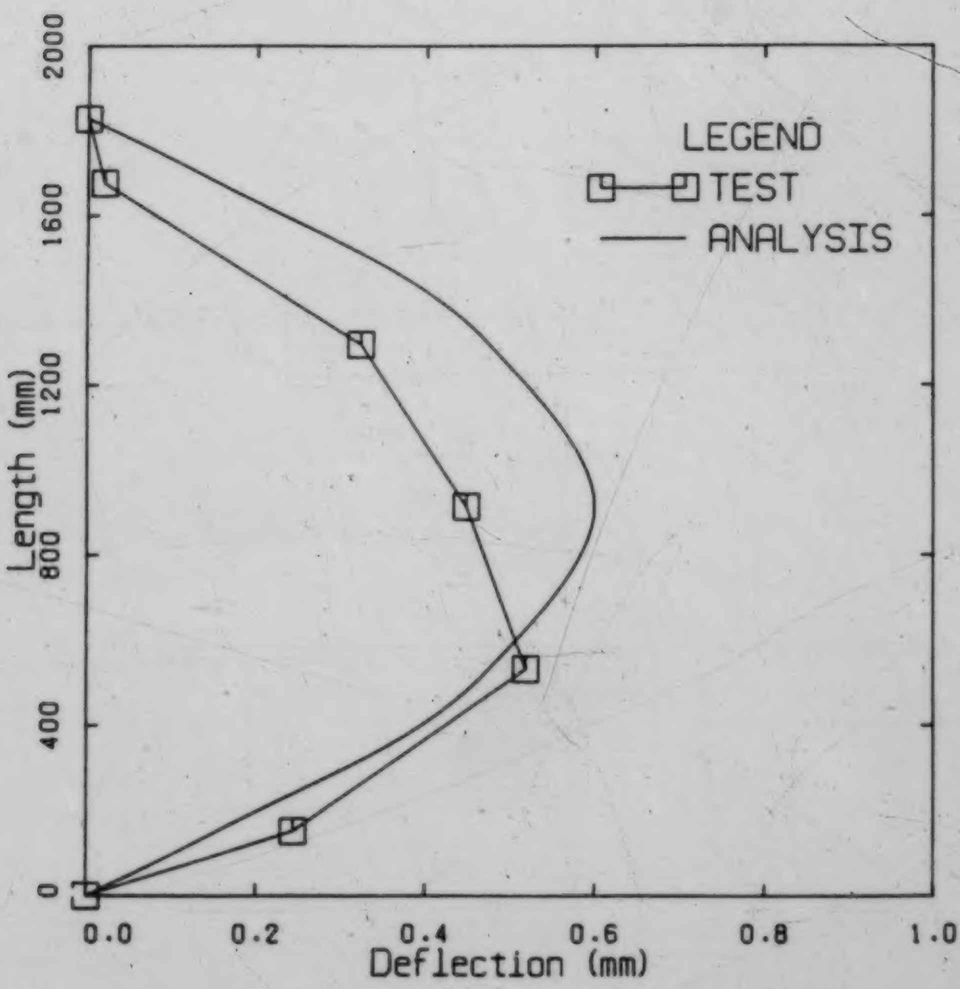

Figure 5.10 Initial Deflected Shape in x Direction For Specimen A2

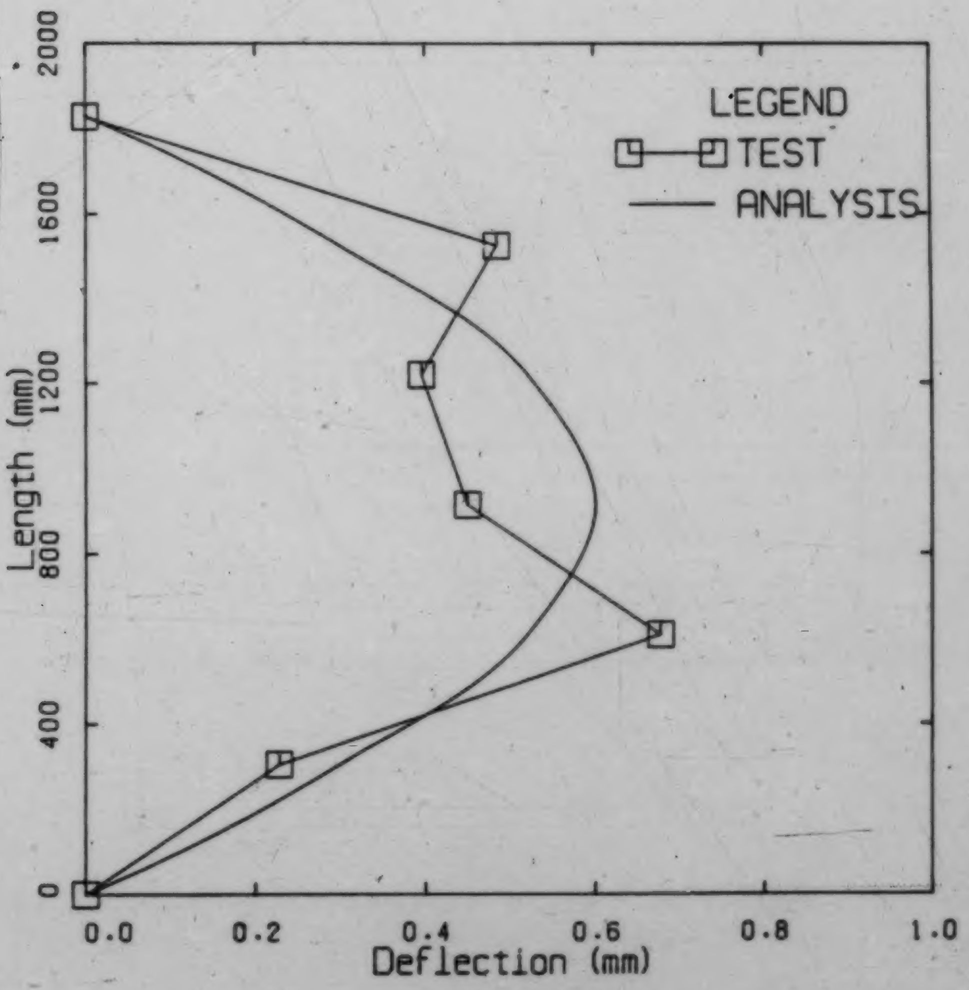

Figure 5.11 Initial Deflected Shape in y Direction For Specimen A2

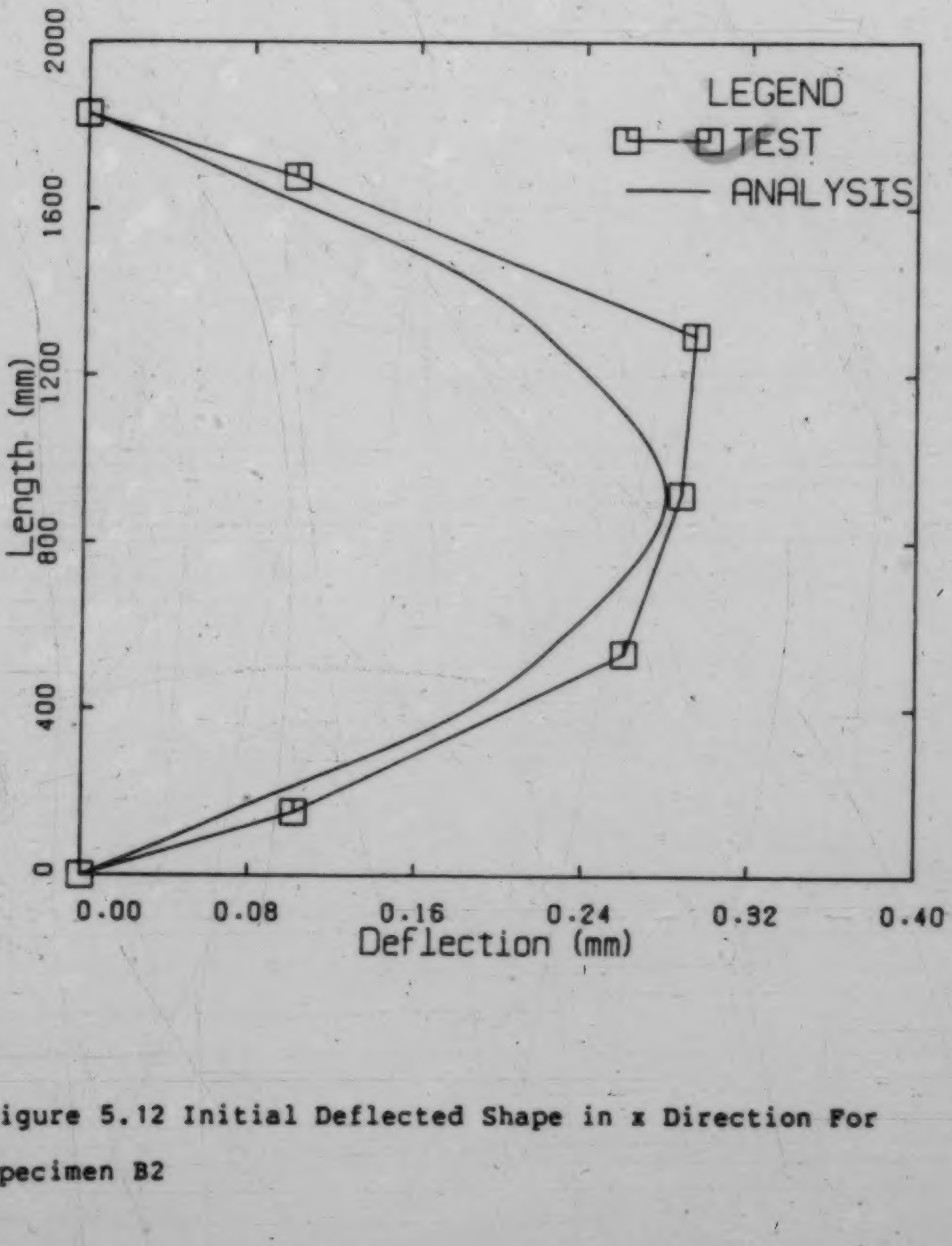

Figure 5.12 Initial Deflected Shape in x Direction For Specimen B2

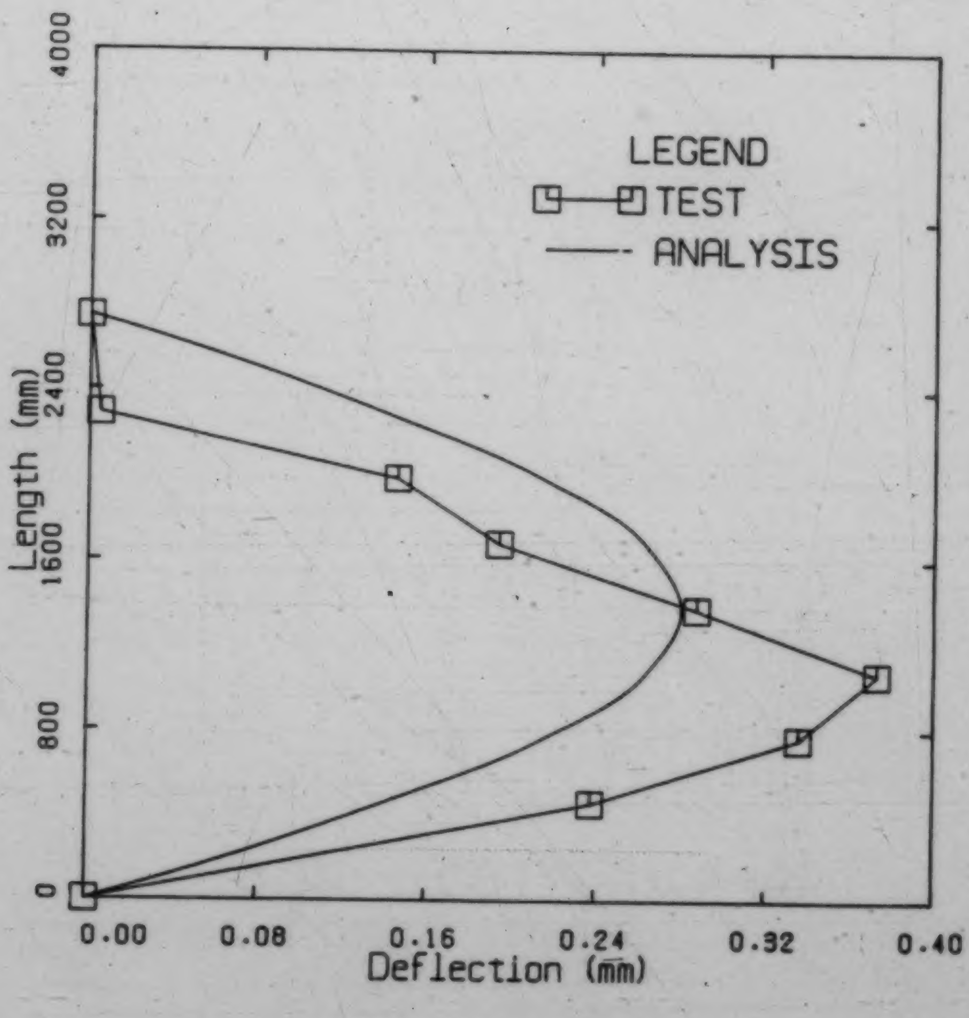

Figure 5.13 Initial Deflected Shape in y Direction For Specimen B2

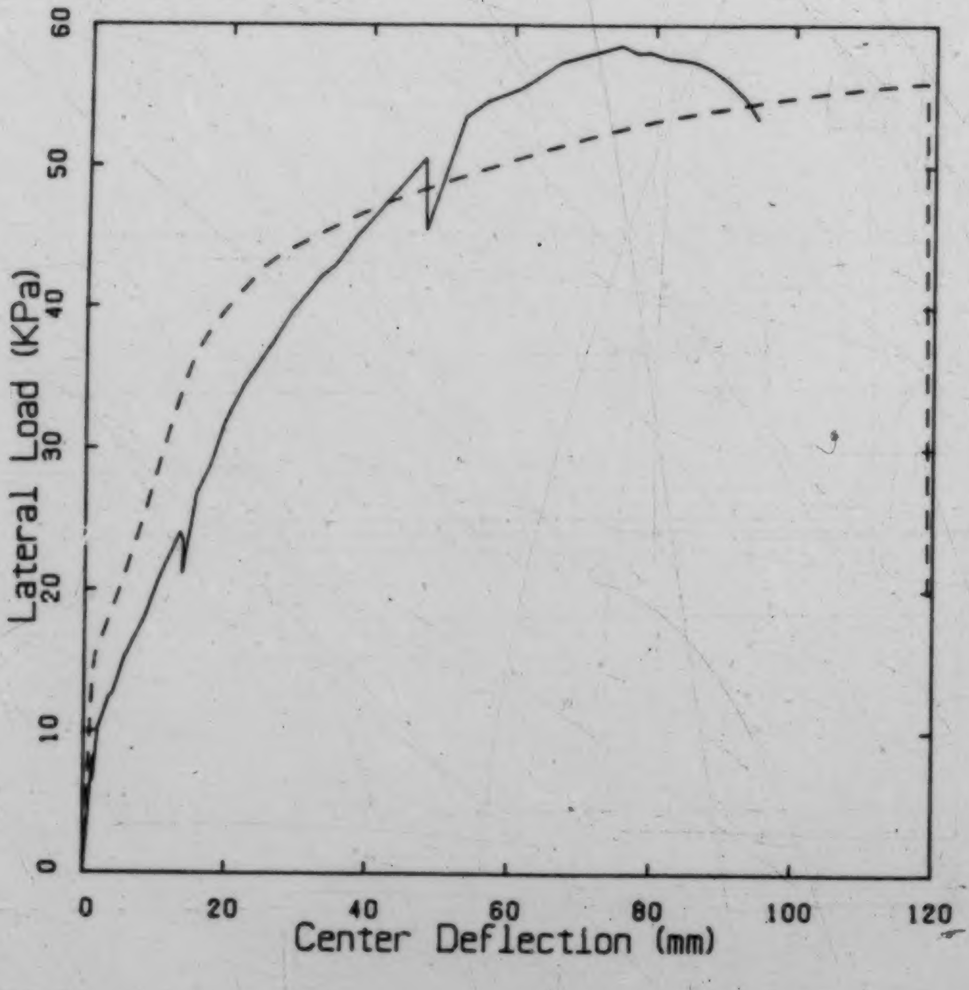

Figure 5.14 Lateral Load Deflection Curves for Specimen A3: Test versus Analytical Predictions.

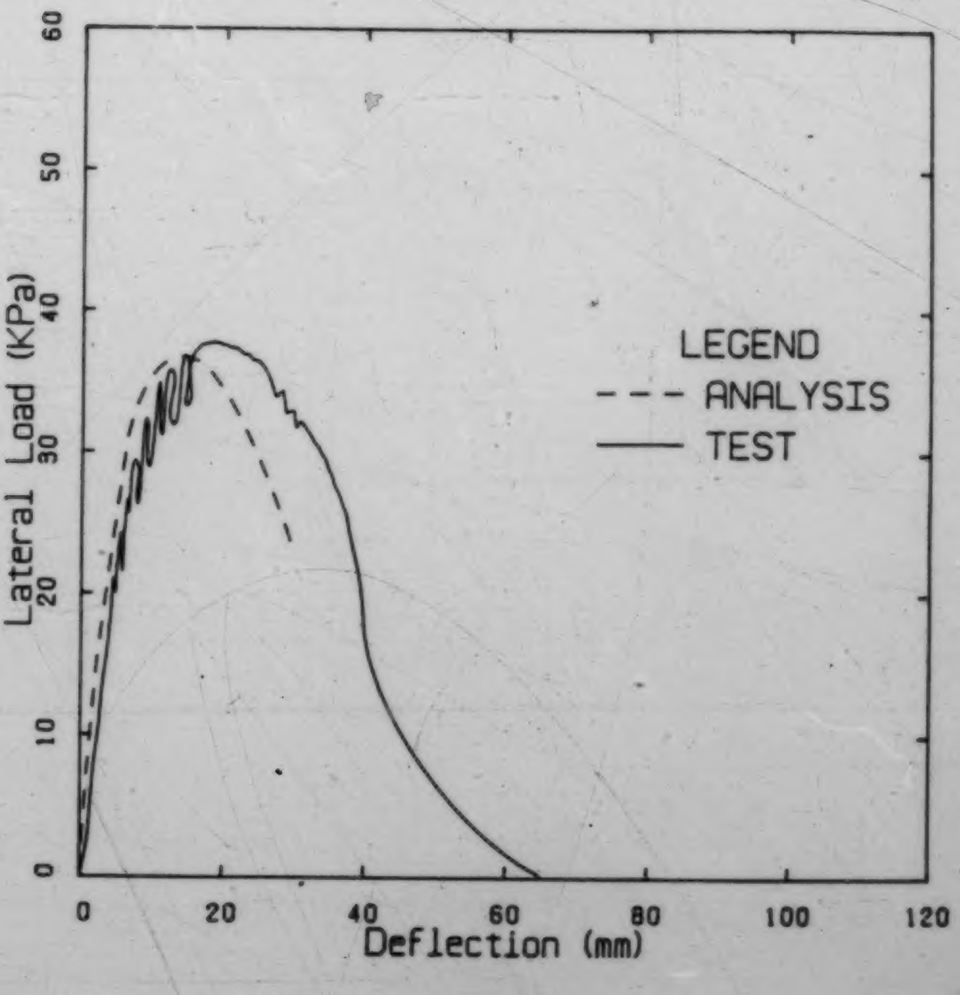

Figure 5.15 Lateral Load Deflection Curves for Specimen A2: Test versus Analytical Predictions.

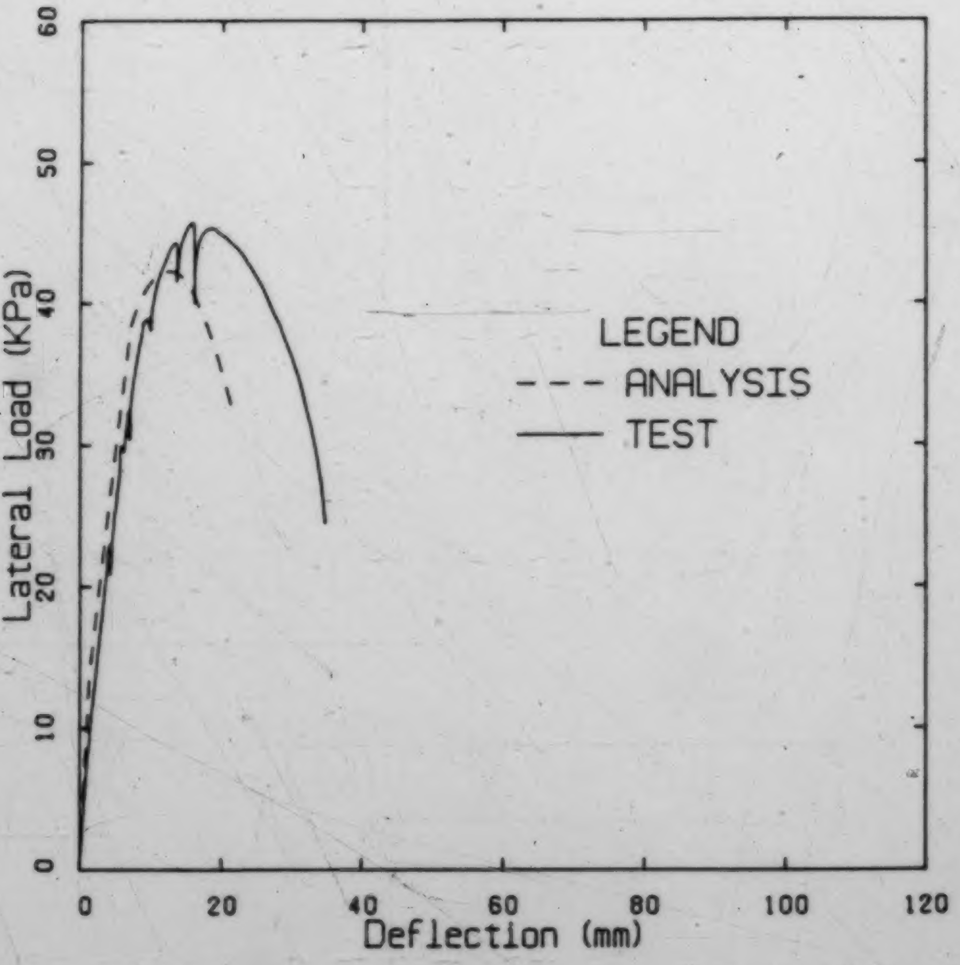

Figure 5.16 Lateral Load Deflection Curves for Specimen A1: Test versus Analytical Predictions.

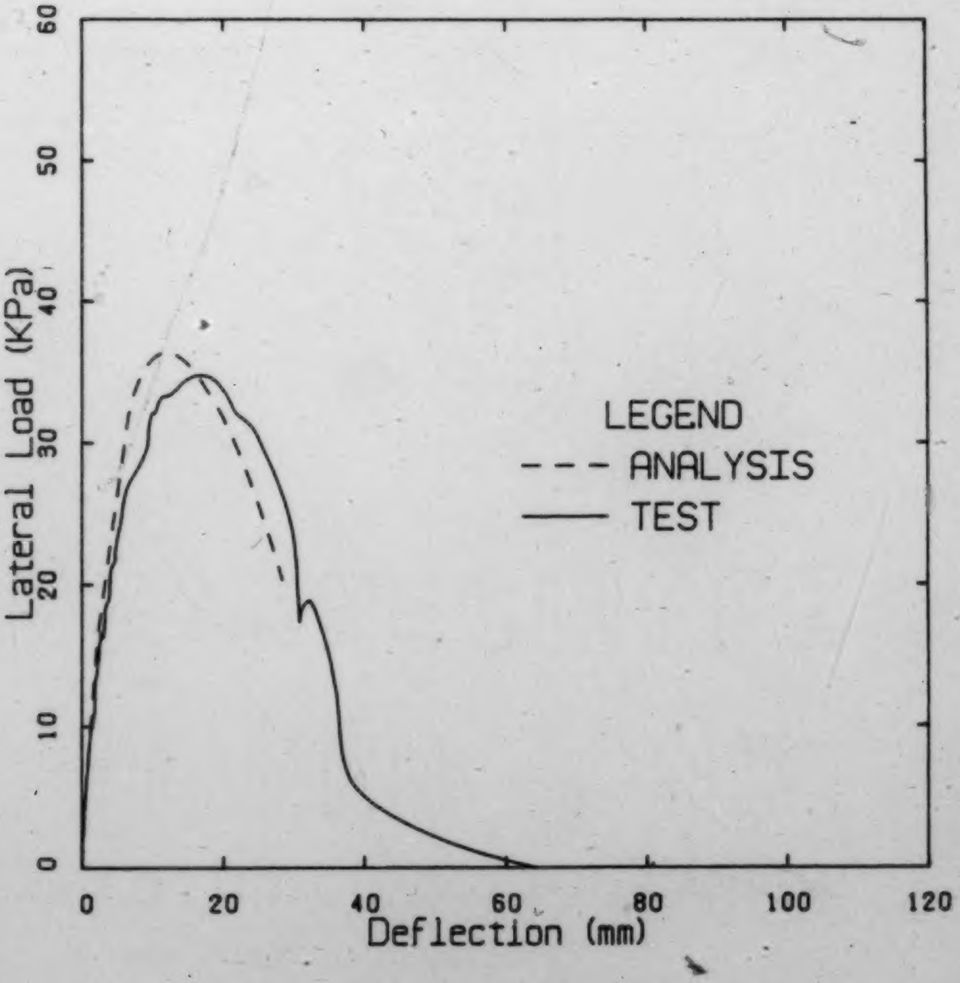

Figure 5.17 Lateral Load Deflection Curves for Specimen C1: Test versus Analytical Predictions.

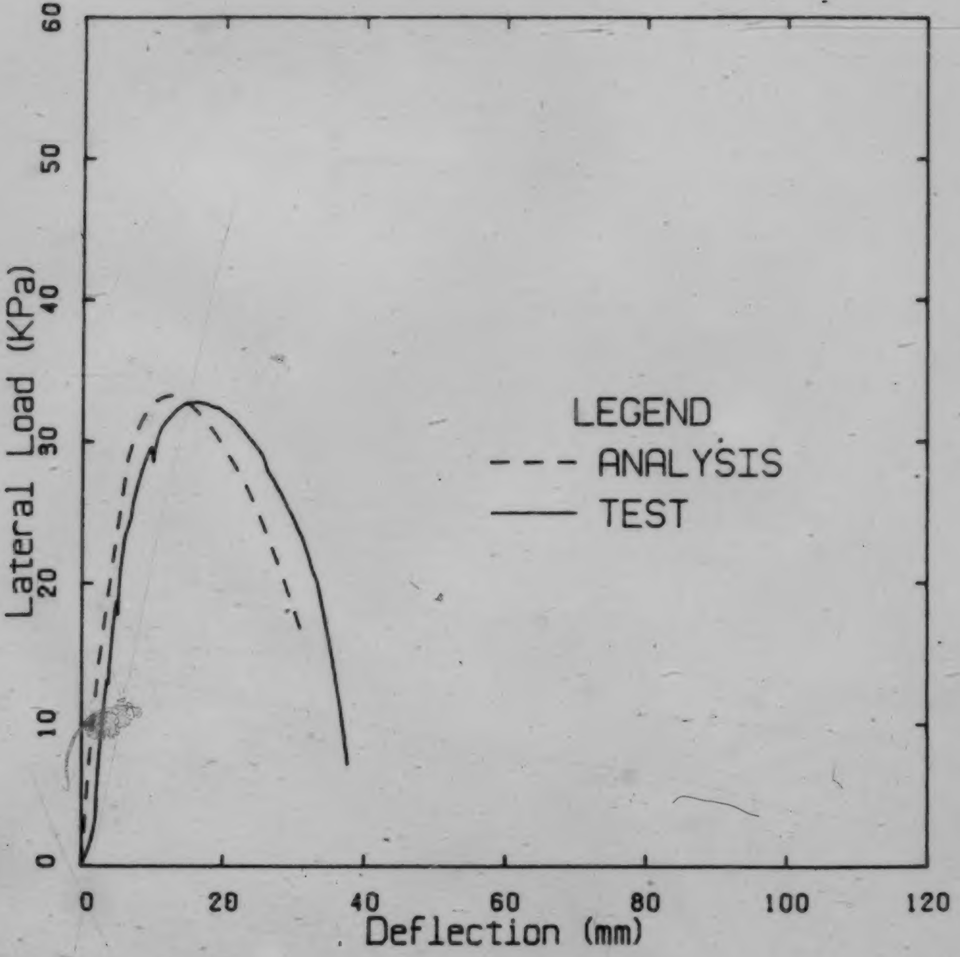

Figure 5.18 Lateral Load Deflection Curves for Specimen C2: Test versus Analytical Predictions.

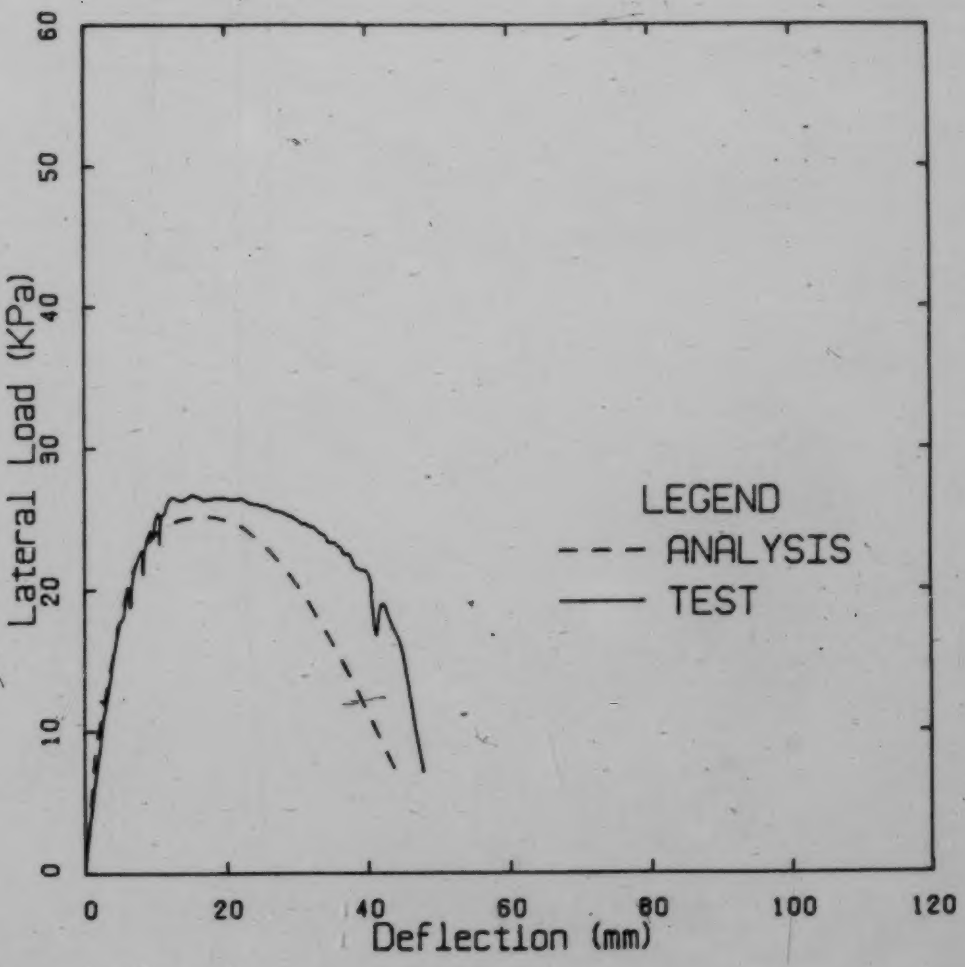

Figure 5.19 Lateral Load Deflection Curves for Specimen D1: Test versus Analytical Predictions.

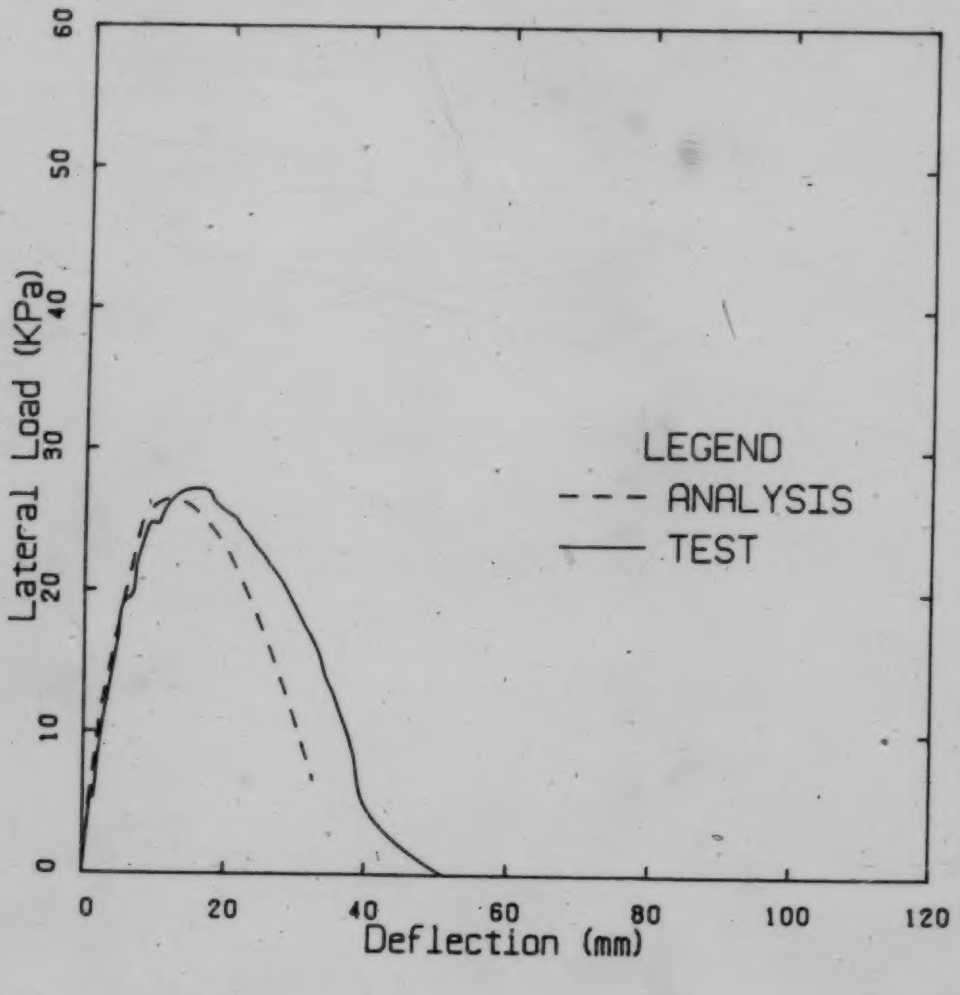

Figure 5.20 Lateral Load Deflection Curves for Specimen D2: Test versus Analytical Predictions.

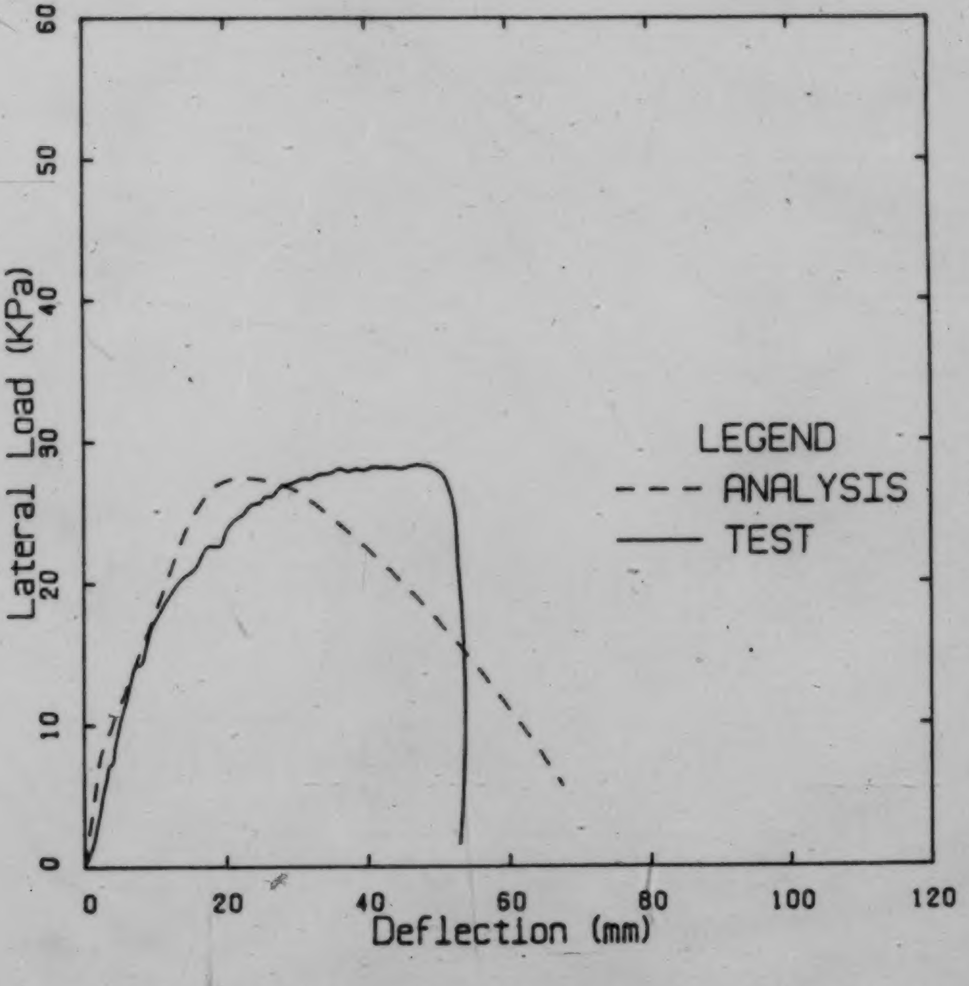

Figure 5.21 Lateral Load Deflection Curves for Specimen B1: Test versus Analytical Predictions.

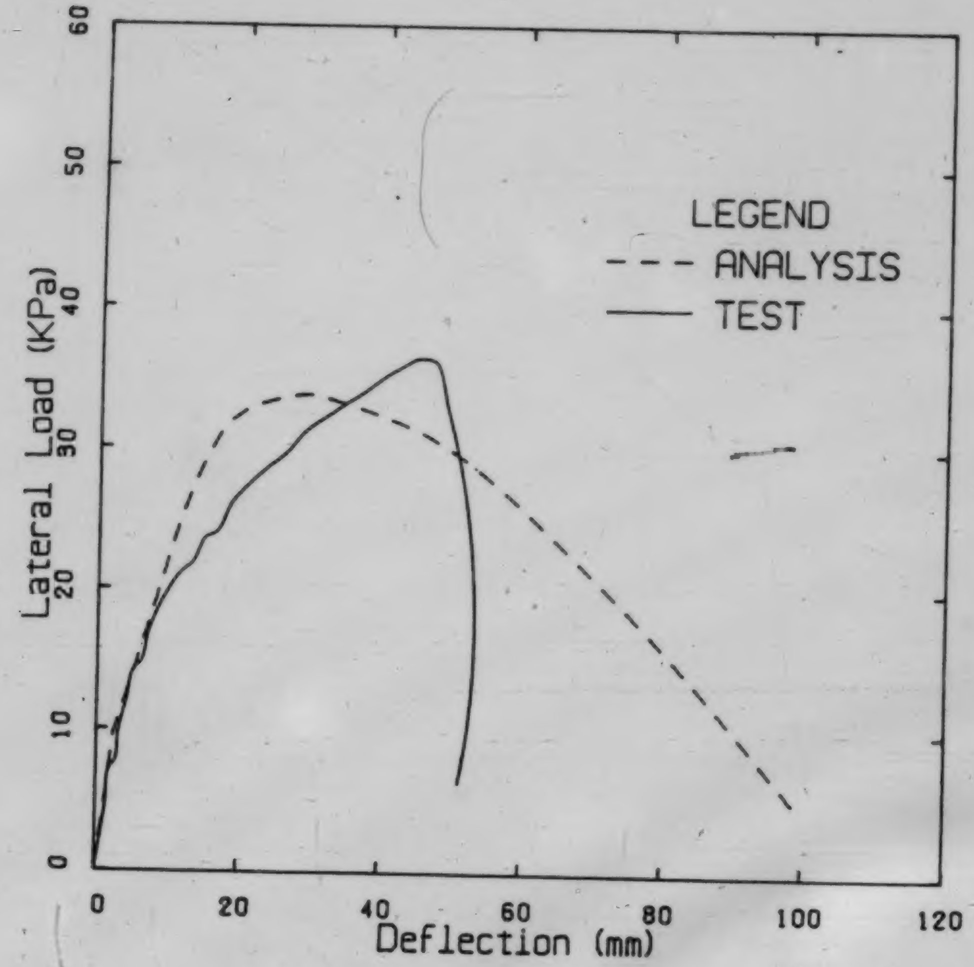

Figure 5.22 Lateral Load Deflection Curves for Specimen B2: Test versus Analytical Predictions.

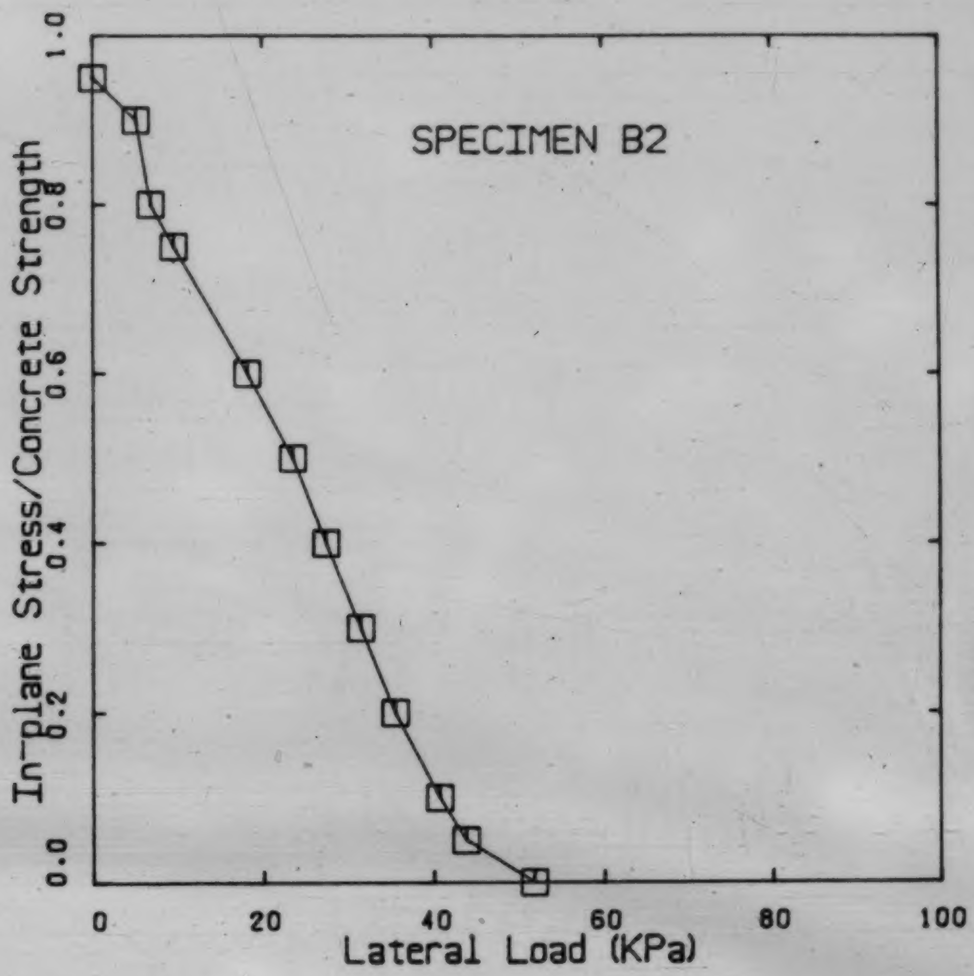

Figure 5.23 Lateral Load In-plane Load Interaction Diagram: Specimen B2

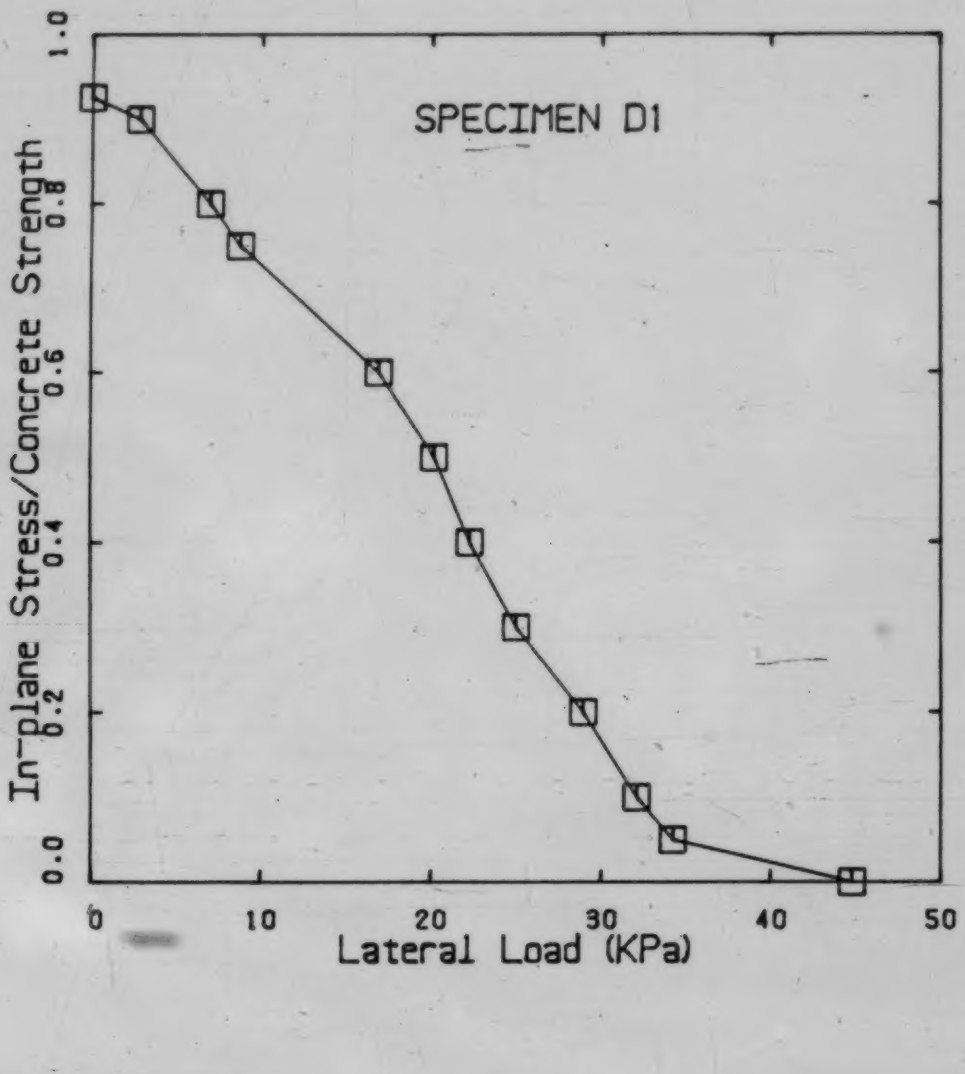

Figure 5.24 Lateral Load In-plane Load Interaction Diagram: Specimen D1

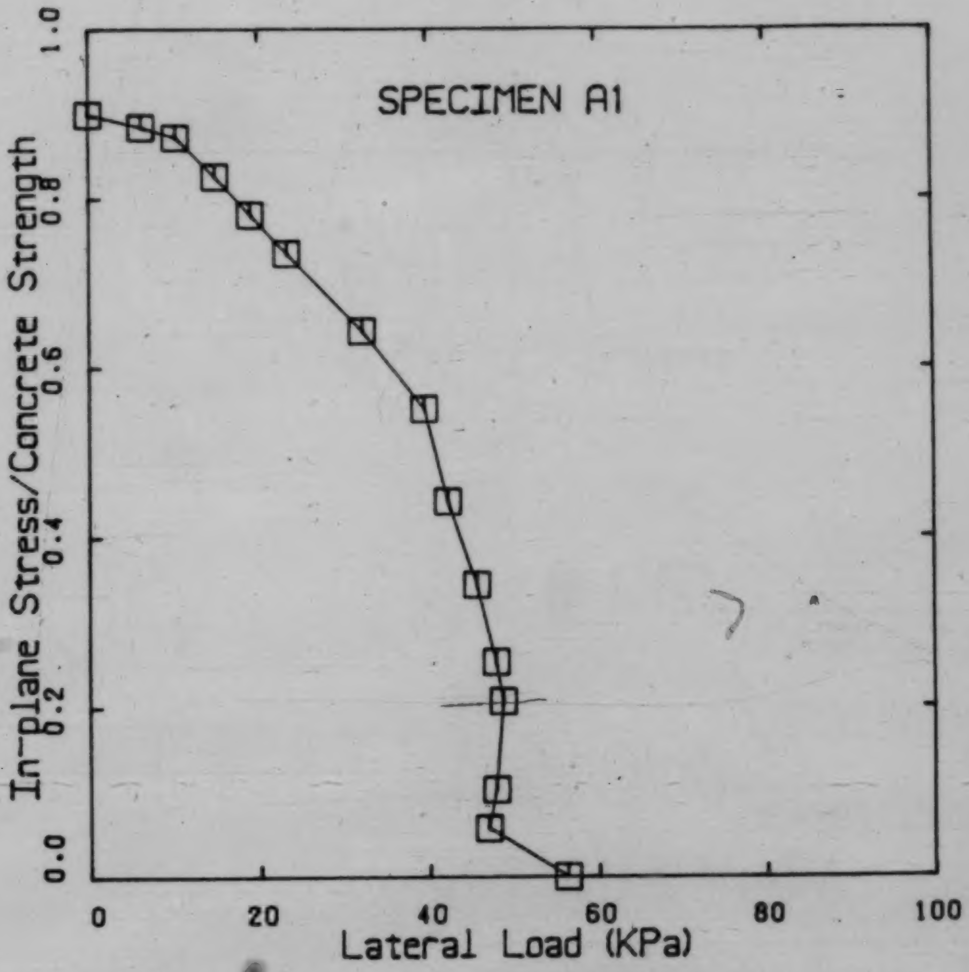

Figure 5.25 Lateral Load In-plane Load Interaction Diagram: Specimen A1

6. SUMMARY, CONCLUSIONS AND RECOMMENDATIONS

6.1 Summary

A test frame has been developed for applying uniformly distributed lateral load combined with uniaxial compression to concrete plates with simply supported conditions. This frame was used for testing eight reinforced concrete plates with aspect ratios of 1.0 and 1.5 under combined uniform lateral and uniform uni-axial compressive in-plane loads. The uniform lateral load was applied to the plate using several discrete point loads. Uniform in-plane compression was approximated by a set of four discrete point loads acting at the loaded edges of the plate. In all but one test the in-plane load was applied first and then held constant while lateral load was applied until failure of the specimen. In the remaining test the in-plane load and lateral load were applied simultaneously. Width-to-thickness ratios varied between 27.3 and 33. From the test results, it was observed that the presence of a compressive in-plane load led to a reduction in the lateral load capacity of the plate.

An analytical method based on a modified lower bound limit analysis and using an assumed deflection function has been developed to determine the lateral load capacity of axially loaded plates. The differential equation of equilibrium of a plate is used to derive an equation for the lateral load capacity which includes geometric nonlinearities. Equilibrium between external loads and internal resistance is required only at the center and corner of the plate. This leads to a simplification of the otherwise complex problem. Material nonlinearities are taken into account using analytically derived load-moment-curvature relationships which include tension stiffening effects. These M-N-ϕ relationships are determined in the two orthogonal directions of the plate. Good agreement was obtained between the analytically derived lateral load capacity and the test results. The model is quite efficient in terms of computer time used. It took approximately 2 CPU seconds to analyze all the eight plates tested under combined loads.

This model could be extended to take into account support conditions other than simply supported or plates under biaxial compression and lateral loads and could be used to prepare design interaction diagrams for concrete plates under combined in-plane and lateral loads for various slenderness, aspect and reinforcement ratios.

A design procedure similar to the ACI code moment magnifier method is developed using a Fourier series expression for the lateral load and deflection. This design method gave an acceptable prediction of the measured maximum loads.

6.2 Conclusions

The results of this investigation led to the following conclusions:

1. The presence of in-plane load can lead to a reduction in the lateral load capacity of a concrete plate. This reduction depends on the in-plane load level, width-to-thickness ratio, the concrete strength and amount of reinforcement and the aspect ratio of the plate.
2. The higher the length-to-thickness ratio of an axially loaded plate, the lower the lateral load capacity.
3. The mode of failure of the axially loaded square specimens was an instability failure mode followed by material failure (concrete crushing) as a secondary cause of collapse.
4. The mode of failure of the rectangular specimens was a material failure (concrete crushing). An increase in the length of the plate in the direction of the in-plane load would increase the chances of a material failure mode as opposed to an instability type of failure.
5. The crack patterns after failure for the axially loaded specimens approached that of a similar plate under lateral load only.
6. The sequence of loading had a very minor effect on the load capacity of the plate.
7. For the range of in-plane loads applied, none of the plates buckled under in-plane loads only.

8. The analytical model and design method developed gave good predictions of the measured maximum lateral loads.
9. The test frame developed performed satisfactorily. The frame could be adapted for testing plates with rotational edge restraints under combined loads.

6.3 Recommendations for Future Research

Further research and development in the following areas would be of interest:

1. More tests should be carried out for ratios of in-plane load-to-uniaxial cross-sectional capacity from 0.10 to 0.80 to enable the complete in-plane/lateral load interaction response to be obtained.
2. Tests of concrete plates under biaxial compression combined with lateral load should be pursued.
3. Tests are needed for plates with boundary conditions other than simply supported.
4. More tests are needed for rectangular plates under combined loads.
5. Tests should be carried out to study the effects of eccentricity of in-plane load.
6. The developed analytical method should be extended to the case of plates with rotational edge restraints.
7. Design aids in the form of in-plane/lateral load interaction diagrams could be produced for various slenderness, aspect and reinforcement ratios.

BIBLIOGRAPHY

AALAMI, B., and CHAPMAN, J.C. 1969. Large Deflection Behavior of Rectangular Orthotropic Plates Under Transverse and In-plane Loads. Journal of the Institution of Civil Engineers, Paper 7112.

AALAMI, B.,MOUKHTARZADE, A., and MAHMUDI-SAATI, P. 1972. On the Strength Design of Ship Plates Subjected to In-plane and Transverse Loading. Royal Institution of Naval Architects,Supplementary Papers,Vol 114, pp. 519-534.

AAS-JAKOBSEN, K. 1983. Buckling of Walls. Committe European du Beton, Bulletin D'Information # 155, pp. 223-250.

AAS-JAKOBSEN, A. and AAS-JAKOBSEN, K. 1978. CEB/FIP Manual of Buckling and Instability. The Construction Press, 135 pp.

ALCOCK, W.J. and Nathan, N.D. 1977. Moment Magnification Tests of Prestressed Concrete Columns. PCI Journal, July/August, pp. 51-61.

AMRHEIN, J.E. *et al*. 1985. Tests on Tall Thin Bearing Walls. Concrete International, January, pp. 53-58.

BELL, J.C. and ELMS, D.G. 1971. A Finite Element Approach to Post-Elastic Slab Behavior. ACI SP-30: Cracking, Deflection, and Ultimate Load of Concrete Slab Systems, pp. 325-344.

BLEICH, F. 1952. Buckling Strength of Metal Structures. McGraw Hill Book Company,New York.

BROMS, B. and VIEST, I.M. 1961. Long Reinforced Concrete Columns. ASCE Transactions, Vol 2.

BROWN, J.C. and HARVEY, J.M. 1969. Large Deflections of Rectangular Plates Subjected to Uniform Lateral Pressure and Compressive Edge Loading. Journal of Mechanical Engineering Sciences,Vol 11,# 3, p. 305.

BULSON, P.S. 1969. The Stability of Flat Plates. American Elsevier Publishing Company, 470 pp.

CANADIAN STANDARDS ASSOCIATION (CSA). 1977. Methods of Test for Concrete. National Standard of Canada. CAN3-A23.2-M77, Canadian Standards Association, Rexdale, Ontario.

CEB BULLETIN D'INFORMATION # 159. 1983. Simplified Methods of Calculating Short Term Deflections of Reinforced Concrete Slabs.

CEB PERMANENT COMMISSION 111-BUCKLING AND INSTABILITY. 1984. Minutes of 7th Meeting, Technical University of Praha, Czekoslovakia.

CHAJES, A. 1984. Principles of Structural Stability Theory. Prentice-Hall,Englewood Cliffs,New Jersey, 336 pp.

CHEN, W.F. and ATSUTA, T. 1976. Theory of Beam Columns, Vol 1:In-plane Behavior and Design, McGraw Hill Inc., 513 pp.

CHEN, W.F. and CHEN, A.C.T. 1974. Strength of Laterally Loaded Reinforced Concrete Columns. IABSE Symposium on Design and Safety of Reinforced Concrete Members, Preliminary Report, Quebec, Canada.

CHEN, W.F. and HAN, D.J. 1985. Tubular Members in Offshore Structures. Pitman, pp. 100-103.

CHIA, C.Y. 1980. Nonlinear Analysis of Plates. McGraw-Hill Book Company,New York, 600pp.

COPE, R.J. and CLARK, L.A. 1984. Concrete Slabs, Analysis and Design. Elsevier Publishers, 502 pp.

DESAYI, P. and KRISHNAN, S. 1964. Equation for The Stress-Strain Curve of Concrete. ACI Journal, pp 351.

DIER, A.F. and DOWLING, P.J. 1980. Strength of Ships' Plating,Plates Under Combined Lateral Loading and Biaxial Compression. Imperial College, London, CESLIC Report SP8.

DET NORSKE VERITAS. 1977. Rules for the Design, Construction and Inspection of Offshore Structures, Appendix D: Concrete Structures. Hovik, Norway.

ELLINAS, C.P., SUPPLE, W.J. and WALKER, A.C. 1984. Buckling of Offshore Structures: A State-of-the-art-review of the Buckling of Offshore Structures. Granada, pp. 301-385.

EMI, H. ET AL. 1981. Design Standard for Sea Transportation of Large Concrete Structures. Proceedings of the Third International Symposium on Offshore Engineering, Federal University of Rio De Janeiro, Brazil.

ERNST, G.C. 1952. Stability of Thin-Shelled Structures. American Concrete Institute Journal, December, Vol 4,# 24.

FLORIN, G. 1980. Theory and Design of Surface Structures:

Slabs and Plates. Trans Tech Publications, 214 pp.

FURNES, O. 1981. Buckling of Reinforced and Prestressed Concrete Members- Simplified Calculation Methods. Prestressed Concrete Institute Journal July/August.

FJELD, S. ET AL. 1978. Special Problems in Structural Analysis and Design of Offshore Concrete Platforms. Offshore Technology Conference Proceedings, Paper 3087.

FEDERATION INTERNATIONALE DE LA PRECONTRAINTE. 1986. Recommendations for the Design and Construction of Concrete Ships. Thomas Telford, London, 12 pp.

FUJITA, Y. ET AL. 1979. Ultimate Strength of Rectangular Plates Subjected to Combined Loading (2nd Report)- Rectangular Plates under Compression and Lateral Pressure. Journal of the Society of Naval Architects of Japan,Vol 146, pp 289-299.

GALAMBOS, T.V. and KETTER, R.L. 1959. Column under Combined Bending and Thrust. Proceedings, ASCE, Vol 85, EM2, April.

GHALI, A. and FAVRE, R. 1986. Concrete Structures:Stresses and Deformations. Chapman and Hall, New York, 352 pp.

GURFINKEL, G. and ROBINSON, A. 1967. Determination of Strain Distribution and Curvature in a Reinforced Concrete Section Subjected to Bending and Longitudinal Load. American Concrete Institute Journal, July.

HARDING, J.E., HOBBS, R.E. and NEAL, B.G. 1977. The Elasto-Plastic Analysis of Imperfect Square Plates Under In-plane Loading. Proceedings of the Institution of Civil Engineers, Vol 63, Part 2, pp 137-158.

HERZOG, M.A.M. 1987. Simplified Design of Unstiffened and Stiffened Plates. ASCE ST 10, October.

HOGNESTAD, E. 1952. Fundamental Concepts in Ultimate Design of Reinforced Concrete Members. Proceedings, ACI, v 48, p 809.

HOLMES, M. and STEEL, K.A. 1964. Upper and Lower Bound Solutions to the Collapse of a Continuous Slab under Uniform Load. Magazine of Concrete Research, Vol. 16, No. 47, pp. 83-88.

HUGHES, O. 1983. Ship Structural Design: A Rationally-Based Computer-Aided Optimization Approach. John Wiley and Sons, New York, 566 pp.

JOHNS, D.J. 1967. Static Instability of Rectangular

Orthotropic Panels Subjected to Uniform In-plane and Deflection Dependent Lateral Loads. British Aeronautical Research Council, Reports and Memoranda, R&M # 3569.

JONES, N. 1976. Plastic Behavior of Ship Structures. Society of Naval Architects and Marine Engineers, Transactions, Vol 84, pp 115-139.

KEMP, K.O. 1962. A Lower Bound Solution to the Collapse of an Orthotropically Reinforced Slab on Simple Supports. Magazine of Concrete Research, Vol 14, # 41, pp. 79-84.

KENNEDY, J.B. and BALI, S.K. 1979. Rigidities of Concrete Waffle-Type Slab Structures. Canadian Journal of Civil Engineering, Vol 6.

KORDINA, K. and STORKEBAUM, K.H. 1973. Untersuchungen Uber Die Traglasten Ausmitting Beanspruchter Stahlbetonwande. Institute Fur Baustoffkunde Und Stahlbetonbau, Technischen, Universitat Braunschweig.

KORDINA, K. and TIMM, R. 1979. Experimentelle Untersuchungen Zum Stabilitatsverhalten Von Bewhrten Und Unbewehrten Betonwanden. Institute Fur Baustoffkunde Und Stahlbetonbau, Technischen, Universitat Braunschweig.

KORDINA, K. and KIEL, M. Stabilitat Mehseitig Gelagertes Betonwande, 2. Stufe. Institut Fur Baustoffkunde Und Stahlbetonbau, Techniscen, Universitat Braunschweig.

KOROL, R.M. and SHERBOURNE, A.N. 1972. Strength Predictions of Plates in Uniaxial Compression. ASCE Structural Division, September, pp 1965-1986.

KUPFER, H., HILSDORF, H.K. and RUSCH, H. 1969. Behavior of Concrete Under Biaxial Stresses. ACI Journal, Vol. 66, # 8, pp. 656-666.

LaNIER, M. ET AL. 1986. The Possibilities for Concrete Floating Structures as a Transportation Medium. ACI Publication SP-93, International Conference on Concrete in Transportation, Vancouver, September 8-10.

LEE, T. 1961. Elasto-Plastic Analysis of Simply Supported Rectangular Plates under Combined Axial and Lateral Loading. PhD Dissertation, Lehigh University, 175 pp.

LERTBANNAPHONG, S. 1979. Analysis and Design of Tilt-up Concrete Walls. Ph.D. Dissertation, The University of Texas at Airlington.

LEVY, S.,GOLDENBERG, D. and ZIBRITOSKY, G. 1944. Simply Supported Long Rectangular Plates under Combined Axial Load and Normal Pressure.NACA Technical Note # 949.

LITTLE, G.H. 1987. Efficient Large Deflection Analysis of Rectangular Orthotropic Plates By Direct Energy Minimization. Computers and Structures, Vol 26, No 5, pp. 871-884.

MAST, R.F. 1975. The Arco LPG Terminal Vessel. Conference on Concrete Ships and Vessels, University of California, Berkeley, Sept. 15-19.

MACLEAY, F.R. 1949. Thin Wall Concrete Ship Construction. ACI Journal, November, Vol. 21, No. 3, pp. 193-204.

MCPHERSON, A.E., LEVY, S. and ZIBRITOSKY, G. 1946. Effect of Normal Pressure on the Strength of Axiall Loaded Sheet-Stringer Panels. NACA Technical Note 999.

MACGREGOR, J.G., BREEN, J.E. and PFRANG, E.O. 1970. Design of Slender Columns. ACI Journal, Vol 67, pp 6-28.

MACGREGOR, J.G., OELHAFEN, U.H. and HAGE, S.E. 1975. A Re-Examination of the EI Value for Slender Columns. ACI Publication SP-50, pp 1-40.

MACGREGOR, J.G. 1986. Stability of Reinforced Concrete Frames. In Concrete Framed Structures: Stability and Strength. Edited by R. Narayanan. Elsevier Applied Science Publishers.

MAGURA, D.D. and MAST, R.F. 1979. Ocean Thermal Energy Conversion (OTEC) 10MWe Preliminary Plant Ship Design. Offshore Technology Proceedings, Vol 3, pp 2059.

MANSOUR, A. and NAGLER, R. 1970. Bending of Stiffened Plates under Combined Lateral and In-plane Loads. Offshore Technology Conference Proceedings, Paper 1231.

MANSOUR, A. 1971. On the Non-Linear Theory of Orthotropic Plates. Journal of Ship Research, December.

MUSPRATT, M.A. 1969. Behavior of Simply Supported Slabs. ASCE Structural Division, Vol 95, # ST12.

MUSPRATT, M.A. 1970. Destructive Tests on Rationally Designed Slabs. Magazine of Concrete Research, Vol 22, # 70, pp 25.

NATHAN, N.D. 1983. Slenderness of Prestressed Concrete Columns. PCI Journal, March-April, pp. 50-77.

NATHAN, N.D. 1985. Rational Analysis and Design of Prestressed Concrete Beam Columns and Wall Panels. PCI Journal, May/June, pp 82.

NAWY, E.G. 1968. Crack Control in Reinforced Concrete

Structures. ACI Journal, Vol. 65, No. 10.

NEALE, K.W. and LIND, N.C. 1970. Limit Analysis of Plates under Combined Loads. ASCE Engineering Mechanics Division, Vol 96, # EM5.

NIELSEN, M.P. 1971. On The Strength of Reinforced Concrete Discs. Acta Polytechnica Scandinavica, Civil Engineering and Building Construction Series # 70.

OBERLANDER, G.D. and EVERARD, N.J. 1977. Investigation of Reinforced Concrete Walls. ACI Journal, June.

O'FLYNN, B. 1987. Composite Ice-Resisting Walls. PhD Dissertation, University of Alberta.

PARK, R. and GAMBLE, W.L. 1980. Reinforced Concrete Slabs. John Wiley & Sons, New york, 618 pp.

PARK, R. and PAULAY, T. 1975. Reinforced Concrete Structures. John Wiley & Sons, New York, 769 pp.

PARSANEJAD, S. 1985. Large Deflection Elasto-Plastic Analysis of Plates under Combined Loads using Finite Elements. Institution of Engineers, Australia, Civil Engineering Transactions, vol .

PARSANEJAD, S. 1986. Nonlinear Analysis of Orthogonally Stiffened Plates Under Combined Loads. Civil Engg. Trans. I.E.Aust., Vol CE28, #3, pp. 207-215.

PFRANG, E.O., SIESS, C.P. and SOZEN, M. 1964. Load-Moment-Curvature Characteristics of Reinforced Concrete Cross-sections. ACI Journal, July.

QUAST, U. 1986. Stability of Compression Members. In Concrete Framed Structures: Stability and Strength. Edited by R. Narayanan. Elsevier Applied Science Publishers.

SABNIS, G.M. *et al.* 1983. Structural Modelling and Experimental Techniques. Prentice-Hall Inc, Toronto, 585pp.

SCANLON, A. 1972. Time Dependent Deflections of Reinforced Concrete Slabs. PhD Dissertation, Dept. of Civil Engineering, University of Alberta.

SCANLON, A. and MURRAY, D.W. 1982. Practical Calculation of Two-way Slab Deflections. Concrete International, vol. 4, #11, pp. 43-50.

SEELY, F.B and SMITH, J.O. 1955. Advanced Mechanics of Materials, 2nd Edition. John Wiley and Sons,New York.

SHARMAN, P.W. and HUMPHERSON, J. 1968. An Experimental and Theoritical Investigation of Simply-Supported Thin Plates Subjected to Lateral Load and Uniaxial Compression. Journal of the Royal Aeronautical Society, vol 72, pp 431.

SWARTZ, S.E. ET AL. 1974a. Buckling Tests on Rectangular Concrete Panels. ACI Journal, January, pp 33.

SWARTZ, S.E. and ROSEBRAUGH, V.H. 1974b. Buckling of Reinforced Concrete Plates. ASCE Structural Division, Vol 100, # ST1, pp 195.

SWARTZ, S.E. *et al*. A Method for Determining the Buckling Strength of Concrete Panels. Experimental Mechanics, April, pp 138.

SUBBA RAO, K.S., RANGAIAH, N. and RANGANATHAM, B.V. 1977. Lower Bound Limit Analysis of Rectangular Slabs. ASCE Structural Division, Vol 103, # ST11, pp 2193-2209.

SUPPLE, W.J. 1979. Buckling of Plates under Axial Load and Lateral Pressure. Proc. International Conference on Thin-walled Structures, University of Strathclyde, Glasgow, pp 693-704.

SZILARD, R. 1974. Theory and Analysis of Plates. Prentice-Hall Inc, New York.

TAYLOR, R. *et al*. 1966. Effect of Arrangement of Reinforcement on the Behavior of Reinforced Concrete Slabs. Magazine of Concrete Research, Vol 18, # 55, June.

TODESCHINI, C.E., BIANCHINI, A.C. and KESLER, C.E. 1964. Behavior of Columns Reinforced with High Strength Steels. ACI Journal, Vol. 61, pp. 701-715.

TIMOSHENKO, S.P. and WOINOWSKY-KRIEGER, S. 1959. Theory of Plates and Shells, Second Edition. Mcgraw-Hill.

TOMA, S. and CHEN, W.F. 1983a. Analytical Models of Tubular Columns. IABSE Proceedings P-67/83.

TOMA, S. and CHEN, W.F. 1983b. Post-Buckling Behavior of Tubular Beam-Columns. ASCE Structural Division, August.

TROISKY, M.S. 1976. Stiffened Plates:Bending, Stability and Vibrations. Elvevier Publishing Company, New York.

TSINKER, G.P. 1986. Floating Ports: Design and Construction Practices. Gulf Publishing Company, 380 pp.

WEBB, S.E. and DOWLING, P.J. 1980. Large Deflection

Elasto-Plastic Behavior of Discretely Stiffened Plates. Proceedings of the Institution of Civil Engineers, Part 2, June, pp 375-401.

UGURAL, A.C. 1981. Stresses in Plates and Shells. McGraw-Hill Book Company, New York, 317pp.

VAN den BEUKEL, IR.A. 1977. Nonlinear Analysis of Concrete Members. HERON, Vol 22, # 2.

VAN GREUNEN, J. 1979. Nonlinear Geometric, Material and Time Dependent Analysis of Reinforced and Prestressed Concrete Slabs and Panels. PhD Dissertation, Dept. of Civil Engineering, University of California, Berkeley, Report No. 79-3.

VEBO, A. and GHALI, A. 1977. Moment-Curvature Relation of Reinforced Concrete Slabs. ASCE Proceedings, Vol. 103, # ST3, pp. 515-531.

VEBO, A.L. 1982. Nonlinear Behavior of Reinforced Concrete Beams and Slabs. Ph.D. Dissertation, Department of Civil Engineering, University of Calgary.

WANG, T. 1948. Large Deflection Analysis of Plates . NACA Technical Note 1425.

WEILER, G. 1982. Approximate Methods for Analysis of Tilt-Up Concrete Wall Panels. Concrete International, November, pp. 16-22.

WIEGAND, E. 1970. Ein Beitrag Zur Beulstabilitat Von Stahlbetonwanden Mit Nichtlinear-elastichen Werkstoffgesetz. Technischen Hochschule, Darmstadt.

YAMAMOTO, Y. *et al*. 1970. Buckling of Plates Subjected to Edge Thrusts and Lateral Pressure. Journal of Society of Naval Architects of Japan, Vol 127, pp 171.

YOSHIKI, M. *et al*. 1965. Buckling of Plates Subjected to Edge Thrusts and Lateral Pressure. Journal of Society of Naval Architects of Japan, Vol 118, pp 249.

YOUNG, A.G. 1957. Ship-Plating Subjected to Loads Both Normal to and in the Plane of the Plate. Transactions, RINA, Vol 99, pp 578.